HIGHWAY RESEARCH RECORD

Number 370 | Concrete
8 Reports

HIGHWAY RESEARCH BOARD
NATIONAL RESEARCH COUNCIL
NATIONAL ACADEMY OF SCIENCES—NATIONAL ACADEMY OF ENGINEERING

1971
HIGHWAY RESEARCH BOARD

OFFICERS

Charles E. Shumate, *Chairman*
Alan M. Voorhees, *First Vice Chairman*
William L. Garrison, *Second Vice Chairman*
W. N. Carey, Jr., *Executive Director*

EXECUTIVE COMMITTEE

A. E. Johnson, *Executive Director, American Association of State Highway Officials* (ex officio)
F. C. Turner, *Federal Highway Administrator, U.S. Department of Transportation* (ex officio)
Carlos C. Villarreal, *Administrator, Urban Mass Transportation Administration* (ex officio)
Ernst Weber, *Chairman, Division of Engineering, National Research Council* (ex officio)
Oscar T. Marzke, *Vice President, Fundamental Research, United States Steel Corporation* (ex officio, Past Chairman 1969)
D. Grant Mickle, *President, Highway Users Federation for Safety and Mobility* (ex officio, Past Chairman 1970)
Charles A. Blessing, *Director, Detroit City Planning Commission*
Hendrik W. Bode, *Gordon McKay Professor of Systems Engineering, Harvard University*
Jay W. Brown, *Director of Road Operations, Florida Department of Transportation*
W. J. Burmeister, *Director of Bureau of Engineering, Division of Highways, Wisconsin Department of Transportation*
Howard A. Coleman, *Consultant, Missouri Portland Cement Company*
Harmer E. Davis, *Director, Institute of Transportation and Traffic Engineering, University of California*
William L. Garrison, *Edward R. Weidlein Professor of Environmental Engineering, University of Pittsburgh*
George E. Holbrook, *E. I. du Pont de Nemours and Company*
Eugene M. Johnson, *President, The Asphalt Institute*
A. Scheffer Lang, *Head, Transportation Systems Division, Department of Civil Engineering, Massachusetts Institute of Technology*
John A. Legarra, *State Highway Engineer and Chief of Division, California Division of Highways*
William A. McConnell, *Director, Operations Office, Engineering Staff, Ford Motor Company*
John J. McKetta, *Department of Chemical Engineering, University of Texas*
J. B. McMorran, *Consultant, Troy, New York*
John T. Middleton, *Acting Commissioner, National Air Pollution Control Administration*
R. L. Peyton, *Assistant State Highway Director, State Highway Commission of Kansas*
Milton Pikarsky, *Commissioner of Public Works, Chicago*
Charles E. Shumate, *Executive Director-Chief Engineer, Colorado Department of Highways*
David H. Stevens, *Chairman, Maine State Highway Commission*
Alan M. Voorhees, *Alan M. Voorhees and Associates, Inc.*

EDITORIAL STAFF

Stephen Montgomery, *Senior Editor*
Mildred Clark, *Associate Editor*
Beatrice G. Crofoot, *Production Manager*

HIGHWAY RESEARCH RECORD

Number 370 | Concrete
8 Reports

Subject Area

32 Cement and Concrete

HIGHWAY RESEARCH BOARD
DIVISION OF ENGINEERING NATIONAL RESEARCH COUNCIL
NATIONAL ACADEMY OF SCIENCES—NATIONAL ACADEMY OF ENGINEERING

WASHINGTON, D.C. 1971

ISBN 0-309-01988-5

Price: $3.00

Available from

Highway Research Board
National Academy of Sciences
2101 Constitution Avenue
Washington, D.C. 20418

CONTENTS

SPONSORSHIP OF THIS RECORD

GROUP 2—DESIGN AND CONSTRUCTION OF TRANSPORTATION FACILITIES
John L. Beaton, California Division of Highways, chairman

Committee on Mechanical Properties of Concrete
Sandor Popovics, Northern Arizona University, chairman
John D. Antrim, Howard T. Arni, R. S. Barneyback, Jr., Richard L. Grey, Frank L. Holman, Jr., Ignatius D. C. Imbert, Clyde E. Kesler, V. M. Malhotra, Bryant Mather, Robert G. Mathey, Leonard J. Mitchell, Richard Alan Muenow, Adam M. Neville, R. E. Philleo, V. Ramakrishnan, Charles F. Scholer, Surendra P. Shah, V. R. Sturrup, Janos Ujhelyi, Harold R. J. Walsh

Committee on Chemical Additions and Admixtures for Concrete
Richard D. Walker, Virginia Polytechnic Institute and State University, chairman
Frederick E. Behn, Delmar L. Bloem, Kenneth E. Daugherty, W. L. Dolch, Fred A. Dykins, H. C. Fischer, Bruce E. Foster, C. E. Lovewell, Bryant Mather, Harry H. McLean, Richard C. Mielenz, William Grover Prince, Jr., Melville E. Prior, Raymond J. Schutz, Peter Smith, Patrick H. Torrans, Rudolph C. Valore, George J. Verbeck

Committee on Basic Research Pertaining to Portland Cement and Concrete
Katharine Mather, U.S. Army Engineer Waterways Experiment Station, Vicksburg, Mississippi, chairman
Horace A. Berman, Stephen Brunauer, L. E. Copeland, Sidney Diamond, Ludmila Dolar-Mantuani, W. L. Dolch, Wilhelm Eitel, G. J. C. Frohnsdorff, Kenneth T. Greene, P. E. Halstead, Waldemar C. Hansen, Gunnar M. Idorn, George L. Kalousek, Clyde E. Kesler, Kenneth R. Lauer, Richard C. Mielenz, R. E. Philleo, T. C. Powers, Della M. Roy, Peter J. Sereda, Ali A. Tabikh, H. F. W. Taylor, Rudolph C. Valore, R. P. Vellines, George J. Verbeck, Robert Brady Williamson, Julie C. Yang

William G. Gunderman, Highway Research Board staff

The sponsoring committee is identified by a footnote on the first page of each report.

FOREWORD

The 8 reports included in this RECORD show the diversity of approaches and techniques available to the research worker whose task it is to stimulate progress toward improvement of the properties of concrete. The breadth of the subject matter treated emphasizes the variety of materials, processes, and properties that require consideration as the highway engineer continues to seek improvement of concrete for the many demanding uses and environments to which it is exposed in modern transportation systems.

The paper by Patterson takes as its domain for the study of admixtures 6 spans in 2 bridges in service under traffic. Isenburg and his co-workers study the behavior of admixtures in the laboratory and include photographs of a single cement grain that occupies almost an entire printed page. Feldman utilizes data from very sophisticated past and current studies to derive a model of hydrated portland cement. The comparatively recent advent of scanning electron microscopy such as described by Isenburg et al. has substantiated many of the essential ideas related to the structure of cement paste and derived by reasoning from fundamental research such as that described by Feldman.

The use of admixtures of many types to improve the properties of concrete is widespread and is reflected in 3 of the 8 reports. Lovewell and Hyland present information on concretes containing both chemical and mineral admixtures, whereas Isenburg, Rapp, Sutton, and Vanderhoff as well as Patterson discuss specific chemical admixtures.

Ballinger's study of the fatigue life of concrete provides experimental confirmation that the behavior of concrete under variable loads follows an earlier developed theoretical hypothesis. The improvement of the mechanical properties of concrete by pretreatment of the aggregates is demonstrated by Lees and Singh.

The ultimate justification for research on new materials, processes, and techniques is the improved or more economical performance of concrete in service. A vital ingredient in the translation of new processes and materials to field practice is assurance that the proportions and processes actually achieved are as specified. Rapid quality control and assurance tests are essential. Hudson and Steele present data for predicting compressive strengths from tests at early ages.

When performance or tests indicate that the specified proportions have not been achieved, a determination of the amount of cement in the concrete is often necessary. This is a complex chemical determination, often impossible for certain combinations of materials. The new method proposed by Tabikh, Balchunas, and Schaefer holds promise for overcoming many of the difficulties associated with current methods.

A METHOD USED TO DETERMINE CEMENT CONTENT IN CONCRETE

A. A. Tabikh, M. J. Balchunas, and D. M. Schaefer, Research Laboratory, Marquette Cement Manufacturing Company, Chicago

•THE CEMENT content in hardened concrete must frequently be determined in order to rebut those who tend to blame the cement whenever the concrete does not meet specifications. Although cement failure is indeed a significant factor, other factors that are often overlooked can be equally important. Thus, a method is needed for determining the cement content of hardened concrete so that the possibility of cement failure can be eliminated and other parameters can be examined. Existing methods, which are handicapped by inconvenience, error, or expense, lack the requirements to meet this need.

The standard ASTM Method C 85 (Test for Cement Content in Hardened Portland Cement Concrete), although tedious, usually gives reliable results when information concerning both the cement and the aggregate is available. Kossivas (4) has proposed an alternate method in which the sulfate ion content is determined. However, to obtain a satisfactory cement determination requires that the sulfate content of the cement be known, and that all the sulfates be derived from the cement. The authors have found aggregates, in a number of instances, that contain sulfates in sufficient quantities to cause serious errors.

Some instrumental methods based on neutron activation and isotopic measurement techniques have been used for cement determinations (2, 3). These nuclear methods have been used primarily for field measurements. However, errors caused by common elements exist, as in the previously mentioned methods. Another deterrent is the high cost of equipment.

The method presented in this study is intended to satisfy the need for a method to determine the cement content of hardened concrete and to circumvent the difficulties discussed in existing methods. No prior knowledge of the chemical composition of either the cement or the aggregate is required. The suggested method involves an extraction of the concrete sample with a methanolic solution of maleic acid.

In a previous study (5), maleic acid was used to extract the silicates from portland cement. Subsequently, it was established that all hydration products are soluble in maleic acid. Because the ideal method of determining cement content in concrete would involve a solution of the cement only, maleic acid extraction seemed a plausible approach. This has in fact been confirmed by a study in which a variety of aggregates were extracted by using an alcoholic solution of maleic acid. In no case was aggregate weight loss observed.

Sponsored by Committee on Basic Research Pertaining to Portland Cement and Concrete and presented at the 50th Annual Meeting.

EXPERIMENT

Materials Used

Anhydrous methanol and a practical grade of maleic acid are used to prepare 2 liters of 20 percent maleic acid solution. This solution is usable for approximately 2 weeks. Fuller's earth (Matheson Catalog No. L-400) is used as a filtering aid. Filtration is made in a 10-cm Büchner funnel fitted with a tared S and S red ribbon paper. A 200-ml Erlenmeyer vacuum flask is used to receive the filtrate.

The concrete specimens studied are part of a concrete research program. Thus, reliable cement content data are available under a controlled mix design program. A number of cement types were included. Also, a number of mortar cubes made according to ASTM Method C 109 (Test for Compressive Strength of Hydraulic Cement Mortars Using 2-in. Cube Specimens) were analyzed.

Procedure

As illustrated in the block diagram shown in Figure 1, the specific gravity of the concrete is determined first. An adaptation of ASTM Method C 127 (Test for Specific

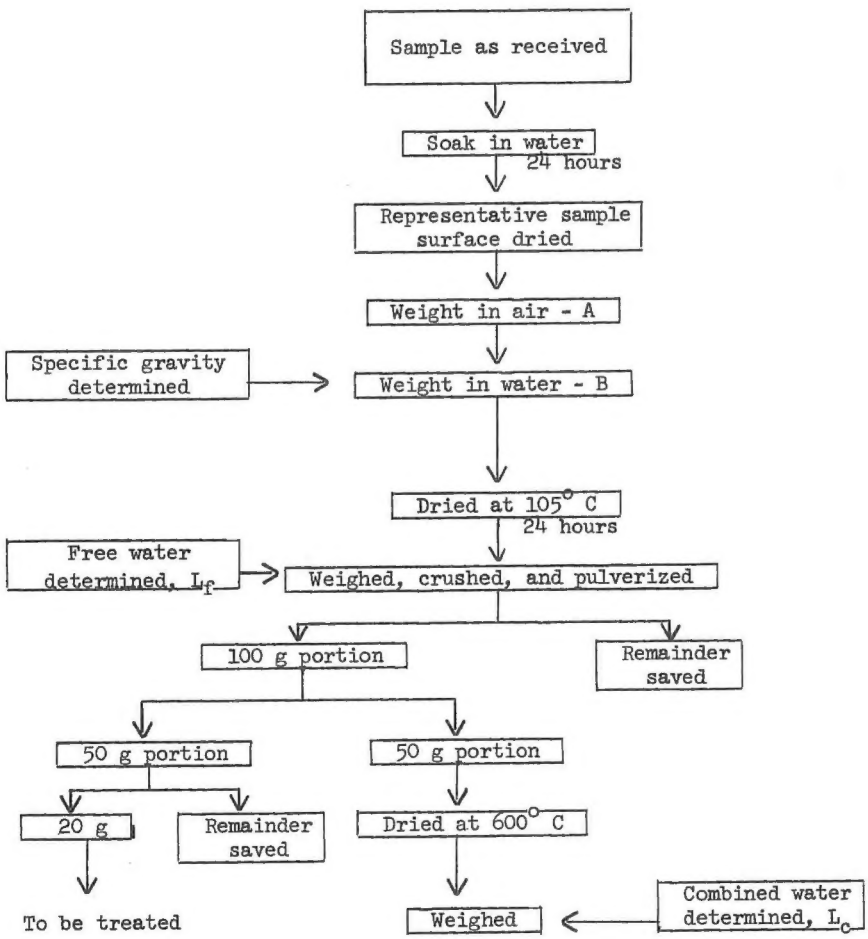

Figure 1. Specific gravity determination and sample preparation of concrete sample.

Gravity and Absorption of Coarse Aggregate) is followed. A sample of the concrete at least 3 times the size of the largest aggregate used in the concrete mix is dried at 105 C to constant weight (overnight is usually sufficient). After soaking for 24 hours, the sample is surface-dried and weighed in air, and then weighed again in water. The bulk specific gravity (saturated surface-dried) is then determined as

$$\text{Bulk sp gr (ssd)} = \frac{A}{A - B}$$

where A = weight in grams of saturated surface-dried sample in air, and
B = weight in grams of saturated sample in water.

At times when speed is essential, a very good approximation of the specific gravity can be made by soaking a sample as received for 1 hour, surface-drying, and weighing as described in the preceding.

If the results are to be incorporated as the content of cement in hardened concrete, the concrete sample should be soaked in water and surface-dried at 105 C for 20 to 24 hours, and the weight loss (L_f) representing the free water in the sample should be calculated.

After the sample has been dried, it is crushed and pulverized to -20 mesh. It is then split to 100 grams. Half of this sample is weighed into a tared dish and dried at 600 C for 4 hours and then weighed and cooled in a desiccator; the loss, L_C, represents combined water.

From the other half of the sample, a 20-gram aliquot is taken for the extraction procedure shown in Figure 2. Three grams of fuller's earth are added with the sample to 800 ml of the maleic acid methanol solution and stirred for 10 min. All but the

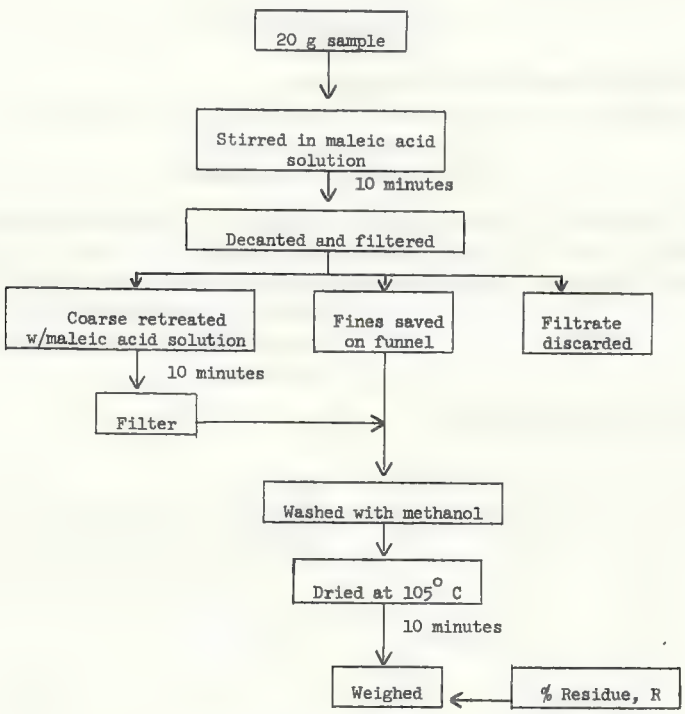

Figure 2. Maleic acid extraction.

coarse particles are filtered through the Büchner funnel. These coarse particles are then re-treated with 400 ml of maleic acid solution, stirred for 10 min, and then washed into the funnel. After the solution has been filtered, the funnel must be carefully washed with methanol to remove all remaining soluble material. The residue is then dried at 105 C for 10 min, cooled in a desiccator, and weighed. The residue, R, is calculated as percentage of residue of the sample.

Calculations

The following calculations give the results of the extraction procedure:

$$L_f = \frac{C - D}{C} \times 100$$

where L_f = free water loss,
C = weight in grams of saturated surface-dried sample, and
D = weight in grams of the same sample after 24 hours at 105 C.

$$L_c = \frac{E - F}{E} \times 100$$

where L_c = combined water loss,
E = weight in grams of pulverized 105 C dried sample, and
F = weight in grams of the same sample after heating at 600 C for 4 hours.

$$C_p = (100 - R - L_c)(1 - \frac{L_f}{100})$$

where C_p = percentage of cement in the concrete, and
R = percentage of residue.

$$\text{c.c.} = (\frac{C_p}{100})(\frac{1}{94})\ (\text{sp gr})\ (K)$$

where c.c. = cement content in bags/cu yd; and
K = conversion factor of metric to English units, 1,685.56.

RESULTS AND DISCUSSION

The cement contents of a large number of hardened concrete specimens have been tested by the maleic acid extraction procedure. The results of some of the tests, representing a number of cement types and concrete mix designs are given in Table 1. In addition, a number of cement content determinations of mortar cubes are given in Table 2.

TABLE 1

COMPARISON OF DETERMINED VERSUS ACTUAL VALUES OF CEMENT CONTENT IN HARDENED CONCRETE

Cement Type	Age of Concrete (day)	Cement Content (bags/cu yd)		
		Actual	Determined	Difference
II	23[a]	7.0	6.7	-0.3
III	28	6.1	5.7	-0.4
III	28	5.1	5.1	0
III	28	4.0	4.0	0
III	28	6.1	6.0	-0.1
I	7	6.0	6.0	0
I	7	6.0	5.7	-0.3
I	91	6.1	5.8	-0.3
II	7	6.1	6.1	0
IA	3	6.1	5.6	-0.5

[a]Months.

TABLE 2

COMPARISON OF DETERMINED VERSUS ACTUAL VALUES OF CEMENT CONTENTS IN MORTAR CUBES MADE ACCORDING TO ASTM METHOD C 109

Age of Mortar (day)	Actual	Determined	Difference
1	23.6	21.9	-1.7
3	23.6	22.1	-1.5
7	23.6	22.0	-1.6
28	23.6	22.1	-1.5

The results given in both tables are shown in Figure 3 where they are expressed as the actual and determined percentages of cement in the total concrete sample. This is a linear relationship that is expressed by

$$Y = a_0 + a_1 x$$

where $a_0 = 1.135$,

$a_1 = 0.885$, and

Coefficient of correlation = 0.99848.

From these statistical considerations, it is clear that the correlation is good. The results would be accurate within ±0.27 bags/cu yd at a 95 percent confidence level when the preceding equation (or curve) is used. Even without the preceding equation, the absolute value determined is very acceptable when one considers the level of precision attained in a field or plant batching operation.

When the age of the concrete is considered, there appears to be no definite trend in the concrete results given in Table 1. By contrast, the mortar cubes (Table 2) do show a trend where the negative bias diminishes with age. This is attributed primarily to the slow hydration rate of the ferrite phase of portland cement. The calcium silicates are readily soluble in methanolic maleic acid, whereas the aluminates and ferrites are normally insoluble. However, in an aqueous phase, the aluminates hydrate rapidly and become soluble in the maleic acid solution, leaving only ferrites in the residue.

The difference between the actual and the experimental cement contents in the mortar cubes, expressed as percentage of unhydrated C_4AF versus time of curing, is shown in

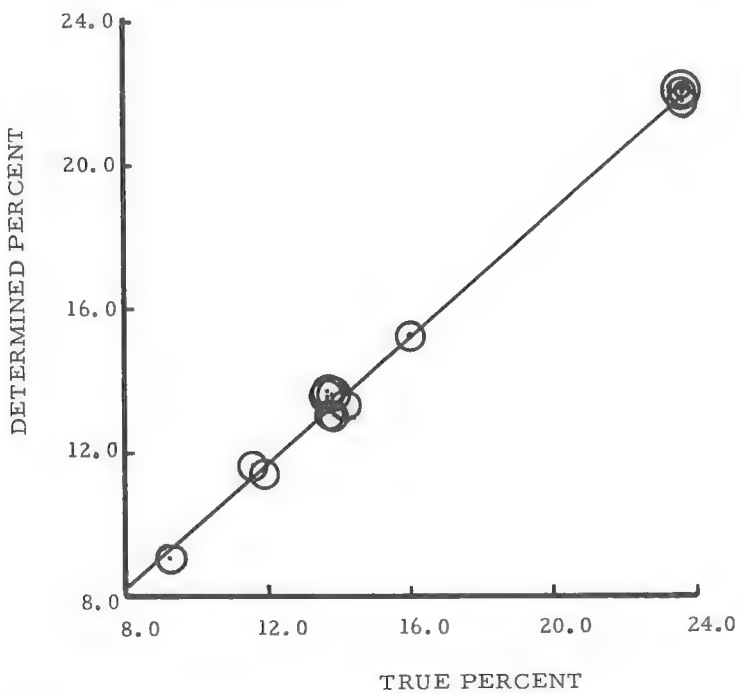

Figure 3. A linear regression line of determined and actual percentages of cement content in total concrete sample.

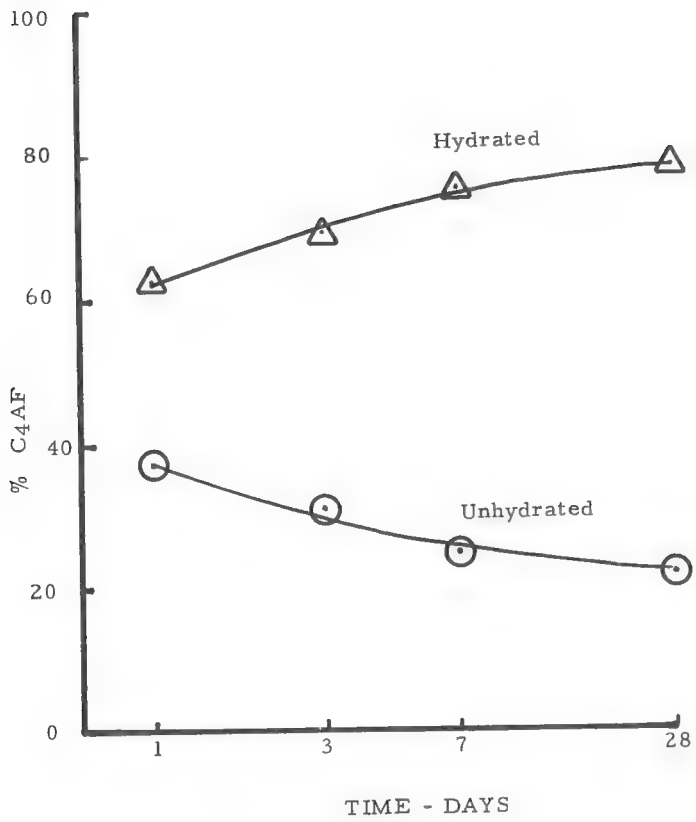

Figure 4. Differences between actual and determined values of cement content in mortar cubes (hydrated curve is obtained by difference).

Figure 4. This plot clearly shows that these differences are a function of the hydration rate of the ferrite phase. It is interesting to note the reaction rate, as shown by the hydration curve in Figure 4. This rate seems to be in general agreement with the results reported by Copeland et al. (1) in their study of the reaction kinetics of cement compounds. Because the hydrated ferrite phase is also soluble, the only insoluble fraction of the cement left after an extraction is the unhydrated ferrite phase. An X-ray diffraction study of the extracted residue lends further support to this conclusion. Unfortunately, the amount of unextracted ferrites is so highly diluted with the other insoluble residues that it was found impractical to determine its amount by a quantitative X-ray diffraction method.

Although the methanolic maleic acid will leave nearly all igneous and calcareous aggregates unaffected, it will probably give erroneously high values when pozzolanic materials are included in the concrete.

REFERENCES

1. Copeland, L. E., Kantro, D. L., and Verbeck, G. Chemistry of Hydration of Portland Cement. Research and Development Laboratories, Portland Cement Association, Bull. 153.
2. Covault, D. O., and Poovey, C. E. Use of Neutron Activation to Determine Cement Content of Portland Cement Concrete. HRB Bull. 340, 1962, pp. 1-29.

3. Iddings, F. A., Arman, A., Perez, A. W., II, Kiesel, D. W., and Woods, J. W. Nuclear Techniques for Cement Determination. Highway Research Record 268, 1969, p. 118-130.
4. Kossivas, K. G. Cement Content Determination in Hardened Concrete. Rock Processing Chemical Research Seminar, W. R. Grace and Company, Chicago, March 6, 1969.
5. Tabikh, A. A., and Weht, R. G. A Study of Portland Cement by X-Ray Diffraction. 21st Pacific Coast Regional Meeting, American Ceramic Society, Oct. 1968.

ASSESSMENT OF EXPERIMENTAL EVIDENCE FOR MODELS OF HYDRATED PORTLAND CEMENT

R. F. Feldman, Division of Building Research, National Research Council of Canada, Ottawa

The relative merits of the "new" and "old" models of hydrated portland cement are presented together with an assessment of published and some unpublished evidence relating to the models. The chief areas of evidence discussed are those pertaining to surface energy of calcium-silicate-hydrate material (C-S-H) by heat of solution, stoichiometry of C-S-H, and the effect of interlayer rehydration of D-dried C-S-H on density measurements, c-axis and hydrated radii calculations, length and weight change isotherms, and porosity and mechanical property correlations. A new technique of measuring the flow rate of helium into interlayer spaces is discussed in terms of evidence it produces. It is concluded that the "new" model of hydrated portland cement more accurately accounts for its nature as indicated by a wide variety of properties.

•THERE ARE many terms used throughout this discussion to describe elements and conditions of hydrated portland cement. These are defined in the following:

1. C-S-H is the poorly crystallized, layered calcium-silicate-hydrate material found in well-hydrated portland cement, C_3S and C_2S.
2. A layer is the basic unit of the C-S-H structure; it is about 9 Å thick in the c-direction. This term is used synonymously with sheet.
3. Interlayer space is the space between layers, when essentially parallel, separated by no more than about 5 Å. Disorientation of layers may lead to greater distances in local areas.
4. Interlayer water occupies space between adjacent layers of C-S-H and is less mobile than free or physically adsorbed water.
5. Physically adsorbed water is water that is held to an open surface and that has energies not much more than the latent heat of evaporation. It does not have a role in the structure, nor does it contribute to the mechanical properties of the material. As defined here, it does not include interlayer water.
6. Nitrogen area is the surface area calculated from nitrogen adsorption results. It does not include the area between adjacent C-S-H layers.
7. Water area is the surface area calculated from water sorption results. The physical significance is difficult to specify because interlayer water appears to reenter interlayer space in an unpredictable way throughout the BET region normally used for surface area calculations.
8. Solid volume is the volume of the C-S-H layers, the volume of the interlayer water, and the unoccupied interlayer space.

Sponsored by Committee on Basic Research Pertaining to Portland Cement and Concrete and presented at the 50th Annual Meeting.

9. The D-dried condition is the condition in which a sample has been dried to equilibrium at the water-vapor pressure of 5×10^{-4} mm of mercury.

10. The P-dried condition also involves drying but at a pressure of 8.15×10^{-3} mm of mercury.

11. Density is of 3 types: (a) density of undried material at 11 percent relative humidity (RH) that includes the interlayer water and interlayer space as solid volume in the calculation (physically adsorbed water is not counted as solid volume); (b) density of D-dried material that does not include the partially collapsed interlayer spaces as solid volume in the calculation (an approximation of this value is obtained by using water as the medium in the determination); and (c) density of D-dried material that includes the partially collapsed interlayer spaces as solid volume in the calculation.

Scientific interest in the experiments that provide evidence for a model for hydrated portland cement paste is currently at a high level. A new model subsequently called the F-S model (Feldman-Sereda model) has recently been proposed (1) that has given rise to extensive discussions (2, 3) comparing it with earlier ones.

The F-S model of hydrated portland cement is based ultimately on 3 fundamental assumptions (considered here as established facts) concerning the nature of the hydrated calcium silicates (assumed to be layered) normally found in hydrated portland cement. These assumptions are as follows:

1. The fundamental physical properties, such as density, equivalent c-spacing, Ca-Si ratio, H_2O-Si ratio, of hydrated portland cement or of the hydrated silicates and surface area vary with conditions of preparation. These conditions include water-solid ratio, temperature, and perhaps the content of alkali, sulfate, and admixtures.

2. When the hydrated material is D-dried, interlayer water is removed from the silicates. When it is reexposed to water vapor, water reenters the interlayer spaces even at low humidities.

3. In light of this conclusion, water surface areas and densities are therefore not correct, but the respective measurements by nitrogen and methanol are approximately correct.

These assumptions were considered wholly or partly incorrect in 1958 (4), even though surface areas determined by nitrogen before that date were given some credence by Kalousek (5) and Brunauer, Copeland, and Bragg (6). The basis of the old model, subsequently called the B-P model (Brunauer-Powers model), was that these assumptions were essentially incorrect, and a great deal of effort was spent in attempting to correlate and understand new data. As more and more data were accumulated, the assumptions had to be reevaluated. In 1964, Feldman and Sereda (7) suggested that assumptions 2 and 3 were true. In 1968 they described the F-S model (1), which is based on data from a variety of measurements on both compact and paste samples. These data included sorption, length change (8), strength, and other mechanical measurements (9), as well as surface area, chemical, and mineralogical considerations.

Other authors have also raised questions about aspects of the B-P model. Taylor (10) has expressed doubt about the supposed similarity of the hydrated silicates to the tobermorites and thus about the relevancy of the term "tobermorite gel"; hence, his preference for the nomenclature C-S-H. He considered the silicates to be very variable in composition and very heterogeneous. He has also questioned the very high density values used by Brunauer, Kantro, and Copeland (4) for a c-axis calculation. Locher (11) and Kurczyk and Schwiete (12) have questioned assumptions and methods used in the Ca-Si ratio determinations and results that show that the Ca-Si ratio varies inversely with the water-cement ratio (13). Seligmann (14) has analyzed nuclear magnetic reso-

nance measurements that he and others obtained and concluded that a large portion of what was considered as physically adsorbed water is interlayer water. Verbeck and Helmuth (15) have gone further and have concluded that the water formerly considered as gel water is interlayer water and that gel pores are, in fact, interlayer spaces. These conclusions all fit in with the descriptions and predictions of the F-S model.

There still remain, however, several areas of experimental evidence that are considered to cast doubt on the F-S model (2). These will be discussed in the following sections, and a considerable amount of new experimental evidence will be introduced. It is believed that the analysis of all the results makes the case for the F-S model convincing and provides the basis for a revision of the stiochiometry and "average interlayer spacing" of C-S-H gel.

SURFACE ENERGY OF C-S-H BY HEAT OF SOLUTION

The greatest difference between the F-S and B-P models of hydrated portland cement arises from assumptions 2 and 3 given earlier. The measurement of the surface energy of C-S-H gel by the heat-of-solution technique (16) has been considered by some (2) to be the strongest supporting evidence for the B-P model. It has been claimed that this measurement indicates that the surface area is correct when determined by water adsorption and is incorrect when determined by nitrogen adsorption. The following points indicate that this claim is doubtful:

1. Consideration of the surface energy of a material must include an assessment of the nature of the material and the type of surface involved. C-S-H is considered to be a layered crystal, the thickness of each layer being about 9 Å. Surface energy is the excess energy between the surface and the bulk. One is, therefore, immediately confronted with the difficult task of establishing whether the term "surface energy" has any meaning in layered materials; i.e., there is no real "bulk state."

2. As in the case with many clays of a layered nature, such as montmorillonite, C-S-H hydrates have both an internal and external surface. Nitrogen surface areas yield the external surface. If the unit cell structure or surface area per layer as proposed by Brunauer, Kantro, and Copeland (4) is correct, the internal plus the external surfaces are approximately 755 m^2/g; thus, without even considering the dubiousness of the concept of surface energy as considered in point 1, one evidently cannot use water areas or nitrogen areas for computing correct overall surface energies.

3. The discussion in point 2 shows that it was erroneous to reason (2) that surface energies, based on nitrogen areas, give values that are too high or too low (negative). In fact, if 755 m^2/g were used as a total area, a value closer to that of amorphous silica (16) would be expected. This emphasizes the irrelevance of the geometric mean of the surface energies of $Ca(OH_2)$ and amorphous silica that has been quoted by some workers (16). It can be questioned why these workers selected the values of crystalline $Ca(OH)_2$ and amorphous silica (2) for this calculation of surface energy because the $Ca(OH)_2$ in C-S-H is not crystalline.

4. The determination of specific surface energy by the heat of solution method is based on a very important assumption: The materials being studied are alike in every way except for their surface areas. Unfortunately, because the C-S-H materials were prepared by different methods, the materials would not be alike, as was pointed out earlier in assumption 1. To start with, the Ca-Si ratio of the C-S-H is now known (13) to vary inversely with the water-cement ratio for normal paste hydrated samples. This leaves several possibilities: (a) If the change in Ca-Si ratio is due only to additional Ca^{++} deposited between the layers (in an unknown state), then the internal surface energy can be changed because the surfaces are different with different amounts of

Ca^{++} and because the separation of the layers will vary. Evidence for the last statement has been obtained and will be discussed later (see section on density measurements and C-spacing). (b) The change in Ca-Si ratio might also be due either to silicone being substituted by calcium within the layer or to a different degree of silica condensation that, as has been shown by Lentz (17), occurs continuously. Owing to the diverse methods of preparing and starting materials, there is a clear possibility that the degree of polymerization of silica varies from preparation to preparation. In other words, variation in body structure and, therefore, body energy is a distinct possibility.

5. An evaluation of a paper by Brunauer, Kantro, and Wiese (16) on surface energy measurements on C-S-H gel led to the following observations: (a) The heat of solution for all their samples varied between 473 and 487 cal/g, a difference of 14 cal/g; for 2 identical samples, the difference was about 3.75 cal/g. It must be concluded that the precision of the data is not enough to make far-reaching conclusions. (b) The data fell into 3 clusters. Each cluster was almost completely composed of samples prepared by the same method: either the ball-mill, the paste, or the bottle-hydrated method. Within each cluster the results were scattered and, in some instances, negative surface energies could be calculated from the data when plotted against the water surface area. (c) Brunauer, Kantro, and Wiese (16) cited 2 samples, D-28 and D-35, when they discussed computation of surface energy. They suggested that if the surface areas of the samples as determined by nitrogen adsorption were used a negative surface energy would result. These samples, however, were made not only from different groups with regard to preparation but also from different materials. Sample D-28 was prepared by ball-milling β-C_2S for 46 days; D-35 was prepared by bottle-hydrating C_3S for 47 days. If one plots the nitrogen area for a group and makes comparisons for the same starting material, negative energies are not obtained. The data for nitrogen area, however, are very sparse.

6. A subsequent paper by Kantro, Wiese, and Brunauer (18), which contained heat of solution data, attempted to correct empirically for variation of Ca-Si ratio and water content. The application of regression analysis here raises the question, Did the variation in Ca-Si ratio cause the observed change in heat of solution, or did it change something else that in turn caused the change? The change in Ca-Si ratio most probably changed the nature of the surface as well as the surface area, body energy, and total heat of solution.

Kantro, Wiese, and Brunauer (18) attempted a difficult task with many inherent complications. It appears, however, that the ideas behind this work were based on the early concept of the nature of C-S-H (see 3 assumptions in first part of paper). With the present knowledge (assumption 1), which Kantro, Wiese, and Brunauer helped in a large measure to accumulate, it is clear that the heat of solution measurements should be reevaluated.

INTERLAYER WATER AND RELATED PROBLEMS

Density Measurements

Assumption 2 presents an important concept concerning interlayer water reentering D-dried material. The significance of this concept has been emphasized in the literature (2), and important questions concerning surface-area determinations by water and density determinations by lime-saturated solutions have been raised. If interlayer water reenters the structure—and several researchers (14, 15, 19) now believe that this is what happens—measured densities obtained by pycnometric techniques would approach that of the individual layers, if the value of the density of interlayer water is known and included in the calculation. It has been assumed, however, that

the layers completely collapse on D-drying, but this does not occur (20, 21). This incorrect assumption will lead to errors in estimates of a c-spacing or density and of a c-spacing of higher hydrates (e.g., P-dried specimens). The interlayer space is normally occupied by the maximum amount of hydrate water under normal conditions of concrete use, and so porosity or density calculations with the space included as solid matter are most relevant. This point will be discussed in detail in a later section.

In an experiment by Brunauer, Kantro, and Copeland (4), the weighed D-dried sample was soaked in a bottle or similar arrangement until the liquid was eventually brought to a certain level, after which the container was weighed. By this time the interlayer water would already have reentered the sample, with the result that the solid volume would appear low and the density too high; this is precisely what resulted (4). If the interlayer water had reentered very slowly subsequent to the measurements, a gradual increase in apparent density for both completely or partially dried samples would have resulted. Some authors, however, reported a gradual decrease in density when measurements were made in this way on partially dried samples, and they explained it by assuming gradual interlayer penetration (4). Some other explanation will have to be found; progressive changing in the state and position of Ca^{++} ions between the layers is perhaps a solution.

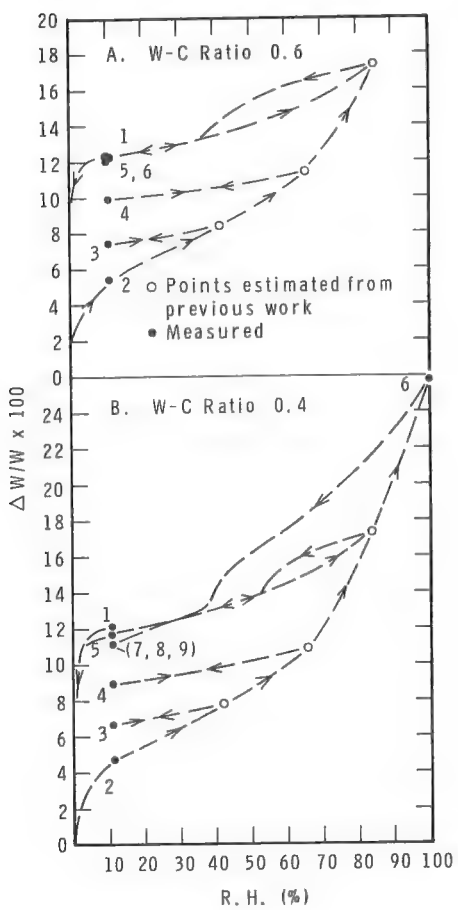

Figure 1. Isotherms for hydrated portland cement pastes.

This author is not aware of any evidence that shows that water cannot reenter the spaces between the C-S-H layers. In fact, much evidence exists to the contrary. Figure 1 shows recent work by this author on 0.6 and 0.4 water-cement ratio pastes hydrated for 2.5 years. These samples were stored for more than 2 and 4 months respectively at 11 percent RH, were then dried in stages well beyond the D-dried position during a period of 40 days, and were finally heated under vacuum to 190 C. They were then exposed to various humidities but always taken back to 11 percent RH before being advanced to a higher humidity.

The dashed lines shown in Figure 1 illustrate the significance of returning to 11 percent RH and how these paths are reversible (8). In an ideal adsorption system, all the numbered points at 11 percent RH should be identical, but in this case the position changes with each further advance of humidity. (An ideal adsorption system is one in which the system can be uniquely defined by temperature and relative pressure for constant surface area and other adsorbent properties in all but the primary hysteresis region. This region rarely exists below 35 percent RH and 11 percent RH should uniquely define such a system.) Previous work (8) has shown that this phenomenon is related to the reentrance of interlayer water. The numbered points are given in Table 1 and show the length of time the samples were retained at each condition. The results clearly show that not only had all the interlayer water

TABLE 1

RESULTS OF TESTS ON PORTLAND CEMENT PASTES HYDRATED FOR 2½ YEARS

Condition	Relative Humidity (percent)	Water-Cement Ratio 0.6				Water-Cement Ratio 0.4			
		Time (days)	Final Weight (gram)	Percent Change From Dry	Point on Figure 1	Time (days)	Final Weight (gram)	Percent Change From Dry	Point on Figure 1
Stored	11	117	16.2645	12.33	1	56	18.6848	12.14	1
Dried incrementally beyond D-dried condition		40	14.4790	—		49	16.6627	—	
	11					4	17.2807	3.71	
	11	41	15.2587	5.39	2	45	17.4416	4.68	2
	42	20	—[a]	—		15	—[a]	—	
	11	9	15.5570	7.45	3	29	17.7717	6.66	3
	66	26	—[a]	—		27	—[a]	—	
	11	9	15.9138	9.91	4	10	18.1393	8.86	4
	84	36	—[a]	—		28	—[a]	—	
	11	28	16.2676	12.35	5	11	18.6064	11.67	5
	11	27	16.2431	12.18		—	—	—	
Immersed in saturated $Ca(OH)_2$ solution						5	20.9562[b]	25.77	6
	11					22	18.5148	11.12	7
	11					9	18.5253	11.18	8
	11					17	18.5120	11.10	9

[a]Estimated. [b]Damp dry.

reentered the sample after exposure to 85 percent RH but also it had done so progressively from low relative humidities. It should be mentioned that this result is exactly the same as that obtained by Feldman (8) when vacuum balance techniques were used and when the desiccator technique on the same sample was used. The same result has been subsequently obtained on other samples when even longer times of equilibration were used. In this case a clear differentiation of interlayer and adsorbed water was made by thermal analysis (DTA and TGA) (22).

Density Measurements and c-Spacing

In the last section it was suggested that both water surface area and a certain density measurement are in error for the same reason; i.e., water reentering the interlayer spaces was not taken into account. This density value was used by Brunauer, Kantro, and Copeland (4) in 1958, however, with certain assumptions to calculate a c-spacing, and a value of 9.3 Å resulted. This density value (2.86 g/cc) is much higher than any listed by Taylor (23, 24) on the relationship between calcium silicates and clay minerals. In addition, Taylor lists a much lower value (2.44 g/cc) for the density of C-S-H than that published in 1956 by Brunauer, Copeland, and Bragg (6). It should be pointed out that a calculation of c-spacing from density assumes that the material is homogeneous in composition, is layered, and has a regular arrangement. As already discussed, this material does not strictly conform in at least two of these requirements—homogeneity of composition and regularity of arrangement. Thus, the calculation of the c-spacing must be considered as yielding, at best, only the average value of layer separation. As such it must still be considered as useful; revised calculations will be made.

A measured c-axis spacing of 9.3 Å is obtained by dehydrating (heating to 300 C) 11.3-Å natural tobermorite (25). Megaw and Kelsey (25) suggested that the packing of adjacent layers in the dehydrated products differed from that in 11.3-Å tobermorite; in 9.3-Å tobermorite the ribs of 1 layer were likely to pack into the grooves of the next. Brunauer, Odler, and Yudenfreund (2) assumed that the same thing occurs when C-S-H is D-dried; they state that "the layers stick to each other with such force that even soaking in water does not separate the layers. Obviously, therefore, at the relative humidi-

ties of 0.07 to 0.33, used in the BET surface area determinations, water cannot enter between the layers."

It appears that the 9.3 Å value for C-S-H obtained by Brunauer, Kantro, and Copeland (4) was approximately the thickness of the layers themselves, if the layers were like tobermorite. This led to the belief that the layers had completely collapsed. Results from helium comparison pycnometry by this author (details to be published later) have shown that the measured density varies directly with water-cement ratio. The density for the D-dried C-S-H, calculated from hydrated C_3S paste prepared at a water-cement ratio of 0.5, is approximately 2.25 g/cc. The results also show that collapse on D-drying is not very great because the undried C-S-H at 11 percent RH has a density of approximately 2.34 g/cc (this value being corrected for adsorbed water). The value of the D-dried sample would be the higher if drying were accompanied by complete collapse (20, 21). The degree of collapse did not compensate for the loss in weight due to hydration; thus, this resulted in the lower density for the D-dried sample. These values correlate well with those published for various calcium silicates of the tobermorite group, where none exceeds 2.35 g/cc (23, 24).

Several comments can be made concerning the following calculations:

1. It was assumed by Brunauer, Kantro, and Copeland (4) that the density of C-S-H did not vary with preparation or Ca-Si ratio. This is contrary to assumption 1, given earlier. The observed variation in density leads to the conclusion (assuming one can calculate c-spacing from density) that c-spacing also varies with preparation and with the water-cement ratio. The measured densities would give an average c-spacing of 11.8 Å for D-dried C-S-H prepared from C_3S paste at a water-cement ratio of 0.5 This is within the range of values found by Taylor (23) for artificial tobermorites. However, the reservations stated in the preceding concerning this calculation are still maintained.

2. The collapse of a badly oriented and organized material with varying amounts of Ca^{++} ions between the layers has been assumed (4) to be similar to the collapse of natural tobermorite. It appears that the large amount of Ca^{++} ions between the layers or their poor orientation are responsible for preventing a greater collapse. It is interesting to note that nonswelling clays like vermiculite, although not the same structure as tobermorite, do allow water to reenter between the layers after they have been strongly dried (24). As has been shown by density and X-ray measurements, such materials suffer greater collapse than does C-S-H.

3. The high-density value of 2.73 g/cc obtained by Brunauer, Kantro, and Copeland (4) for the P-dried sample was high for much the same reason that the value obtained for the D-dried sample was high. A c-spacing of 10.2 Å was calculated on the basis of this density. On immersion of a P-dried sample in water during the course of a density determination, one could expect that the remainder of the interlayer water rapidly enters. Thus, the measured density will be only somewhat less than that of the layers themselves.

4. The reasoning by some authors with regard to the stoichiometry of C-S-H is considered incorrect. In 1958 Brunauer, Kantro, and Copeland (4) stated, ". . . that one molecule of Ca_3SiO_5 reacts with exactly three molecules of water and one molecule of β - Ca_2SiO_4 with two molecules of water could not be demonstrated in the present investigation. The reason for this is that a reliable method is lacking to distinguish quantitatively between adsorbed water and chemically bound water in tobermorite."

No new method has been applied by Brunauer, Odler, and Yudenfreund (2) in their recent discussion of the F-S model to separate the types of water. The original conclusion that the chemical formula of P-dried C-S-H was $Ca_3Si_2O_7 \cdot 254H_2O$ is based

on the assumption that on reexposure to 33 percent RH neither the P-dried nor the D-dried samples experience reentry of interlayer water. This assumption has now been proved incorrect. Brunauer, Kantro, and Copeland (4) continued in their paper in 1958 that " . . . the molecular formula of the tobermorites in C-18 and D-43, corrected for adsorbed water, is $Ca_3Si_2O_7 \cdot 2.54H_2O$. It is clear that drying at a vapour pressure greater than 8×10^{-3}mm would have led to a higher water content. On the basis of arguments advanced in an earlier paper, as well as on the basis of the present results, it seems reasonable to suppose that in a saturated $Ca(OH)_2$ solution tobermorite contains 3 molecules of combined water." It is this author's opinion that the formula $Ca_3Si_2O_7 \cdot 3H_2O$ should be considered as not having been established; a sounder based estimation can, however, be made.

It will first be shown that the area of the internal plus external surfaces of D-dried C-S-H, usually taken as 755 m^2/g, is of the right order. This is the value generally assumed for one layer of C-S-H.

In a recent paper, Feldman (8) showed that the total interlayer water for a sample of hydrated portland cement was 7.54 percent by weight of D-dried material, with the sample having a nitrogen area of 30 m^2/g. If it is assumed that the interlayer water molecule covers 10.8 $Å^2$/molecule on 1 surface, the internal area is $274 \times 2 m^2/g$ (i.e., 548 m^2/g) and, if nitrogen measures the external area correctly, the total area is thus 578 m^2/g. If corrections are made for incomplete hydration, the equivalent total area is thus 670 m^2/g. If one assumes that completely hydrated Type II portland cement is composed of 80 percent C-S-H (27) and assigns the area of internal plus external surface of 755 m^2/g to the C-S-H portion, the expected value of surface area would be 80 percent of 755 m^2/g (i.e., 604 m^2/g). This agrees fairly well with the 670 m^2/g figure when one considers that in hydrated portland cement some of the water generally termed "interlayer" may have come from the aluminates and sulfoaluminates.

A further series of calculations may be used to establish the stoichiometry and the calculated c-axis spacing of C-S-H derived from C_3S. Hydrated C_3S pastes, when first D-dried from about 12 percent RH by Helmuth (19), yielded a water content of approximately 28.4 percent of the ignited weight. According to Brunauer, Kantro, and Copeland (4) and to Feldman (8), at 12 percent RH the sample contains approximately all the interlayer and 1 monolayer of adsorbed water. Hydrated C_3S paste, containing C-S-H dehydrated to $Ca_3Si_2O_7 \cdot 2H_2O$ (approximately D-dried), contains 19.7 percent water based on the ignited weight. The difference between 28.4 and 19.7 percent (8.7 percent) is made up of the interlayer and the adsorbed water. For a surface area of 73 m^2/g determined by this author on 0.5 water-cement ratio paste with nitrogen adsorption, the equivalent value of a monolayer of water is 2.0 percent by weight, leaving 6.7 percent as interlayer water. This corresponds to 1.7 molecules per formula unit at about 12 percent RH. This gives a formula of $Ca_{3+x}Si_2O_7 \cdot 3.7H_2O$ for this C-S-H at 12 percent RH. For a molecule coverage of 10.8 Å/molecule, the 6.7 percent interlayer water is equivalent to $244 \times 2 = 488$ m^2/g of internal area. Adding internal to external area previously calculated made a total area of 561 m^2/g. One gram of hydrated Ca_3SiO_5 paste on the ignited weight basis contains 0.71 g of D-dried C-S-H, giving the expected value of 755×535 m^2. This compares well with the 561 m^2 in the preceding. When only 1 molecule of interlayer water per formula unit is used for the calculation instead of 1.7 molecules, a value of only 357 m^2/g is obtained as the total surface area. (In the formula, x represents the variation that is normally found from Ca-Si ratio of 3 to 2.)

Assuming the composition at 12 percent RH to be $Ca_{3+x}Si_2O_7 \cdot 3.7H_2O$, assuming, as Brunauer, Kantro, and Copeland (4) did, that a unit cell contains a formula unit and that it is orthorhombic with $\underline{a}$ = 5.59 Å and $\underline{b}$ = 3.64 Å, and using a value of 2.34 g/cc

for density, one obtains the value of the average c-spacing of 12.4 Å, as opposed to 11.8 Å for the D-dried C-S-H prepared from C_3S paste at a water-cement ratio of 0.5. This value of 12.4 Å must be regarded as tentative for some assumptions that were in the calculation. The preceding calculation of average c-spacing is still subject to the previously mentioned reservations with regard to homogeneity in spacing and composition.

Another interesting point about hydrated C_3S paste was observed by Helmuth (19). After the paste was D-dried and reexposed to water vapor, the total water content at 12 percent RH was approximately 25.5 percent or 2.9 percent less (on the ignited weight basis) than that found from the desorption branch. When the paste was exposed to increasing humidities as high as approximately 100 percent RH and then returned to 12 percent RH, all the water initially present was regained. This evidence, which is similar to that for portland cement as shown in Figure 1, shows clearly that the interlayer water had completely reentered the sample.

Phenomena Related to Hydraulic Radius of Hydrated Portland Cement

Brunauer, Odler, and Yudenfreund (2) presented the calculations, based on the concept of hydraulic radius, as evidence against the F-S model. Table 1 in the paper by Brunauer, Odler, and Yudenfreund gives the hydraulic radius of the pores not penetrable by nitrogen as being much larger than the diameter of the nitrogen molecule. Faced with the question of why nitrogen cannot enter these pores, Mikhail, Copeland, and Brunauer (28) suggested that these pores have necks smaller than the diameter of the nitrogen molecule. This conclusion was based on the assumption that the interlayer water did not reenter the D-dried sample. Brunauer, Odler and Yudenfreund concluded that the values they derived in column 10 of Table 1 in their paper (2) for the "internal" hydraulic radius are too large to be attributed to water occupying interlayer spaces. This author suggests that in references to interlayer spaces, however, other calculations would have been more appropriate. Because the area of a sheet of C-S-H, according to Brunauer, Kantro, and Copeland (4), is 755 m^2/g, the interlayer area would be 755 S_{N_2} and not $S_{H_2O} - S_{N_2}$ as used by Brunauer, Odler, and Yudenfreund (2). If the figure is corrected for $Ca(OH)_2$ in the hydrated portland cement, the interlayer area per gram would be approximately $600 - S_{N_2}$ and the hydraulic radius should be calculated by the expression $V_{H_2O} - V_{N_2}/600 - S_{N_2}$.

In this calculation the correction for $Ca(OH)_2$ giving the amount of C-S-H gel in hydrated portland cement was due to Powers (27); this was approximately 80 percent of the hydrated cement. No correction was made to 755 m^2/g for the other components because they are considered to be incorporated with the C-S-H gel. However, it is clear that corrections for other components would be minor and would not alter the results significantly. Table 2 gives calculations made according to this mode for hydraulic radius of the pastes cited by Brunauer, Odler, and Yudenfreund (2).

TABLE 2

SURFACES, POROSITIES, AND HYDRAULIC RADII OF PORTLAND CEMENT PASTES

Water-Cement Ratio (1)	S_{N_2} (m^2/g) (2)	$600 - S_{N_2}$ (3)	V_{H_2O} (ml/g) (4)	V_{N_2} (ml/g) (5)	$V_{H_2O} - V_{N_2}$ (ml/g) (6)	r_{ln} Brunauer (Å) (7)	r_{ln} Corrected (Å) (8)
0.35	56.7	543.3	0.1264	0.0748	0.0516	3.4	0.95
0.40	79.4	520.6	0.1776	0.1059	0.0717	5.8	1.38
0.50	97.3	502.7	0.2615	0.1792	0.0823	8.5	1.64
0.57	132.2	467.8	0.3110	0.2493	0.0617	10.0	1.32
0.70	139.5	460.5	0.4008	0.2758	0.1250	20.8	2.78
Montmorillonite	15	735[a]	—	—	0.0964	—	1.26

[a] 750 - 15 = 735.

Column 7 gives the calculations from Table 1 in Bruno, Odler, and Yudenfreund's paper (2) and column 8 gives the suggested corrected values. Also included is a calculation for montomorillonite, a well-known layer-structured clay. The similarity between the average of the first 4 pastes, 1.32 Å, and montmorillonite, 1.26 Å, is very significant. The 0.7 water-cement ratio paste gives a value of 2.78 Å (col. 8) which is much lower than that given in column 7. This author believes, however, that the value in Table 1 (2) $V_{H_2O} - V_{N_2}$ for this paste is much too high. The values of S_{H_2O} and S_{N_2} for water-cement ratios of 0.57 and 0.70 in the same table are almost the same, and there is no trend of $V_{H_2O} - V_{N_2}$ increasing with water-cement ratio. Furthermore, this author has made determinations on 14 different preparations at a water-cement ratio of 0.8 and has found that for these the value for $V_{H_2} - V_{N_2}$ varied between 0.06 and 0.08. Thus, it is thought that the hydraulic radius of the water-cement ratio 0.7 paste would also be similar to that of montmorillonite. The hydraulic radius, then, gives further supporting evidence of the interlayer nature of the so-called gel water.

LENGTH- AND WEIGHT-CHANGE ISOTHERMS

The Question of D-Drying

The writer has now cited considerable evidence to indicate that the D-dried samples do allow water to reenter between the layers. It has been argued (2), however, that the samples discussed in Feldman's recent work (8) were not properly D-dried and that this fact explains his results. The following points should clearly establish that the samples were D-dried.

1. The amount of water removable from a state in equilibrium with a relative humidity of 11 percent was determined by conventional D-drying. It was then found that heating replicate samples at 85 C for 3 hours in a thermal balance under high-vacuum conditions gave an equivalent weight loss. One sample was heated at 95 C for 3 hours and at 97 C for 2 hours more without any major change in the weight loss.
2. The vapor pressure at the "dry" condition was measured with a sensitive Bourdon gage of 1μ repeatability. It indicated a pressure of less than 1μ.
3. Helmuth (19) on measuring isotherms of hydrated C_3S paste dried the samples (in the form of 1-mm thick specimens) for 3 months by conventional means. His results for both sorption and length-change isotherms were qualitatively and quantitatively similar to those of Feldman (8); they showed similar hysteresis, complete regain of interlayer water, and irreversibilities of length and weight change.
4. Brunauer, Odler, and Yudenfreund (2) also argued that the nitrogen areas published by the present writer (8) suggested that his samples were not D-dried. In point of fact, the paste sample hydrated at a water-cement ratio of 0.5 was D-dried by the conventional method for determining surface area by nitrogen adsorption. Then the sample was heated to progressively higher temperatures (up to 400 C) and the area measured at each temperature decreased from 47 to 42 m^2/g. Tomes, Hunt, and Blaine (29), working with pastes that were 50 percent hydrated at a water-cement ratio of 0.5, obtained surface areas by nitrogen adsorption of 10 to 25 m^2/g, a maximum surface area of 50 m^2/g for complete hydration; a value of 97 m^2/g was obtained by Mikhail, Copeland, and Brunauer (28) and republished by Brunauer, Odler, and Yudenfreund (2).

It is not being suggested here that the value of 97 m^2/g is incorrect but rather that nitrogen area can be affected by several factors. These may include water-cement ratio, admixture dosage, and perhaps alkali and sulfate content. This suggests the importance of nitrogen area and of its proper interpretation. With this valuable tool one can detect the sensitivity of hydrated portland cement to various agents and

understand its variability in relation to the mechanical and physical properties of the hydrated cement. Certain trends in properties of hydrated portland cement are functions of water-cement ratio and admixture addition. It is interesting to observe that as water-cement ratio increases the nitrogen area increases, the Ca-Si ratio decreases, and the first drying shrinkage and density increase. Large dosages of some admixtures (e.g., calcium lignosulfonates) enhance the effect of high water-cement ratio. The nitrogen area reflects the change in Ca-Si ratio and predicts differences in first drying-shrinkage properties.

Scanning Loops

Data used in developing the F-S model (1) indicate that interlayer water reenters D-dried samples in increments as the relative humidity they are exposed to increases. When some water reenters the interlayer spaces at, for example, 30 percent RH, it goes on sites that will retain it to a very low RH. Thus, one obtains an irreversibility in the isotherm, a scanning loop (8). This is probably caused by the collapsed layers mechanically blocking the water from entry to high-energy sites; the layers, however, subsequently reopen. One may refer to this as a changing nature of the adsorbent. One of the assumptions made in adsorption equations is that the adsorbent surface remains constant qualitatively and quantitatively. In contrast, the water-scanning isotherms of weight and length change showed that the interlayer water reenters at very low humidities and right through the BET range. Naturally then, any calculation of the monolayer capacity using this isotherm will be incorrect. A similar difficulty occurs in an attempt to calculate the surface area of some montmorillonites from water vapor adsorption.

In addition, above 7 percent RH a quantitative separation of the interlayer and physically adsorbed water was made through interpretation of the scanning isotherms. It was also made clear that, even below 7 percent RH, a considerable portion of the water put on by the sample was interlayer. The use of a trial-and-error procedure or, alternatively, the assumption that the nitrogen area was approximately correct has shown that (a) the Gibbs and Bangham equations (30) properly described the length change and sorption data for physical adsorption; and (b) calculation of Young's modulus of the solid material from the length-change adsorption data yielded a value of 4.35×10^6 lb/in.^{2}, which is very similar to that obtained by direct measurement of E as a function of porosity and extrapolation to zero porosity, 4.5×10^6 lb/in.^{2} The latter work was done by Helmuth and Turk (31) and they concluded that the interlayer spaces are "gel pores." In their extrapolation they considered the porosity to be that obtained by water saturation methods, not recognizing that the water reentered between the layers causing a higher porosity. Soroka and Sereda (32) confirmed the work of Helmuth and Turk and made a similar extrapolation. Verbeck and Helmuth (15) reassessed this work. They then came to the conclusion that gel pores were interlayer spaces, and so their new extrapolation excluded these spaces. Brunauer, Odler, and Yudenfreund (2) refer to the work of Soroka and Sereda (32), state that "Feldman rejects the values of his colleagues," and find an inconsistency in this. Subsequent to the submission of the Soroka and Sereda paper (32), this author (8) found that the total volume of interlayer water derived by calculation from scanning isotherms was approximately equal to the difference between the total volume of water sorbed and the total volume of nitrogen or methanol, as given by the following:

$$V_{(H_2O)} - V_{(N_2 \text{ or methanol})} = V \text{ (interlayer water)}$$

Subsequently, this author obtained helium comparison pycnometry data (21) indicating that helium occupied essentially the same volume as methanol.

When the physically adsorbed water is deducted from the observed adsorption isotherm, one obtains an isotherm showing how the interlayer water reenters as a function of RH. This enabled Feldman and Sereda to propose the model that emphasizes the interrelationship of E, $\Delta w/w$, $\Delta \ell/\ell$, and RH (1).

Reversibility and Equilibration Time

The question of reversibility is always related to that of equilibration time. If weeks were allowed for equilibration, months or years could be suggested if one did not wish to accept the data. In the following paragraphs, data cited by this author (8) are used to counteract this type of argument. In these paragraphs also is a substantiation of the conclusion that there are 2 processes occurring simultaneously. One is essentially in thermodynamic equilibrium with the water-vapor pressure and involves adsorption on the same surfaces on which nitrogen adsorbs. This occurs fairly rapidly and is represented by the scanning loops. The other process involves intercalation of the layers and strong attachment to internal surfaces. The latter process is slow and does not represent a path of thermodynamic equilibrium and is not reversible. At lower humidities (below 50 percent RH), the process, to all practical purposes, ceases at the various RH steps. The system is not in "thermodynamic" equilibrium with the relative vapor pressure at those points.

1. The experimental points were very closely spaced. When the pressure was changed by a small increment, a very rapid increase of weight took place and was followed by a very slow rate. Equilibrium was judged not only by weight change but by pressure change, pressure being measured with a sensitive Bourdon gage with repeatability of 1 μ. A pressure change of less than 10 μ a day was used as the pressure criterion for equilibrium. Below 50 percent RH on the adsorption loop, 2 to 3 days per closely spaced point were adequate to meet this criterion

2. Figure 1 in Feldman's paper (8) shows isotherms and numbered scanning loops. Loops 2, 5, 6, 7, and 8 show clearly how, after desorption on the loop, the readsorption meets the exact point on the main curve where the loop commenced; in the case of loop 7 the complete cycle took $3\frac{1}{2}$ weeks.

3. On the main desorption curve, loops 9 and 10 also return exactly through the point they started from 1 week earlier. If they were so far removed from an equilibrium position, it seems unlikely that they would have rejoined; instead the point would have been well below at the same pressure on the return of the loop.

4. It was found that, in a preliminary experiment on the desorption curve using 7 days per point, there was no change after 1 day of using high-vacuum conditions. The data shown in Figure 1 and given in Table 1 of this paper support this indication; from 100 percent RH to 11 percent RH, no further change was observed beyond the first measurement taken after 2 weeks. Further conditioning of $1\frac{1}{2}$ months at this point produced no further change.

5. It is clear from the length-change data that the 2 types of water separated by scanning loops are completely different and that the $(\Delta \ell/\ell)/(\Delta w/w)$ relationship for the interlayer water is 4 times that for the physically adsorbed water. The length change due to physically adsorbed water is governed by the Gibbs and Bangham equations. When the interlayer water reenters, a considerably larger expansion per unit weight of adsorbed water than that predicted by these equations must be expected. Work in the same paper by Feldman (8), using methanol as adsorbate, shows that there is also interlayer penetration by methanol, although not nearly to the same extent as by water. Contrary to what is generally felt about methanol and length change caused by its sorption on hydrated portland cement, however, the $(\Delta \ell/\ell)/(\Delta w/w)$ is larger for the inter-

layer penetration of methanol than of water. This, of course, is not surprising on the basis of molecular sizes.

6. The isotherms of both length and weight change for water sorption on hydrated portland cement have been measured with great precision and detail (8) in a high-vacuum apparatus using exceedingly sensitive measuring devices. Water isotherms have been previously published by many authors (33, 34, 35) including Powers and Brownyard (36), and recently Helmuth (19), Mikhail, Kamel, and Abo-el-enein (37) with none of them exhibiting closing secondary hysteresis loops (neither does the isotherm shown in Figure 1 of this paper).

The early work of Powers and Brownyard (36) is almost completely devoid of desorption isotherms although this is not generally realized. There are, however, 2 such curves and the following statements are made:

> As shown in Figure 2-6, the adsorption and desorption curves coincided only at pressures below 0.10 p_s. (As a matter of fact, it is not certain that the curves coincided over this range, but it seems probable that they did so. Powers and Brownyard then show (in essence) some scanning isotherms and continue.) Although the phenomenon has not been investigated extensively here, there is little reason to doubt that portland cement pastes all show essentially the behaviour described above. This matter of hysteresis is significant. . . . At any rate the whole phenomenon cannot be understood until these loops can be adequately interpreted. However, practically all the measurements reported in this paper were of adsorption only. Therefore, the interpretation of the adsorption curve is the only part of the problem that can be considered here.

It is now clear that without complete understanding of these loops the adsorption curve could not be interpreted either.

In addition, in the work by Powers and Brownyard, the point at approximately 10 percent RH on first drying was reattained after further drying and a subsequent cycle of wetting and redrying to the above humidity. This means that all the water, including the interlayer water that had been removed, reentered during rewetting.

Helmuth (19) D-dried from low humidities continually for 3 months and, in his work as stated previously, all the interlayer water also returned. This, it must be reemphasized, is a crucial point as has been pointed out by others (2).

Helmuth's results (19) on C_3S paste contain a further interesting point. The desorption isotherm appeared to rejoin in the primary hysteresis region at high humidities, but as desorption continued there reappeared a very large secondary hysteresis equal in magnitude to that of this author's at the lower humidities. The preceding behavior is probably related to the primary hysteresis and may involve recrystallization of $Ca(OH)_2$ and a changing of the pore size, shape, and distribution. This might explain the unpublished work of J. Hagymassy referred to by Brunauer, Odler, and Yudenfreund (2).

Mikhail, Kamel, and Abo-el-enein (37) have recently published water isotherms on various cement hydration products. In every case large hysteresis loops were obtained without any closure. Mikhail, Kamel, and Abo-el-enein found that only 48 hours were necessary between successive measurements. On samples prepared in paste form, Mikhail states that 12 days should be allowed between measurements. The experimental points, however, are spaced quite far apart, e.g., from 15 to 35 percent RH. He also states, "Desorption was then carried down to extremely low relative pressures. The sample was then exposed to out-gassing at 30° C for a period of 30 hours, to remove all the adsorbate and the sample weight was brought back to its original value."

7. Numerous data have been compiled by this author since the International Symposium work (8). The data were obtained after allowing much longer times for equilibrium (in the order of months) in both high-vacuum apparatus and in desiccators and by using the same samples. Some of the data are shown in Figure 1 and given in Table 1. They have confirmed the existence of scanning loops, the equilibrium of sorption points, and the complete reentry of interlayer water after very severe drying and after a cycle of rewetting and drying to 11 percent RH.

8. The accepted method for D-drying has been worked out and published by Copeland and Hayes (38) who state that it takes 4 to 7 days for equilibrium. This involves drying from fairly wet conditions to removal of both the tightly held first layer and the even more tightly held interlayer water from the very narrow spaces. The slower-than-normal times required for equilibrium of water during the adsorption stage is probably due to the lengthy process of reopening the layers.

NEW EXPERIMENTAL EVIDENCE

Recently this author has done an entirely new type of work (20, 21, 22) that not only provides further evidence for the F-S model but also provides powerful new techniques to study hydrated cement. A few of the results will be briefly discussed·

1. When water is removed from C-S-H materials, the prime concern is what happens to the spaces vacated by the water and what happens to the solid. A method of studying the spacing is to measure rates of diffusion of helium gas (a small atom) into them (20). When hydrated portland cement equilibrated for several months at 11 percent RH was exposed to helium, helium very quickly entered the pores of even 20 Å radius. When the gas was compressed to 2 atmospheres, rate curves could be measured for helium diffusing into the vacated spaces. As water was removed incrementally from the sample, the diffusion rate and absolute quantity at each water content increased at first; but as more water was removed, the rate decreased although the quantity continued to increase. Finally, the quantity also decreased, and at D-dry conditions the diffusion rate was very low. These results can best be explained by the collapse of layers in the same manner as the F-S model has suggested (1). On readsorption of water, the helium diffusion rate again increased. After the sample was exposed to high humidities, all the interlayer water had reentered (diffusion experiments were performed at 11 percent RH), and the rate curves were similar to the curves obtained for the sample at the beginning of the experiment. These results indicate that the layers had reopened and that interlayer water had reentered; if it had not, the very low diffusion rate observed at the D-dry condition would have remained the same.

2. Density measurements (21) obtained by a helium penetration technique from hydrated portland cement prepared at water-cement ratios of 0.4 to 1.0 showed that the computed densities of C-S-H gel vary with water-cement ratio from approximately 2.30 to 2.18 g/cm^3. For water-cement ratios of less than 0.6, the density decreased with decreasing water-cement ratio. Because Ca-Si ratio and nitrogen surface area vary with water-cement ratio, one might reasonably expect changes in density and degree of collapse.

3. Measurement of solid volume and length simultaneously as a function of water content on drying to the D-dried position and on rewetting has enabled an independent calculation of the monolayer capacity for water to be made. On the assumption that

$$\Delta V/V - 3\Delta \ell/\ell = \Delta w/V$$

where

$\Delta V/V$ = relative change in volume of solid phase plus adsorbed phase,
$\Delta \ell/\ell$ = external length change,
Δw = change in volume of adsorbed water, and
V = volume of solid,

it was found that the results for D-dried samples yield a surface area varying only by about 15 percent from the result obtained by nitrogen adsorption. Results also suggested that first D-drying reduces the surface area of the hydrated portland cement.

This last group of experiments (20, 21) presents evidence different, and perhaps in a superior form, from that obtained from conventional isotherms. The latter experiments indicate how much water entered or left the specimen; but in these new experiments, as in length change studies, information is gained also about the effect of the removal of the water on the solid body. Thus, it is possible to draw conclusions as to where the water was likely to have come from, the nature of the spaces it occupied, and its role in the structure of the solid.

4. Thermal analysis both DTA and TGA (22) were performed on samples equilibrated at a relative humidity for lengths of time, in the order of months in desiccators, and at relative humidities similar to those reported here for the isotherms. It was found that interlayer water and its reentry could be correlated to an endothermic effect at 90 to 105 C, and the physically adsorbed water to an effect at 65 to 80 C. The results confirmed the fact that 11 percent RH was a nonunique state and also confirmed the conclusions in the previous section concerning scanning loops, equilibration, and hysteresis.

ACKNOWLEDGMENT

The author wishes to acknowledge the valuable discussions had with V. S. Ramachandran and P. J. Sereda, and the experimental work done by S. Dods. This paper is a contribution of the Division of Building Research, National Research Council of Canada, and is published with the approval of the Director of the Division.

REFERENCES

1. Feldman, R. F., and Sereda, P. J. A Model for Hydrated Portland Cement as Deduced From Sorption-Length Change and Mechanical Properties. Matériaux et Constructions, Vol. 1, No. 6, 1968, pp. 509-520.
2. Brunauer, S., Odler, I., and Yudenfreund, M. The New Model of Hardened Portland Cement Paste. Highway Research Record 328, 1970, pp. 89-107.
3. Feldman, R. F., and Sereda, P. J. Discussion of The New Model of Hardened Portland Cement Paste. Highway Research Record 328, 1970, pp. 101-103.
4. Brunauer, S., Kantro, D. L., and Copeland, L. E. The Stoichiometry of the Hydration of β-Dicalcium Silicate and Tricalcium Silicate at Room Temperature. Jour. of Amer. Chem. Soc., Vol. 80, No. 4, 1958, pp. 761-767.
5. Kalousek, G. L. Fundamental Factors in the Drying Shrinkage of Cement Block. ACI Jour. Proc., Vol. 26, 1954, pp. 233-248.
6. Brunauer, S., Copeland, L. E., and Bragg, R. H. The Stoichiometry of the Hydration of Tricalcium Silicate at Room Temperature: Part 2, Hydration in Paste Form. Jour. of Phys. Chem., Vol. 60, 1956, pp. 116-120.
7. Feldman, R. F., and Sereda, P. J. Sorption of Water on Bottle-Hydrated Cement. Jour. Appl. Chem., Vol. 14, 1964, pp. 87-93.

8. Feldman, R. F. Sorption and Length Change Scanning Isotherms of Methanol and Water on Hydrated Portland Cement. Fifth Internat. Symp. on Chemistry of Cement, Tokyo, 1968.
9. Sereda, P. J., Feldman, R. F., and Swenson, E. G. Effect of Sorbed Water on Some Mechanical Properties of Hydrated Portland Cement Pastes and Compacts. HRB Spec. Rept. 90, 1966, pp. 58-73.
10. Taylor, H. F. W. The Calcium Silicate Hydrates. Fifth Internat. Symp. on Chemistry of Cement, Tokyo, 1968.
11. Locher, F. W. The Chemical Reactions of the Hardening of Cement. Zement-Kalk-Gips, Vol. 17, No. 5, 1964, pp. 175-182.
12. Kurczyk, H. G., and Schwiete, H. E. Electron-Microscopic and Thermochemical Investigations on the Hydration of Calcium Silicates, C_3S and β-C_2S and the Effects of $CaCl_2$ and Gypsum on the Process of Hydration. Tonind-Zeitung, Vol. 84, 1960, pp. 585-598.
13. Kantro, D. L., Brunauer, S., and Weise, C. H. Development of Surface in the Hydration of Calcium Silicates. In Solid Surfaces and the Gas Solid Interface, Advances in Chemistry Series, No. 33, Am. Chem. Soc., 1961, pp. 199-219.
14. Seligmann, P. Nuclear Magnetic Resonance Studies of the Water in Hardened Cement Paste. Jour. of PCA Res. and Dev. Laboratories, Vol. 10, No. 1, 1968, pp. 52-65.
15. Verbeck, G. L., and Helmuth, R. A. Structures and Physical Properties of Cement Pastes. Fifth Internat. Symp. on Chemistry of Cement, Tokyo, 1968.
16. Brunauer, S., Kantro, D. L., and Weise, C. H. The Surface Energy of Tobermorite. Canadian Jour. of Chem., Vol. 37, 1959, pp. 714-742.
17. Lentz, C. W. The Silicate Structure Analysis of Hydrated Portland Cement Paste. HRB Spec. Rept. 90, 1966, pp. 269-283.
18. Kantro, D. L., Weise, C. H., and Brunauer, S. Paste Hydration of Beta-Dicalcium Silicate, Tricalcium Silicate, and Alite. HRB Spec. Rept. 90, 1966, pp. 309-327.
19. Helmuth, P. A. Chicago Inst. of Technology, 1965. MSc thesis.
20. Feldman, R. F. The Flow of Helium into the Interlayer Spaces of Hydrated Portland Cement. Cement and Concrete Research, Vol. 1, No. 3, May 1971, pp. 285-300.
21. Feldman, R. F. Density and Porosity Studies of Hydrated Portland Cement. Unpublished paper.
22. Feldman, R. F., and Ramachandran, V. S. Differentiation of Interlayer and Adsorbed Water in Hydrated Portland Cement by Thermal Analysis. Unpublished paper.
23. Taylor, H. F. W. Relationships Between Calcium Silicates and Clay Minerals. Clay Minerals Bull., Oxford, Vol. 3, 1965, pp. 98-111.
24. Howison, J. W., and Taylor, H. F. W. A Method for the Calculation of the Specific Gravities of Calcium Silicates From Their Refractive Indices. Mag. of Concrete Res., London, Vol. 9, 1957, pp. 13-16.
25. Megaw, H. D., and Kelsey, C. H. The Crystal Sequence of Tobermorite. Nature, London, Vol. 177, 1956, pp. 390-391.
26. Van Olphen, H. Thermodynamics of Interlayer Adsorption of Water in Clays: Part 1, Sodium Vermiculite. Jour. of Colloid Sci., Vol. 20, 1965, pp. 822-837.
27. Powers, T. C. The Chemistry of Cements. Academic Press, New York, 1964. Ch. 10.
28. Mikhail, R. S., Copeland, L. E., and Brunauer, S. Pore Structures and Surface Areas of Hardened Portland Cement Pastes by Nitrogen Adsorption. Canadian Jour. of Chem., Vol. 42, 1964, pp. 426-438.

29. Tomes, L. A., Hunt, C. M., and Blaine, R. L. Some Factors Affecting the Surface Area of Hydrated Portland Cement as Determined by Water-Vapor and Nitrogen Adsorption. Jour. of Res., National Bureau of Standards, Vol. 59, No. 6, 1957, pp. 357-364.
30. Sereda, P. J., and Feldman, R. F. Mechanical Properties and the Solid Gas Interface. In The Solid Gas Interface (Flood, E. A., ed.), Vol. 2, Marcel Dekker Inc., New York, 1967, pp. 729-764.
31. Helmuth, R. A., and Turk, D. H. Elastic Moduli of Hardened Portland Cement and Tricalcium Silicate Pastes: Effect of Porosity. HRB Spec. Rept. 90, 1966, pp. 135-144.
32. Soroka, I., and Sereda, P. J. The Structure of Cement-Stone and the Use of Compacts as Structural Models. Fifth Internat. Symp. on Chemistry of Cement, Tokyo, 1968.
33. Krasil'nikov, K. G. Calculation of the Specific Surface of Tobermorite From Its Crystal Lattice Parameters and Adsorption Data. Doklady Akademii Nauk SSSR, Vol. 149, 1963, pp. 891-893.
34. Luk'yanova, O. I., and Rebinder, P. A. Properties of Tobermorite-like Hydrosilicates as a Variable Composition Phase. Doklady Akademii Nauk SSSR, Vol. 184, 1969, pp. 1144-1147.
35. Pihlajavaara, S. E. Some Results of the Effect of Carbonation on the Porosity and Pore Size Distribution of Cement Paste. Rheological Acta, West Germany, Vol. 7, 1968, pp. 397-400.
36. Powers, T. C., and Brownyard, T. L. Physical Properties of Hardened Portland Cement Paste: Part 2, Studies of Water Fixation. ACI Jour. Proc., Vol. 43, 1947, p. 276.
37. Mikhail, R. S., Kamel, A. M., and Abo-el-enein, S. A. Surface Properties of Cement Hydration Products: Part 1, Pore Structure of Calcium Silicate Hydrates Prepared in a Suspension Form. Jour. of Appl. Chem., Vol. 19, 1969, pp. 324-328.
38. Copeland, L. E., and Hayes, J. C. The Determination of Nonevaporable Water in Hardened Portland Cement Paste. ASTM Bull. 194, 1953.

PREDICTION OF POTENTIAL STRENGTH OF CONCRETE FROM THE RESULTS OF EARLY TESTS

S. B. Hudson, Materials Research and Development, Inc., Raleigh, North Carolina; and G. W. Steele, West Virginia Department of Highways

A series of 3 designed experiments was conducted to investigate the practicality of using early tests of concrete cylinders made at the job site as a means of quality control of concrete. The scope of the experiments included concrete of 3 cement constants, 3 brands of cement, and 4 methods of conditioning specimens prior to test. The test results, when analyzed by statistical methods, indicate a definite linear relationship between the logarithm of the maturity of the concrete in degree-hours and the relative compressive strength. When specimens were tested at spaced values of maturity, an equation capable of predicting the 28-day strength of concrete to within about 500 psi was derived. Predicted results are suitable for constructing one-sided confidence limits for quality control purposes. It was found practical to construct a nomograph to expedite the computation of predicted values. A limited amount of simulation was conducted on 8 sets of test cylinders made at the job site and tested at 23 to 42 hours of age. The average difference between the predicted 28-day strengths and the routine 28-day test results was about 300 psi. Practical application of this method requires that a definite early test procedure be established and that equation constants for commonly used concrete mixtures be established by experiment using this procedure. Predicted results from early tests on cylinders made at the job site can then be used for quality control purposes and to provide prompt warning of the production of concrete of unacceptable strength.

•IT IS EVIDENT that effective quality control of concrete requires some means of assessing the potential strength of concrete within several hours of manufacture instead of 4 weeks. The 28-day test is really only a measure of potential strength and, by the time the results are available, they are useful only for historical records. Even 14- and 7-day tests are not satisfactory for quality control purposes because, with current rates of production, large quantities of concrete can be placed and other large amounts superimposed before an indication can be obtained that corrective measures are necessary.

Since the 1930's, a great deal of work has been done in this area in the United States and in other countries. A report by the Ontario Department of Highways (1) lists 87 references relating to methods for use in estimating the later strength of concrete from early test results. Currently, Subcommittee 11-i of ASTM Committee C-9 is writing procedures for estimating potential strength at significantly early times. However, none of these procedures or methods has come into general use in connection with highway construction in this country.

In view of the critical need for an expedient means of detecting concrete of inferior quality, the Materials Control, Soils and Testing Division of the West Virginia Department of Highways conducted a series of designed experiments to investigate the

Sponsored by Committee on Mechanical Properties of Concrete and presented at the 50th Annual Meeting.

possibility of obtaining reliable estimates of the potential strength of concrete from the results of early tests. These results were analyzed by statistical methods, and the equations that have been developed indicate a high probability of success with respect to the ability to classify the quality of concrete at very early ages.

OBJECTIVES

The objectives of the work described here were to evaluate alternate methods of preparing concrete specimens for early tests, to determine the effects of various factors on the relationship between early and potential strength of concrete, and to develop reliable means of predicting minimum potential strength from the results of tests on concrete cylinders made at the job site or laboratory and cured over a range of times and conditions.

RESEARCH APPROACH

A review of the literature indicated that most previous approaches to the problem of relating the strength of concrete at an early age to that at 28-days contained restrictions that should be eliminated or modified, if possible. Procedures required that the early tests be made at fixed times after the forming of the specimens so that they were not very adaptable to conditions associated with highway construction, where there may be differences in early curing temperatures and variations in the time required to transfer specimens from the job site to the location of the testing equipment. The methods of preparing specimens for test were sometimes inconvenient or required extensive equipment. Finally, the mathematical equations that had been previously used did not appear to be suitable for prediction of potential strengths of specimens formed at the job site, and the degree of confidence that could be placed in the prediction under these conditions was unknown.

However, in view of the normal variation in 28-day tests of concrete made and cured under standard conditions and knowledge that, for quality control purposes, all that is required is a prediction of minimum potential strength with an acceptable degree of confidence, it was believed that a satisfactory method could be developed that could be used in evaluating concrete quality at early ages and that would be comparable in significance with 28-day tests.

Designed Experiments

The designed experiments set up for the purposes of obtaining data required for deriving the desired relationships included making and testing 3 series of specimens. All experiments were so designed that test specimens from the same batch were tested at spaced intervals. These equal increments of maturity form the basis to this approach for determining the line of prediction.

Series 1—The purpose of series 1 was to investigate the effect of variation of cement content over a practical range. It consisted of 3 groups of 30 cylinders each with groups made with 4.00, 5.50, and 7.25 bags/cu yd of the same brand of cement.

The order of making the batches was arranged to be pseudo-random so that no consistent pattern of batching occurred. In each batch, duplicate cylinders were designated for testing at the same degree of maturity for the purpose of estimating testing error under the conditions of the experiment. Brand M cement was used in all batches with Ohio River sand and gravel. Air-econ admixture was used to obtain the desired air content. The 2.7 cu ft batches were mixed in a Müller 6-S (6 cu ft) mixer in general accordance with ASTM Method C 192 (Standard Method of Making and Curing Concrete Test Specimens in the Laboratory).

After it was mixed, the concrete from all batches was tested for slump and air content. Concrete used for these purposes was discarded. Cylinders for test purposes were made by the "group" method in the curing chamber and were not disturbed for 24 hours.

At the end of the curing period, the cylinders for early test were stripped and placed in a water bath consisting of half a 55-gal oil drum filled with water. Heat was supplied

by a thermostatically controlled Chromalox electric immersion unit. The bath was agitated with compressed air. The temperature of the bath was maintained at approximately 200 F for the 3½-hour conditioning of the 6 to 7 cylinders placed in the bath at 1 time. The cylinders were placed and removed from the bath by the use of a specially designed tool to avoid accidental injury to the test specimens or to personnel.

At the end of the conditioning period, the cylinders were removed from the bath and allowed to cool in air for 45 min. They were then capped with a commercial sulfur composition capping compound that was allowed to harden before the cylinders were tested in compression.

Comparison cylinders for the 28-day tests were cured and prepared for test in the routine manner. All cylinders were tested in compression by the use of a 450,000-lb Baldwin machine. The test results are shown in Figure 1.

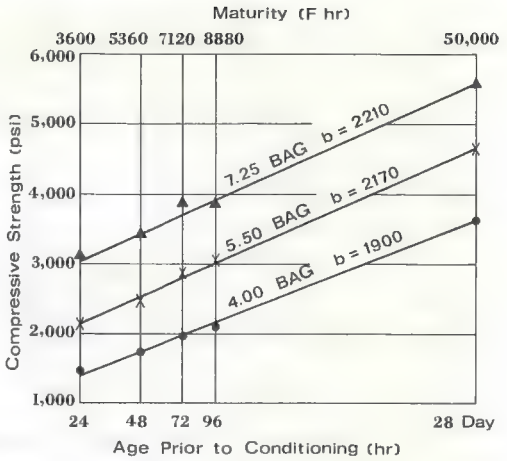

Figure 1. Series 1—relationship of early to 28-day strength.

The lines of relationship shown in Figure 1, computed by the use of Eq. 3, are essentially parallel and indicate an increase in strength of about 2,500 psi over the range of maturity covered. The percentage increase in strength is from about 40 percent to about 55 percent depending on the level of the 28-day test results.

Series 2—Series 2 also consisted of 3 groups of 30 cylinders each. Each group was made with a different brand of cement in common use in West Virginia, but all groups were made with 6.00 bags/cu yd of cement. The purpose was to determine the effect of cement source on strength relationships. Curing, conditioning, and testing of the test specimens were identical to the procedures of series 1. The results of the tests are shown in Figures 2 and 3.

The lines of relationship were computed in the same way as those shown in Figure 1, and they indicate that there is some difference in the level of 28-day results and in the rate of gain of strength when different brands of cement are used under identical

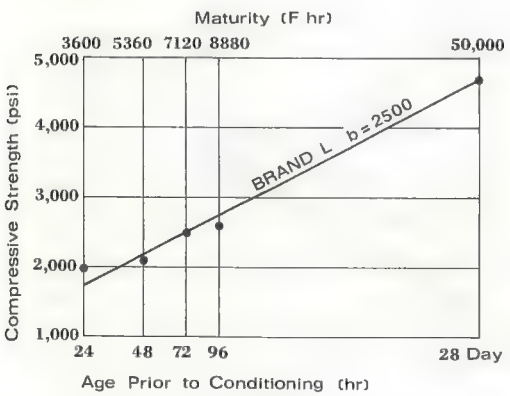

Figure 2. Series 2—relationship of early to 28-day strength.

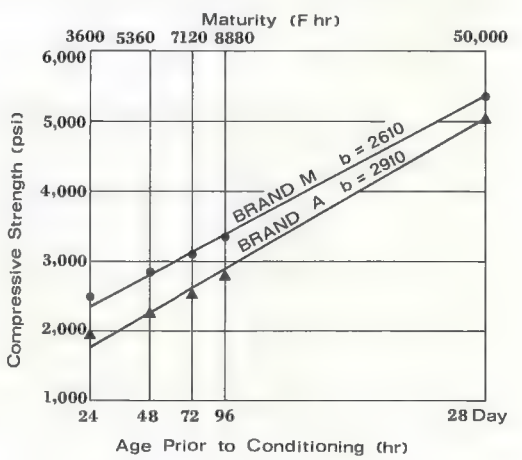

Figure 3. Series 2—relationship of early to 28-day strength.

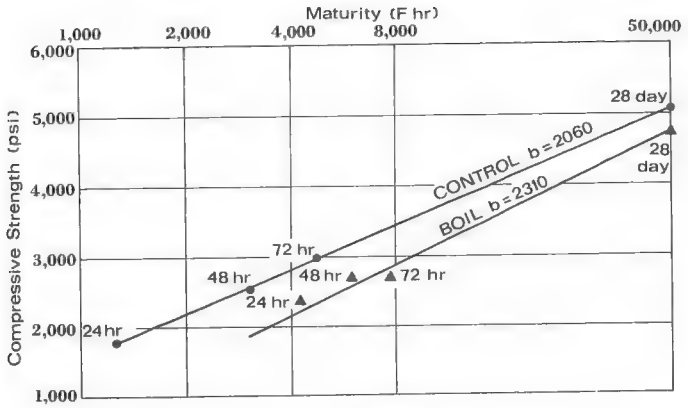

Figure 4. Series 3—relationship of early to 28-day strength.

conditions. The lines are essentially parallel and indicate an increase in strength of about 3,000 psi over the range of maturity covered. The percentage increase in strength is from about 34 percent to about 43 percent but is not directly related to the level of the 28-day test results shown in Figures 2 and 3.

Series 3—The primary purpose of series 3 was to investigate the effect of different methods of preparation for early test on strength relationships. The effect of conditioning 28-day cylinders immediately prior to test was also investigated. This series included 4 groups of 30 cylinders each. Each group was made with 6.00 bags/cu yd of the same brand of cement.

Test results are shown in Figures 4 and 5. Early test cylinders designated as "autoclave" were conditioned, after normal curing, by being heated in a pressure cooker maintained at 15 psi for a period of 3 hours. The temperature of the water in the cooker at time of immersion of the cylinders was about 100 F and the maximum temperature was probably about 245 F. Early test cylinders designated as "boil" were conditioned after normal curing by a $3\frac{1}{2}$-hour immersion in a 200 F water bath. This is the same procedure as used for series 1 and 2. Cylinders designated as "control" were tested after normal curing. No heating or other conditioning was applied to these specimens. Early test cylinders designated as "oven" were conditioned after normal curing by heating in a convection oven for 6 hours. The temperature of the test

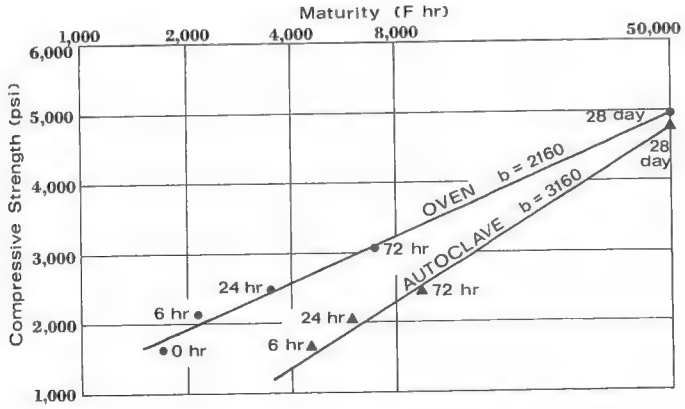

Figure 5. Series 3—relationship of early to 28-day strength.

cylinders was determined by measurements on a dummy cylinder. The temperature varied from about 76 F at the start of heating to 199 F for the last hour with an average of about 175 F. The 28-day boil cylinders were heated for $3\frac{1}{2}$ hours in the 200 F bath at the end of the normal curing for 28 days. All of the heated cylinders were allowed to cool for a period of 45 to 60 min, were capped with sulfur composition caps, and were tested about 30 min after the end of the cooling period. Interior temperature of the concrete at time of test was about 130 F.

The lines of relationship shown in Figures 4 and 5 were computed by the use of Eq. 3, and C-values were determined by iterative graphical methods as described in the Appendix. The lines shown in Figure 4 for the control cylinders and for the boiled cylinders that were conditioned the same as those for series 1 and 2 are essentially comparable and the previous remarks apply. The oven-conditioned cylinders (Fig. 5) also show a relationship comparable to the previous series. However, the cylinders conditioned under pressure in the autoclave appear to have a significantly different rate of gain of strength, as could be expected from the experience of prior investigators (2).

Mathematical Analysis

Several methods of deriving an equation that would predict 28-day strength from the results of early tests were applied to the experimental data, and the results were evaluated. The criterion was the size of the standard deviation of the differences exposed by comparing the value predicted from each early test result with the corresponding 28-day test on a cylinder from the same batch.

Many prior investigators have attempted to develop a factor by which to multiply early results to estimate 28-day results. Others have derived equations in which early results are expressed as a percentage of strengths at later ages. These approaches were investigated but, when applied to the experimental data, the results were not of acceptable accuracy.

The maturity concept advocated by Plowman (3) and others was next investigated. It was found that a reasonably close fit to a straight line was obtained when compressive strength in pounds per square inch (psi) was plotted against maturity in degree-hours on semilog graph paper. This indicated that an equation of the general form $Y = a + bX$, where the slope b of the regression line is found by the method of least squares, could be fitted to the data. Accordingly, the experimental data were first analyzed by fitting the equation

$$S_M = b (\log m) - a \qquad (1)$$

to the data. In this equation,

S_M = predicted compressive strength in psi,
m = maturity in degree-hours at time of test,
b = regression coefficient (slope of line), and
a = a constant.

Parameters for Eq. 1 were computed by machine calculation and computer printout, and a good fit was obtained. However, when the exposures were calculated, it was found that Eq. 1 was not entirely satisfactory with respect to accuracy of prediction.

It seemed that accuracy could be improved by projecting the prediction line from the result of each early test rather than from the intercept a, which is a fixed point. This resulted in Eq. 2 as follows:

$$S_M \approx S_m + b (\log M - \log m) \qquad (2)$$

where

S_M = predicted normal compressive strength (psi) at maturity M;
S_m = measured compressive strength at maturity m;
M = degree-hours of maturity under standard conditions (i.e., when cured at 73.4 F);
m = degree-hours of maturity of specimen at time of early test after conditioning [(hours of age × ambient temperature) + C];

C = degree-hours of maturity determined by autogenous heating, method of preparation or conditioning, residual temperature at time of test, and possible unknown factors; and
b = slope of prediction line.

In this case, the value of b was found by the ratio of the averages, sometimes called the method of zero sum, as follows:

$$b = \frac{\Sigma (S_M - S_m)}{\Sigma (\log M - \log m)} \tag{3}$$

Because, in general, the standard deviation is proportional to the compressive strengths, it is theoretically possible to obtain a better value of b from the average of individual ratios. However, on trial, no large difference was observed, so the zero sum method was used as a matter of convenience.

For series 1 and 2, a pooled value for C of 1,840 degree-hours was used. The value of the maturity m was then the number of hours of age at 73.4 F × 73.4 + 1,840. The regression coefficients and related prediction error terms are given in Table 1.

Because the mean of the differences between predicted and actual values of compressive strengths was zero (or very nearly so), the error standard deviation was computed by the use of the equation

$$\sigma_e = \sqrt{\frac{\Sigma (S_M - S_{28})^2}{2\eta}} \tag{4}$$

This error term can be used to construct a one-sided confidence interval for the predicted value. For example, if

$$S_M - 1.645\ \sigma_e > L \tag{5}$$

there is a 95 percent probability that the true average strength is greater than the designated lower limit L.

Comparisons of predicted and measured values were made by substitution in Eq. 2, as shown in the following example:

$$\begin{aligned} S_M &\approx S_m + b\ (\log M - \log m) \\ &\approx 1{,}540 + 1{,}900\ (4.699 - 3.556) \\ &\approx 1{,}540 + 1{,}900\ (1.143) \\ &\approx 1{,}540 + 2{,}170 \\ &\approx 3{,}710 \text{ psi} \\ S_{28} &= \underline{3{,}790 \text{ psi}} \\ \text{Difference} &= -80 \text{ psi} \end{aligned}$$

An estimate of the maximum error to be expected over a wide range of conditions was obtained by using the pooled values of 2,410 for b and 1,840 for C to compute the exposure of the differences between predicted and measured strengths for all of the series 1 and 2 results. The results in histogram form are shown in Figure 6. This analysis indicates that, over the range of cement constants and cement brands covered in the 2 series, there is a 95 percent probability that the strength predicted from the results of early tests on specimens conditioned for 3½ hours in the 200 F water bath will not exceed corresponding, measured 28-day strengths by more than 800 psi.

TABLE 1

RESULTS OF COMPUTATIONS FOR SERIES 1, 2, AND 3

Series	Batch	Value of Slope b	Degree-Hours of Maturity C	Prediction Error σ_e, psi
1	4.00 bag	1,900	1,840	162
	5.50 bag	2,170	1,840	317
	7.25 bag	2,210	1,840	282
2	Brand M	2,610	1,840	128
	Brand A	2,910	1,840	185
	Brand L	2,550	1,840	392
3	Oven	2,160	1,740	201
	Autoclave	3,160	4,200	142
	Boil	2,310	2,480	292
	Control	2,060	-500	190

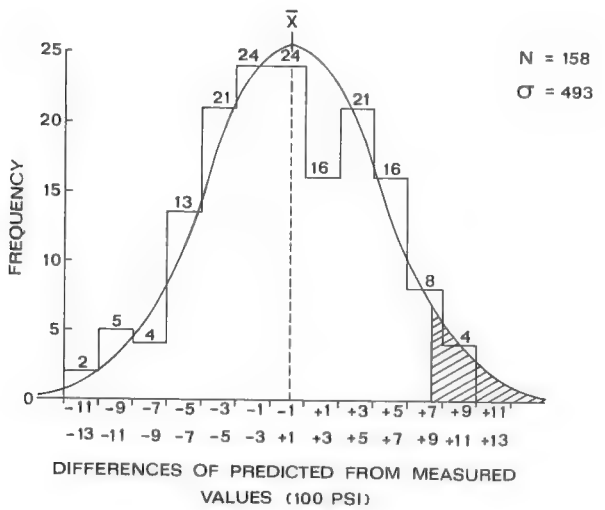

Figure 6. Frequency distribution of differences of predicted value from measured value (28-day concrete compressive strength).

DISCUSSION OF RESULTS

The excellent fit of Eq. 1 to the data confirms the original mathematical assumptions and indicates that, for a specific set of conditions, reasonably accurate predictions of potential strength can be made from the results of early tests of concrete. The accuracy of these predictions is limited by the size of the standard deviation (or coefficient of variation) normally found among 28-day tests.

For general application, over a range of cement constants and brands of cement, accuracy is considerably reduced because these factors influence the slope b of the prediction line. However, use of Eq. 2 should provide sufficient accuracy for a quality control test where the objective is to ensure a minimum potential strength rather than to predict an exact value. This can be accomplished by applying a one-sided confidence interval to the predicted value. For example, if $S_M - 1.645\,\sigma_e > L$ (Eq. 5), there is a 95 percent probability that the true average strength is greater than the designated lower limit L.

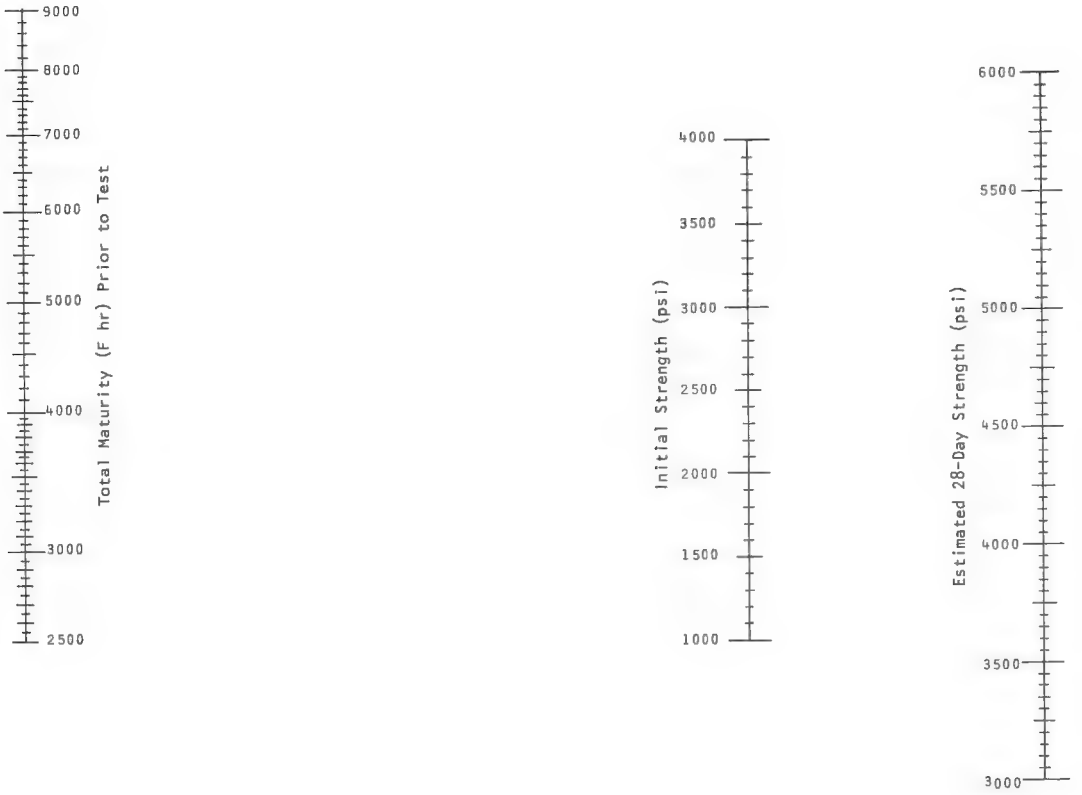

Figure 7. Nomograph for estimating potential 28-day strength from early tests (normal curing).

The necessity of using logarithms may appear to be a disadvantage, but this is easily overcome by the use of a nomograph. A trial nomograph, as shown in Figure 7, has been constructed and found to be practical. A finalized version can be produced after further simulation and acceptance of the philosophy associated with Eq. 5.

CONCLUSIONS

Within the range of the conditions included in the experiment, all test results indicate that a linear relationship exists between the logarithms of the maturity in degree-hours of concrete and the relative compressive strength. This relationship is accurately expressed by Eq. 2, provided that proper values of the constants b and C are used. Reliable values of b and C for a particular combination of conditions can be determined by designed experiment wherein early tests of the concrete are made at uniformly spaced intervals of maturity. Trial values of b and C can be obtained by graphical methods as shown in the Appendix. Final values of b are best obtained by the method of zero sum.

For the purpose of determining potential strength of concrete 24 hours or more of age, prior conditioning does not appear to be necessary. Where results are required at earlier ages, conditioning with either a convection oven or with an autoclave appear to be about equally satisfactory. However, it is advisable to allow concrete to reach the state of final set before conditioning.

When values of b and C have been determined for a particular set of conditions, the potential 28-day strength of concrete can be predicted by the use of Eq. 2 to within about 500 psi 19 times out of 20.

Computations of predicted strengths can be expedited by use of a nomograph that can be easily constructed for any particular value of b.

ACKNOWLEDGMENT

The opinions, findings, and conclusions expressed in this paper are those of the authors and not necessarily those of the West Virginia Department of Highways or of the Federal Highway Administration.

REFERENCES

1. Smith, P., and Tiede, H. Earlier Determination of Concrete Strength Potential. Highway Research Record 210, 1967, pp. 29-66.
2. Budnikov, P. P., and Erschler, E. Y. Studies of the Process of Cement Hardening in the Course of Low-Pressure Steam Curing of Concrete. HRB Spec. Rept. 90, 1966, pp. 431-446.
3. Plowman, J. M. Maturity and Strength of Concrete. Mag. of Concrete Research, London, Vol. 8, No. 22, 1956, pp. 13-22.

APPENDIX

PROCEDURE FOR ESTABLISHING AN EQUATION FOR PREDICTING POTENTIAL STRENGTH FROM EARLY TESTS ON CONCRETE CYLINDERS

1. Prepare laboratory batches large enough to make 6 test cylinders of a design mix to which equation will apply. Repeat on 5 different days. To minimize variation, make cylinders in place where they can remain undisturbed for 24 hours at 73 F ± 3 F.
2. At the end of 24 hours, test 1 cylinder from each batch with or without conditioning such as 3-hour immersion in 200 F bath or 200 F oven. Place remaining cylinders under standard moist cure at 73.4 F ± 3 F.
3. Test 1 cylinder from each batch at end of 48, 72, and 96 hours with or without conditioning, as tested for 24-hour cylinder. Test 2 cylinders for 28-days without conditioning.
4. Average test results ($\bar{X}_s$) for each age.
5. Prepare a sheet of semilog graph paper, 2 cycles by 70 divisions (K and E 46-4970, or similar) by numbering 1-in. divisions in thousands of psi and letting the log scale represent maturity m in thousands of degree-hours at time of test.
6. Draw horizontal lines across graph from psi scale for each average strength. Plot point for 28-day psi at 50,000 degree-hours of maturity.
7. Points for each strength should lie on their respective lines in positions such that a straight line from the 28-day strength point will pass through or near all the early strength points. Because both the slope of the line and the maturity values of the points are unknown, the equation must be found graphically by trial and error. It is known that the maturity values of the points will be 1,760 degree-hours (24 × 73.4 F) apart. Then each point will have a maturity value of some multiple of 1,760 plus some value C determined by conditioning (if any), autogenous heating, and unknown factors. The iterative method of finding the line of prediction is shown in Figure 8. The synthetic data on which the graph is based is given in Table 2. Figure 8 shows that the first series of points, ●, have too flat a slope to intersect the 28-day point. The second trial, X, points have too steep a slope. The third trial, ▲, provides points falling very closely on the line projected to the 28-day point, so the best value of C is 1,240.
8. The slope of b of this line is the vertical scale distance between the intercept on the 10,000 m-line and the intercept on the 100,000 m-line or about 2,850 in the case of the example.
9. The general form of the prediction equation (Eq. 2) is

$$S_M \approx S_m + b\,(\log M - \log m) \qquad (2)$$

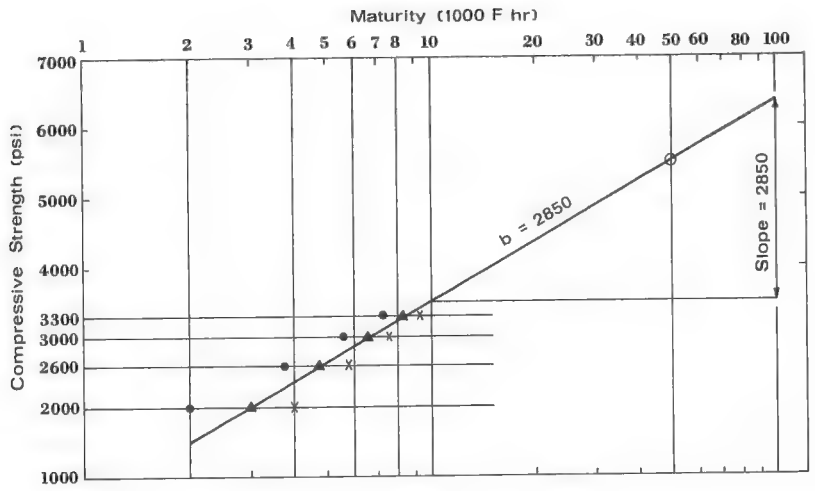

Figure 8. Determining line of prediction.

10. In the case of the example, the potential 28-day strength projected from the 24-hour test would be

$$S_{28} = 2{,}000 + 2{,}850\ (4.699 - 3.477)$$
$$= 2{,}000 + 2{,}850\ (1.222)$$
$$= 5{,}480 \text{ psi}$$

11. The graphical method described in the preceding provides an approximate prediction equation for averages of groups of compressive test results. A better estimate of the value of slope b can be obtained by the method of zero sum using the following equation:

$$b = \frac{\Sigma (S_M - S_m)}{\Sigma (\log M - \log m)} \tag{3}$$

When this method is used, the difference between each early test result and the corresponding 28-day tests on cylinders from the same batch are noted along with the matching difference in the logarithms of the maturities. The total of the differences in compressive strengths is then divided by the total of the difference in the logarithms of the maturities.

TABLE 2
SYNTHETIC DATA FOR FIGURE 8

Age (hour)	S_c (psi)	m′	m = m′ + C		
			C = 240	C = 2,240	C = 1,240
24	2,000	1,760	2,000	4,000	3,000
48	2,600	3,520	3,760	5,760	4,760
72	3,000	5,280	5,520	7,520	6,520
96	3,300	7,040	7,280	9,280	8,280
28[a]	5,500	50,000	50,000	50,000	50,000

[a]Days.

12. The prediction equation is tested by computing an exposure table. The slope b obtained by the method of zero sum (item 11 preceding) is used to predict the 28-day strength from each individual early test result. The algebraic difference between each predicted result and the corresponding, measured 28-day test results are listed and totaled. The total should be zero or nearly so.

13. The prediction error is computed by the use of the formula

$$\sigma_e = \sqrt{\frac{\Sigma (S_M - S_{28})^2}{2\eta}} \tag{4}$$

The best values of b and C are indicated by the lowest value of σ_e. A one-sided confidence limit can be established by

$$S_M - 1.645\ \sigma_e > L \tag{5}$$

which indicates that 95 times out of 100 the true average strength is greater than L.

14. The testing error is computed by the use of the equation

$$\sigma_t = \sqrt{\frac{\Sigma |X_1 - X_2|^2}{2\eta}} \tag{6}$$

where X_1 and X_2 are the paired 28-day test results on cylinders from the same batch.

15. The actual prediction error is

$$\sigma_p = \sqrt{\sigma_e^2 - \sigma_t^2} \tag{7}$$

16. Equation 6 may be used to predict potential strength at any age from a test result of a cylinder of any age, provided that the temperature history of the cylinder prior to test can be estimated. For example, the potential 14-day strength of concrete can be estimated from a cylinder 41 hours old at time of test when the average temperature of the cylinder was 90 F as follows:

$$\begin{aligned}
b &= 2{,}850 \\
C &= 1{,}240 \\
M &= 14 \times 24 \times 73.4 = 24{,}640;\ \log = 4.39164 \\
m &= (41 \times 90) + 1{,}240 = 4{,}930;\ \log = 3.69285 \\
\log M - \log m &= 0.69879 \\
S_m &= 2{,}210 \text{ psi} \\
S_{14} &= 2{,}210 + 2{,}850\ (0.699) \\
&= 2{,}210 + 1{,}990 \\
&= 4{,}200 \text{ psi}
\end{aligned}$$

A NEW DEVELOPMENT IN THE MODIFICATION OF THE PROPERTIES OF CONCRETE FOR USE IN PAVEMENTS

G. Lees and G. Singh,
Department of Transportation and Environmental Planning,
University of Birmingham, England

During the past several years, new mileage of rigid type of pavement has been declining steadily in favor of the flexible type. The greater load spreading capacity of the former, due to the high rigidity of the concrete, is accompanied by a relatively low tensile strength and low capacity to accommodate movements caused by climate variations. Demands made by the structure of the pavement on this multiphase material have been established, and modifications of material properties, so as to achieve an improvement in pavement slab properties, are proposed. Confirmation has been made of the predicted effects of this modification on workability, static flexural strength and deformation, reversed flexural fatigue strength, and free and restrained movements due to temperature and moisture variations. A comparison has been made between the predicted structural behavior of pavement slabs based on their behavior in laboratory tests. This comparison shows that significant improvement in a number of important respects can be expected from the use of the modified concretes. In addition it is considered that the modification proposed in this paper would also enable efficient use to be made of lower quality aggregates.

One of the primary virtues of a concrete pavement slab is its capacity to distribute the loads over a relatively wide area of the underlying layers. This is due to the high flexural rigidity that the concrete slab possesses, with the result that the major portion of the structural capacity of the pavement has to be supplied by the concrete slab itself. Large horizontal stresses are induced in it under the action of traffic loads, climatic variations, and movements of the supporting layers. The tensile strength of concrete, as compared with its rigidity, is very low and its capacity to accommodate movements due to things such as climatic variations is poor. These necessitate the use of thick slabs as well as the provision of means, namely a joint system, frequently accompanied by a system of reinforcement and load-transfer devices to control the magnitude of stresses and the resulting cracks. The joints, apart from adding to the initial and maintenance costs (1), are often a cause of distress in the pavements. Psychological effects, occurrence of resonant vibrations, and effects on the riding quality are all too well known, although good current practice goes some way toward removing these objections. Continuous reinforcement (if present) itself exerts restraint to the contraction of the slab by inducing tensile stresses.

It follows that any means by which these stresses may be reduced would be desirable. Modified concretes, designed with the aim of reducing stresses due to the factors mentioned, have been subjected to a comprehensive series of laboratory tests for the purposes of practical and theoretical evaluation.

The modification proposed is that the aggregate be coated with a chemically stable soft medium before it is incorporated into the mix. Because of its low cost and availability, the coating medium used in this study has been a penetration grade bitumen.

Sponsored by Committee on Mechanical Properties of Concrete.

STRUCTURAL BEHAVIOR OF A CONCRETE PAVEMENT

The major design factor in rigid pavements is the structural strength of the concrete slab. By this is meant the capacity of the concrete slab to endure the following stress-inducing factors:

1. Externally applied static and repeated loading;
2. Restrained temperature and moisture-induced movements including restraint due to incompatibility of the phases in the material, restraint due to continuity of the material, and restraint by the subgrade; and
3. Volume changes in the supporting material, including those caused by frost action, permanent deformation of the subgrade, and loss of support through pumping.

External Loading

In the design of a pavement it is recognized as desirable to know and control the stresses both in the slab and in the subgrade. In this study, use has been made of the analyses of Westergaard and Burmister for approximation of these stresses (2). These studies indicate that reduction in the ratio $E_{slab}/E_{subgrade}$ (Burmister) or E_{slab}/K (Westergaard) reduces the bending stresses in the slab. The increases in the subgrade due to the preceding are insignificant (3), even if the stiffness ratios are reduced to $^1/_{10}$ of their usual value.

For given values of slab thickness and load, there are 2 ways in which the stress in the slab can be reduced—by increasing $E_{subgrade}$ (or K) or by decreasing E_{slab}. In the former case [but not forgetting the cost of increasing $E_{subgrade}$ as given by Ghosh and Dhir (4)], although the traffic stresses in the ideal case of uniform support assumed in the Westergaard and Burmister analyses will be lower, stresses induced by warping effects and subgrade restraint will be greater. In the case where E_{slab} is decreased, not only is the effect of factor 1 reduced but also are the effects of factors 2 and 3.

Satisfactory behavior of a rigid pavement depends on the structural integrity of the concrete slab. Whether the slab will be able to sustain stresses with the required factor of safety (or load factor) depends also on the strength of the concrete in the slab.

In Figure 1 curve AB shows a generalized approximate relationship between the modulus of elasticity E of concrete and its bending strength. Curve CD represents the relationship between the E of the same concrete in a slab and the bending stress in it for given loading conditions, subgrade, and slab thickness. The zone to the left of F (where bending stress in the slab exceeds the bending strength of the material) is representative of the case of lean concrete, and the zone to the right of F represents conditions in which the slab behaves as a rigid pavement.

Let a comparison be made between a normal concrete, the properties of which are represented by point N on the curve AFB, and a concrete being modified, say, to give properties represented by point M. By virtue of the lower E value of the modified concrete, the bending stress in it is less than that in normal concrete by an amount PS. This gives it a factor of safety MQ/SQ, which is more than that of normal concrete NR/TR. This superiority will exist even if the strength of the modified concrete is less (by an amount LM) than that of normal concrete, up to a certain limiting value of LM (not necessarily equal to PS) beyond which the strength of modified concrete will not be enough to take advantage of the stress reduction provided by its low E.

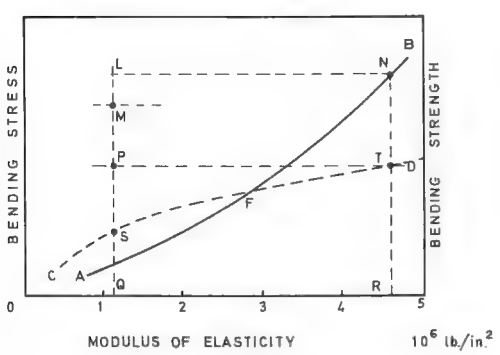

Figure 1. General relationships of bending stress, bending strength, and modulus of elasticity for concrete in road pavements.

The degree of benefit derived from the approach depends on (a) the extent of

modification in E, in which a reduction in E has considerably more effect in the lower range of E values below approximately 1×10^6 lb/in.^{2} (7×10^4 kg/cm^2); (b) the extent of modification in bending strength as compared with normal concrete; and (c) loading conditions, type of subgrade, and thickness of slab.

Restrained Temperature-Induced and Moisture-Induced Movements

The stresses induced in a concrete slab because of restraint against movements in response to temperature and moisture content fluctuations and gradients depend on the following:

1. The free (i.e., unrestrained) thermal and moisture coefficients of expansion and contraction of the concrete (larger values tend, other things being equal, to produce higher stresses);
2. Temperature and moisture diffusivity of the material (a lower diffusivity increases the gradients and hence increases warping stresses but also reduces the mean variation in temperature and moisture content and hence reduces longitudinal restraint stresses, and these stresses are more critical than warping stresses in the case of longer, > 100 ft or 30 m, slabs);
3. The E and creep characteristics of the concrete (a lower value of E accompanied by greater creep reduces the bending stresses due to warping and the longitudinal stresses due to subgrade restraint); and
4. Characteristics of the subgrade or base including surface frictional characteristics, shear strength, load-deformation and creep characteristics, and effect of moisture and temperature variations on these.

Volume Changes in the Supporting Material

Volume changes such as the dilation of a granular subgrade, unequal subgrade settlement or compaction, pumping at joints, swelling and shrinking in the subgrade, and frost heave beneath the pavement produce nonuniform support, resulting in bending stresses. These stresses, in response to loading and self weight of the slab, are proportional to the stiffness of the slab. The reduction, therefore, of stiffness and provision of an increased creep facility provide a reduction and relaxation of stresses. The analysis of Richard and Zia (6)—who used elastic theory and parameters E for slab and K for subgrade, confirms that a reduced value of E provides reduced stress in the slab. The analysis also shows that there are very large pressure concentrations on the subgrade at the boundaries of any such discontinuity in support and that these are also effectively relieved by a reduction in E and an increase in the creep facility in the slab.

MECHANICAL AND PHYSICAL CHARACTERISTICS OF CONCRETE

It is apparent from the discussion in the previous section that the effects of variation in the slab properties should be viewed not in isolation but with reference to the pavement as a structural system, performing under the action of traffic, under climatic variation, and under varying conditions of subgrade support.

The modification in concrete composition proposed, namely the coating of a proportion of the aggregate with a soft medium before it is incorporated in the mix, is here examined in the light of its probable effects on the performance of the structure as a whole.

If other factors are assumed to be constant, the proposed modification can be expected to influence concrete properties as follows:

1. Workability—For most aggregates the roughness of the surface texture and angularity of major projections will be reduced by coating. Hence workability is improved, with the usual consequences that for a given workability the water-cement ratio can be reduced, leading to an increase in paste-mortar strength, or a leaner mix may be employed.
2. Average strength—For many types of aggregate, the coating will produce a drop in bond strength, and this will lead to a fall in average strength as measured in

conventional laboratory tests in compression, tension, indirect tension, flexure, and fatigue. In other cases it is possible that the average strength, for a given water-cement ratio, may be increased because, in normal concrete, parasitic stresses due to thermal, moisture, and modules of elasticity incompatibility between the phases present invariably produce cracks that extend during the life of the structure because of climatic and loading fatigue. Introduction of a soft medium between the aggregate and paste will tend to reduce these stresses.

3. Statistical strength—An important aspect of the Griffith theory is that the fracture strength of materials such as concrete is statistical in nature and depends on the probability that, for a given applied stress, a flaw of sufficient size to propagate further is already present. On the assumption that the bitumen coating will eliminate or tend to reduce the occurrence of random parasitic cracks, the soft coating itself acting as a system of controlled and uniformly distributed flaws, it can be expected that the scatter of results of observed fracture strength will be reduced.

4. Low-quality aggregates—Aggregates that are generally considered to have rather low quality, with respect to high water absorption or potential adverse chemical reactivity, will be rendered innocuous by bitumen coating, and their use will thereby be made more feasible.

5. Modulus of deformation and creep—The effect of coating the aggregate will be to reduce the stiffness of the concrete and to increase the creep facility. These changes of the material properties will enter into any rational design of concrete pavement structures.

6. Coefficients of thermal expansion—In most cases the coefficient of thermal expansion of the concrete will be slightly increased as a result of coating because normally the value of the coefficient for the continuous phase of paste is higher than that of the dispersed aggregate phase, and the coating will allow greater freedom to the independent movements of the 2 phases. Coating may have the reverse effect of lowering the coefficient of expansion of the concrete in those rarer cases where the rigid phase of aggregate particles has a higher coefficient than the paste continuum. The causes of this would be (a) the reduced stiffness of the coated aggregate and (b) the greater opportunity for independent movement that would facilitate internal creep in the form of particle reorientation. In addition, there would be movement of the fluid phase into and out of the pore structure of the paste or mortar phase in response to volume changes in the aggregate. The latter action would also take place with respect to volume changes within the coating itself. These latter effects mean that, in spite of the fact that bitumen has a higher coefficient of expansion than any of the other phases present in the concrete, this in itself could be of minor significance in affecting the coefficient of the composite as a whole.

7. Thermal conductivity—In addition to the effects on thermal coefficients, the coating of the aggregate can be expected to affect the thermal conductivity. This would probably be of minor importance because the modification affects the dispersed phase only.

8. Coefficients of volume change with moisture movement—For reasons similar to those given in item 6, if an aggregate is used that possesses greater dimensional stability in the presence of moisture variations than the paste, then the coating of the aggregate and consequent reduction in bond stiffness will give a concrete with lower stability (i.e., showing higher coefficients of volume change) than normal concrete. On the other hand, if an aggregate is used that has lower dimensional stability than the paste, then the coating will render the mix more stable than the corresponding normal concrete.

9. Moisture diffusivity—The plugging of voids in the concrete by the progressive migration of bitumen toward these sites will reduce its permeability and water absorption. Both resistance to the establishment of moisture content gradients, leading to warping, and resistance to water absorption, leading to the swelling effects just discussed, will be favorably increased. Frost resistance also will be increased by the decrease in water absorption.

EXPERIMENTAL INVESTIGATIONS

Materials Used and Mixes Tested

Because of their common use in concrete mixes, a crushed quartzite gravel and natural sand (Weeford Pit, Staffordshire) were chosen. This type of aggregate has an above-average value of coefficient of thermal expansion (6) but is reasonably stable to moisture variations. Details of grading, concrete mix design, and type and quantity of bitumen used are given in the Appendix.

The investigation has involved the study of the following 3 types of concrete: (a) normal concrete; (b) concrete with coarse aggregate coated, i.e., retained on British standard sieve $^3/_{16}$ in. (4.76 mm); and (c) concrete with 92 percent by weight of all aggregate coated, i.e., all fractions except those passing B.S. sieve No. 52 (0.295 mm).

In the remainder of this paper, these types of concrete will be designated M_0, M_1, and M_2 respectively. In all cases the water-cement ratio was adjusted to give a selected workability of 20 sec (vebe time).

Curing was effected under water during 28-day periods for static tests, 28 to 48 days for fatigue tests, and 14 days for temperature and moisture-movement characteristic tests.

Results of Investigations

1. Flexural testing was done of beams 1.58 in. (40 mm) × 2.47 in. (62.5 mm) × 10.5 in. (265 mm). A third point loading system on a span of 9.3 in. (236 mm) was used for the flexural tests.

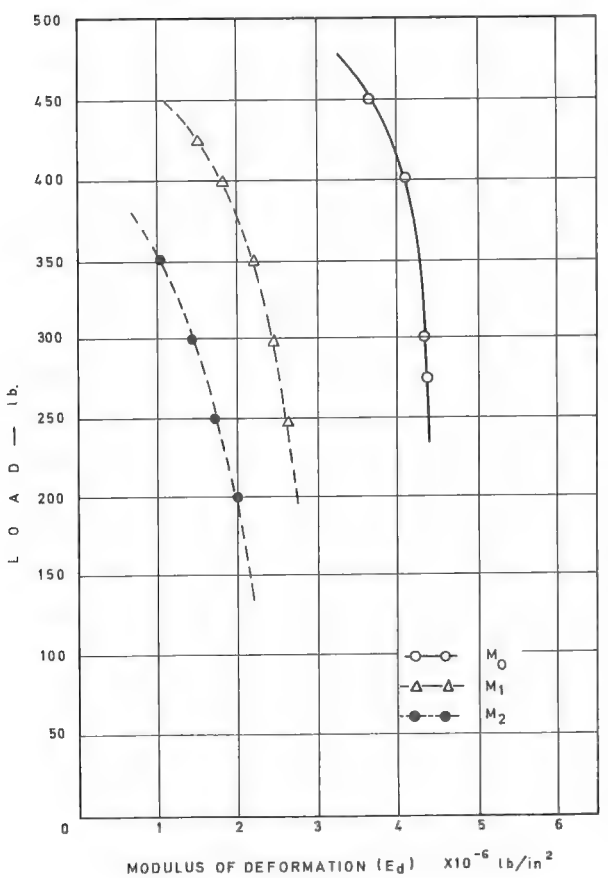

Figure 2. Load versus modulus of deformation for normal and modified concretes.

The modulus of deformation in flexure shown in Figure 2 is seen to be considerably reduced for the modified concrete as compared with the normal concrete, the difference being greater at the higher load levels. This modulus is the effective modulus that should be considered in the design of a pavement and has been used in calculations of expected performance discussed in the concluding section of this paper.

The average flexural strength is also reduced as a result of modification (Fig. 3). This reduction, as compared with normal concrete, is 5.8 and 24.2 percent for concretes M_1 and M_2 respectively. The reduced scatter in the results for the modified concretes means, however, that the difference in strength tends to decrease at lower probabilities of failure. For example, at a probability of failure level of 0.022 (2 standard deviations), M_2 is only 9.5 percent weaker than M_0, and M_1 is 8 percent stronger.

2. In reversed flexural fatigue testing, the average strength (in terms of number of cycles to fracture failure) is, as in the case of

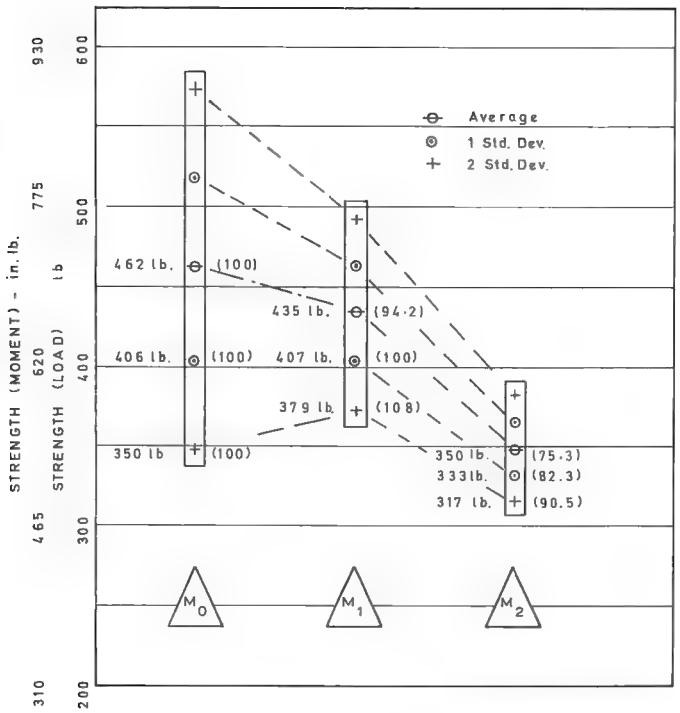

Figure 3. Flexural strength values for normal and modified concretes.

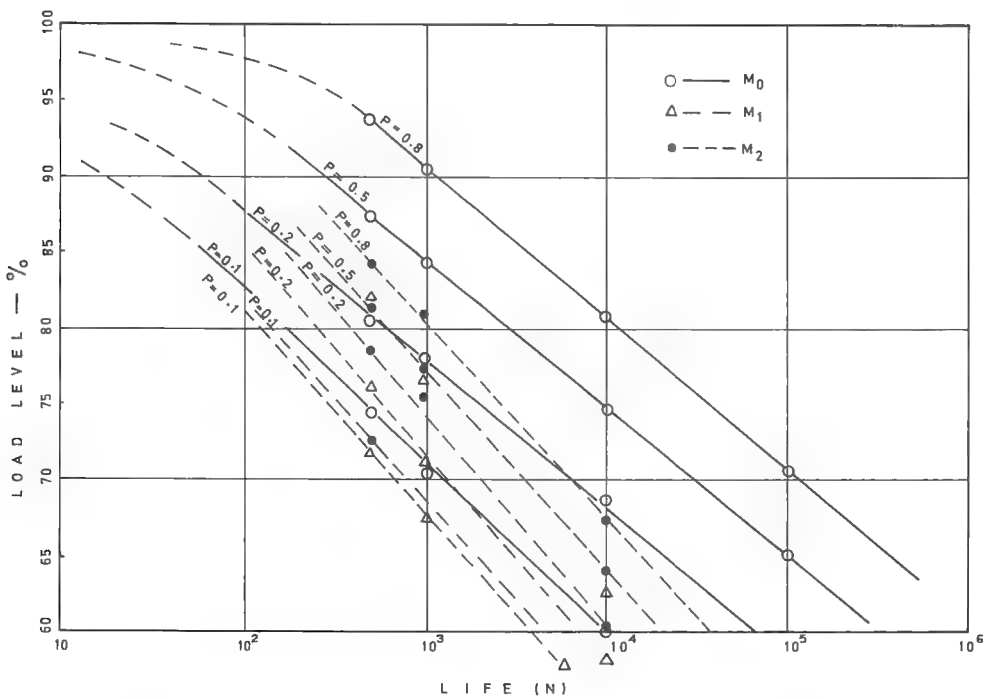

Figure 4. Fatigue lives of normal and modified concretes.

simple flexural testing, lower for the modified concretes than for normal concrete (Fig. 4). This difference, within the measured range, is greater at lower load levels.

In these results also, a reduced scatter was observed in the modified concretes, with the consequence that, at lower levels of probability of failure, the difference in strength is considerably less. This is shown by the proximity of the lines for the 3 concretes at P = 0.1.

It is also to be noted that the fatigue tests were of a constant bending moment type. As discussed in the section on external loading, however, it is important to recognize that, under actual service conditions, the bending stresses experienced by any slab will be a function of the slab's own stiffness. It follows that, under more simulative loading and support conditions, the merits of the modification would appear to considerably greater advantage.

With regard to results 1 and 2, a further point should be added based on the consideration of the scatter of the results and on the assumption that the weakest link theory is applicable. This point is that the average flexural strength (static and fatigue) of the modified concrete will be considerably improved, relative to that of the normal concrete, when measured on specimens of full slab thickness and when tested under realistic conditions such that the volume of the concretes subjected to near maximum bending moment is relevant to their individual stiffnesses.

3. The linear coefficients of thermal expansion (unrestrained) of M_1 and M_2 have been found to be increased by 8.8 and 13 percent respectively as compared with M_0. (Coefficients of expansion are 12.4, 13.5, and 14.0 $\times 10^{-6}$ C for M_0, M_1, and M_2 respectively.)

4. The free drying shrinkage (unrestrained) of M_1 and M_2 are 16 and 25 percent respectively, greater than that of M (Fig. 5). These comparisons refer to a drying period of 23 days at 10 C and 20 percent relative humitidy.

5. Under restrained test conditions (Figs. 6 and 7), which are more simulative of the pavement slab conditions, the stresses induced in M_1 and M_2 because of temperature

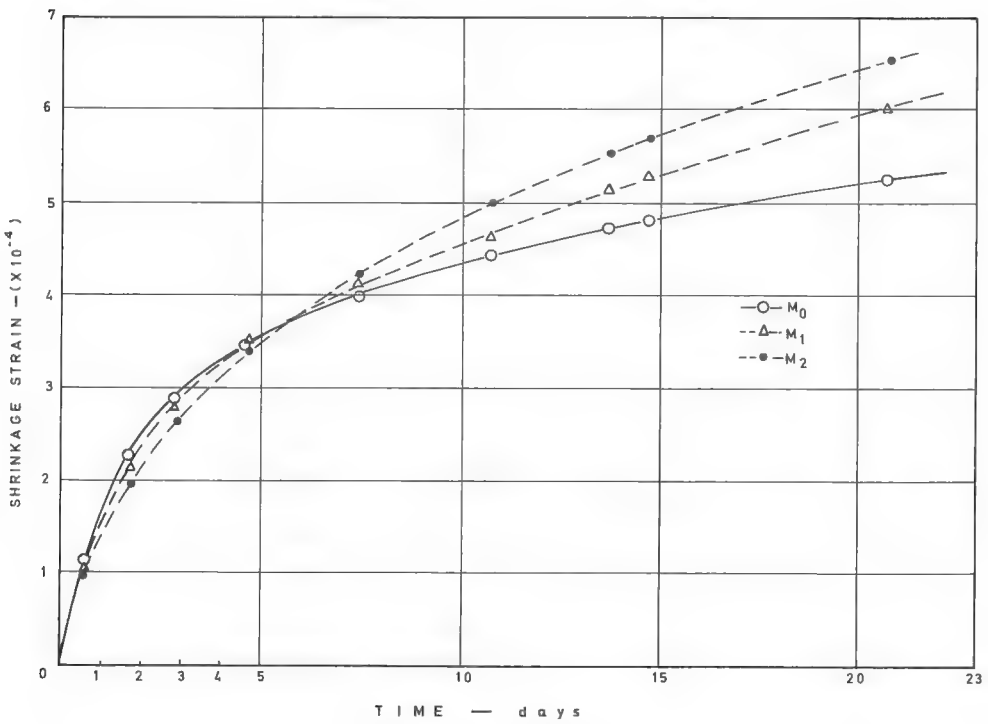

Figure 5. Strains due to unrestrained shrinkage in normal and modified concretes.

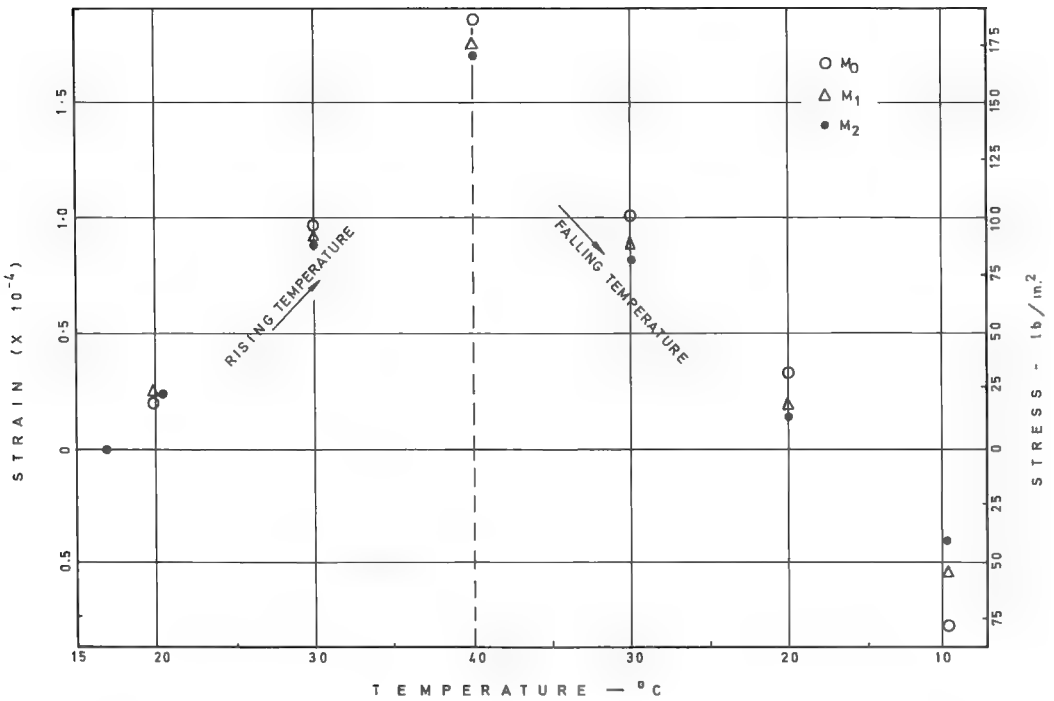

Figure 6. Thermally induced strains and stresses in normal and modified concretes.

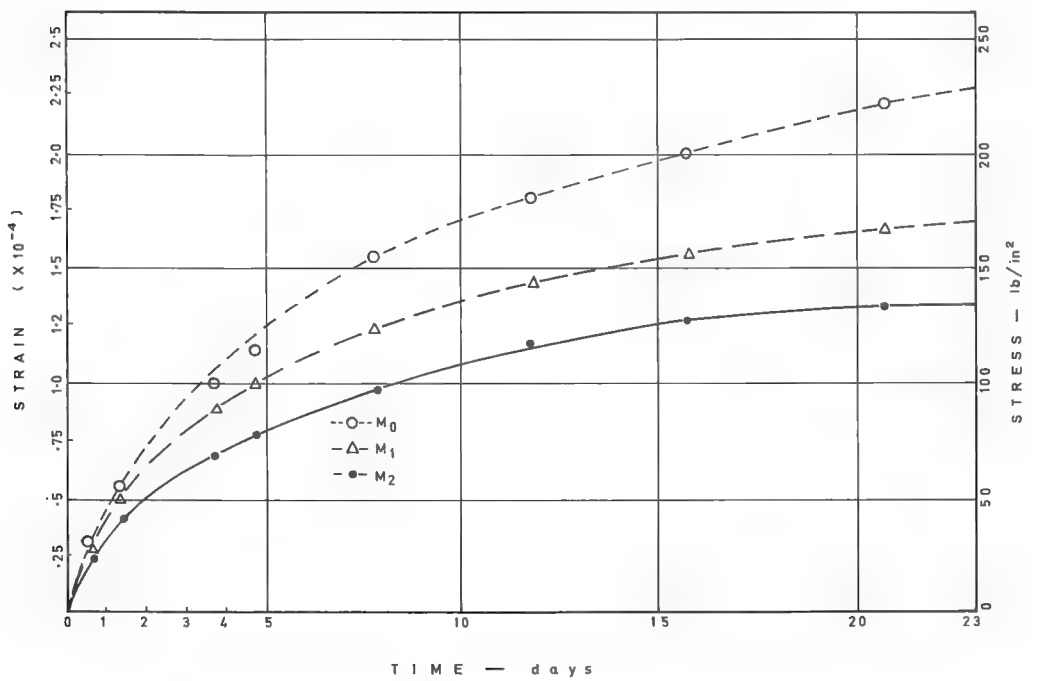

Figure 7. Strains and stresses due to restrained shrinkage in normal and modified concretes.

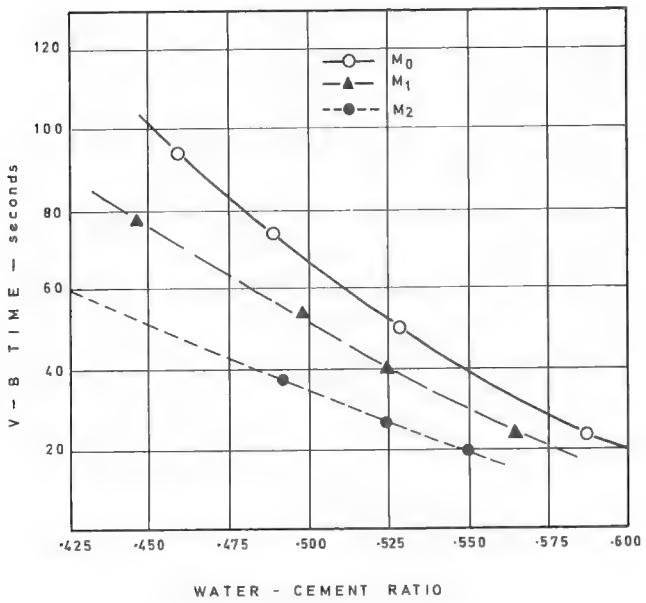

Figure 8. V.B. workability for normal and modified concretes at various water-cement ratios.

and moisture variations are very significantly lower than those in M_0. The corresponding movements are also less in M_1 and M_2. The orders of merit shown in these tests are hence the reverse of those in unrestrained tests (results 3 and 4).

6. The thermal conductivity does not seem to be affected by the modification.

7. As shown in Figure 8, the workability of the mixes M_1 and M_2 is considerably increased as a result of surface texture and shape modification of the aggregate particles by coating.

CONCLUSIONS

A theoretical comparative analysis of the structural behavior of pavement slabs of the 3 concretes based on the experimental results obtained shows the following:

As computed from Meyerhof's (7) method of analysis, the expected ultimate load-carrying capacity of the slabs of modified concretes is considerably greater than that of the slabs of normal concrete (Table 1). This is despite the lower average strength of the former and without taking into account size effects and the statistical probability of failure. This superiority of the modified concrete slabs is more marked for lower slab thicknesses, H, and lower values of the modulus of subgrade reaction, K.

Despite the bias against the modified concretes introduced by the method of fatigue testing (result 2) the data given in Table 1 show that on the whole the modified concretes can be expected to perform better under the fatiguing action of traffic, particularly for low values of H and K. The only cases where the normal concrete showed higher calculated life are marked in Table 1.

The calculated lives given in Table 1 are based on a probability of failure level of 0.1. There is in this analysis an additional bias against the modified concrete because it is certain that a rational method of pavement design should consider levels of probability of failure several orders of magnitude less than the one taken here. In a design based on such lower levels of probability of failure, the superiority of the modified concretes would be apparent over an even wider range of support, thickness, and loading conditions than that given in Table 1.

TABLE 1

COMPARISON OF STRUCTURAL BEHAVIOR OF CONCRETE

Slab Thickness H (in.)	Value of Modulus of Subgrade Reaction K (lb/in.²/in.)	Ultimate Load Capacity (lb)			Value of Load Applied (lb)	Expected Life (no. of load cycles)		
		M_0	M_1	M_2		M_0	M_1	M_2
4	50	8,380	17,300	16,800	5,000	10,500	800,000	960,000
					7,000	77	105,000	114,000
					8,000	13	40,000	40,000
					9,000	>1	15,000	14,000
	100	15,600	27,000	26,000	9,000	34,000	365,000	410,000
					10,000	4,300	195,000	200,000
					12,000	290	54,000	51,000
					14,000	26	15,300	13,400
	300	27,950	48,000	44,000	15,000	36,000	520,000	450,000
					18,000	4,200	180,000	130,000
					21,000	410	62,000	38,500
					25,000	28	14,700	8,200
8	50	46,100	64,500	57,200	24,000	51,000	185,000	105,000
					30,000	3,300	38,500	17,000
					35,000	360	10,000	11,000
					40,000	40	2,510	770
	100	62,100	81,100	70,500	35,000	21,500	68,000	63,000
					40,000	3,900	23,000	8,300
					45,000	720	8,000	2,300
					50,000	140	2,750	640
	300	88,700	106,500	93,000	45,000	62,000[a]	80,000	28,000[a]
					50,000	21,500[a]	41,000	13,400[a]
					55,000	6,550[a]	15,500	5,400[a]
					60,000	2,000	7,000	2,100

[a]Only cases where normal concrete showed higher expected life.

The stresses in the modified concrete slabs due to all other stress-inducing factors will also be reduced very significantly. The possibility of greater spacing or elimination of joints (including contraction joints) is obvious.

Quantification of the exact relative overall merits of the 3 concretes is extremely difficult and, as is usual in such cases, calls for full-scale pavement tests together with further laboratory investigations.

The indications are clear, however, that concretes designed to have properties relevant to their place in the pavement structure are desirable if a rational method of rigid pavement design is to be used to its maximum effect and that such concretes, either as described or similar, are capable of being designed.

ACKNOWLEDGMENTS

The authors are indebted to Professor J. Kolbuszewski, Department of Transportation and Environmental Planning, University of Birmingham, for active interest and for the provision of financial grants and laboratory facilities. Grateful acknowledgment is also made of the useful help received from F. D. Hobbs, Department of Transportation and Environmental Planning.

REFERENCES

1. The Cost of Constructing and Maintaining Flexible and Concrete Pavements Over 50 Years. Road Research Laboratory, RRL Rept. LR 256, Crowthorne Berkshire, 1969.
2. Whiffin, A. C., and Lister, B. S. C. The Application of Elastic Theory to Flexible Pavements. Proc. Internat. Conf. Struct. Design of Asphalt Pavements, 1962, pp. 499-520.

3. Fox, L. Computation of Traffic Stresses in a Simple Road Structure. D.S.I.R., Rd. Res. Tech. Paper 9, His Majesty's Stationery Office, 1948.
4. Ghosh, R. K., and Dhir, M. P. Provision of Bases under Cement Concrete Roads and Airfield Pavements. Australian Road Research Board, Proc. Vol. 2, Part 2, 1964.
5. Richard, F. E., and Zia, P. Effects of Local Loss of Support on Foundation Design. Proc. ASCE, Vol. 128, Part 1, 1963, pp. 1149-1179.
6. Handbook of Physical Constants. Geol. Soc. Am., Spec. Paper 36, 1942.
7. Meyerhof, G. G. Load Carrying Capacity of Concrete Pavements. ASCE Jour., Vol. 88, No. SM3, 1962.
8. Shacklock, B. W., and Walker, W. R. The Specific Surface of Concrete Aggregates and Its Relation to the Workability of Concrete. Cement and Concrete Assoc., Res. Rept. 4, 1958.
9. Singh, G. A Contribution Towards Understanding and Development of Concrete for Pavements. University of Birmingham, England, PhD dissertation, 1968.

APPENDIX

DETAILS OF GRADING, CONCRETE MIX, AND BITUMEN

Grading

Figure 9 shows the grading of the aggregate used. The aggregates were first dried in the laboratory and then screened into separate sizes by using $^3/_8$-in. (9.52-mm), $^3/_{16}$-in. (4.76-mm), No. 7 (2.38-mm), No. 14 (1.41-mm), No. 25 (0.59-mm), No. 52 (0.295-mm), and No. 100 (0.152-mm) British standard sieves. These fractions were kept separately in closed bins until required; the separate sizes were weighed up to give the same grading for each batch of concrete.

Coating

Fraction sizes of $^3/_8$ to $^3/_{16}$ in. (9.52 to 4.76 mm) and $^3/_{16}$ in. to No. 7 (4.76 to 2.38 mm) were coated with 90 to 110 penetration bitumen. The aggregate was heated on a hot plate to about 150 C and transferred to an electrically heated mixer drum maintained at about the same temperature. The aggregate was thoroughly coated by being mixed for about 5 min with a precalculated amount of bitumen. The coated aggregate was then tipped into a cold water bath to prevent the aggregate particles from sticking to one another. The aggregate was dried in the laboratory air before being used in the concrete mix.

Aggregate fractions passing the No. 7 (2.38 mm) British standard sieve were coated with an emulsion of 190 to 210 penetration bitumen. Laboratory dried material from the bins was weighed and transferred to the mixer drum, and a precalculated amount of emulsion was added. A mixing time of about 3 min was found to be sufficient to obtain an adequate coating, but mixing was continued in some cases to aid evaporation of water.

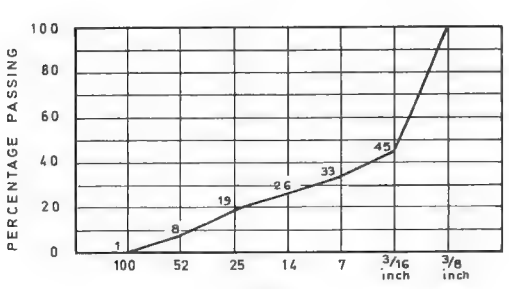

Figure 9. Grading of concrete aggregate used.

The quantity of bitumen used for coating of the $^3/_8$- to $^3/_{16}$-in. (9.52- to 4.76-mm) size fraction was 3 percent by weight. This amount was about the maximum quantity of bitumen that could be added without leading to excessive adhesion between the particles in a cooled state. The criterion for deciding the amount of bitumen or of bitumen emulsion for any of the

finer fractions was the ratio of mean diameter of the particles of the size fraction under consideration to the average thickness of the coating film. This ratio (122.5) was maintained constant for the various fraction sizes, and it was first determined for the $^{3}/_{8}$- to $^{3}/_{16}$-in. (9.52- to 4.76-mm) sized aggregate. The average thickness of the coating was calculated by dividing the volume of the bitumen used by the surface area (8) of the aggregate coated. This thickness was 0.0583 mm for the largest and 0.001715 mm for the smallest fraction sizes.

Aggregate-Cement and Water-Cement Ratios

An aggregate-cement ratio of 6:1 was used for all mixes. Water-cement ratios of 0.60, 0.575, and 0.55 were used for M_0, M_1, and M_2 respectively to give a workability of 20 vebe degrees. Further details of the characteristics of the test specimens and of the results are contained in the thesis submitted by Singh (9) to the Department of Transportation and Environmental Planning, University of Birmingham, England.

CUMULATIVE FATIGUE DAMAGE CHARACTERISTICS OF PLAIN CONCRETE

Craig A. Ballinger, Federal Highway Administration,
U.S. Department of Transportation

A laboratory study was conducted to investigate the fatigue characteristics of plain concrete. The primary goal was to evaluate the effect of variable loads on the fatigue life—to determine whether the Miner hypothesis adequately represents cumulative damage. In the laboratory work, 6- by 6- by 64-in. beams were tested statically and also under monotonic or variable loadings. Most specimens were moist-cured for 7 days and then stored in normal laboratory air for an average of 425 days before testing. The sinusoidal fatigue tests were conducted at a loading rate of 450 cpm, with the ratio of minimum to maximum stress equal to 0.15. The specimens in the variable load series were subjected to 2 levels of loading. A range of conditions was provided by raising or lowering the stress level by varying the number of cycles at the first level and by varying the stress range. The test data indicated a wide scatter in strength for concrete subjected to extended drying conditions. The applied fatigue stresses was normalized by using a multiple linear regression procedure to predict the static strength. The variable load fatigue tests were evaluated against the basic S/N data. It is concluded that the Miner hypothesis represents the cumulative damage characteristics of plain concrete in a reasonable manner. Because of the variability of concrete strength, a more elaborate rationale is not warranted. The accuracy of the S/N diagram is very dependent on the accuracy of the prediction of the normalizing strength values.

•WHEN CONCRETE and other structural materials are subjected to high repetitive stresses, they are subject to failure by fatigue. Therefore, if it is known that structures are going to be subjected to heavy repetitive loads during their service lives, it is essential that this factor be considered in their design. Economics and other considerations also require that the structures not be overdesigned. Therefore, the designer must have accurate criteria for adequately estimating the fatigue life of a structure under the expected service loading.

In the past, numerous research studies have been conducted to evaluate the fatigue characteristics of concrete. However, most of these studies have been restricted to determining the influence of variations in the type or proportion of the component materials on the fatigue life. This basic information was obtained by subjecting individual specimens to repetitive loading at constant stress amplitudes until failure occurred. The results of many tests and studies are plotted on a S/N diagram, which relates the percentage of ultimate stress that the specimens were loaded at to the number of cycles to failure. The line of 'best fit', which represents the data for each variable being considered, is then evaluated. The following conclusions result from these studies: (a) The fatigue response, when expressed in terms of the static ultimate strength, is statistically independent of the nominal strength, air-entrainment, type of aggregate, or the frequency of the repetitions of load; (b) the inclusion of rest periods

Sponsored by Committee on Mechanical Properties of Concrete and presented at the 50th Annual Meeting.

was found to extend the fatigue life, with the effect increasing to a maximum for rest periods of about 5 min; and (c) fatigue life is found to be affected by the range of the applied cyclic stress, and, for a given minimum stress, the life is increased as the stress range is reduced (1).

Unfortunately little research has been conducted to evaluate the effect of variations in repetitive stresses on the fatigue life of concrete. Because the service stresses in structures do vary, many designers feel that the bulk of the existing fatigue information on concrete is only of limited value. Because of this lack of definitive information on concrete, many structures are overdesigned so that service stresses will be below the fatigue limit, and therefore fatigue will not be a real factor. If, however, the cumulative damage due to repetitive stresses of varying magnitudes must be estimated, designers have almost traditionally used the Miner hypothesis. This method assumes that damage is proportional to the stress level and the number of cycles of load. However, Miner's theory is based not on fatigue tests of concrete but rather on notched aluminum specimens (2). In recent years research has shown that this method does not adequately represent the cumulative damage relationship for many metals. Accordingly, there is concern that the Miner equation may not adequately represent the fatigue characteristics of concrete.

OBJECTIVES

A laboratory study was conducted to develop information on the cumulative damage characteristics of plain concrete that is subjected to variations in repetitive loads. Because many designers currently use the Miner equation to estimate such damage, the data from this study were evaluated with respect to that theory to determine whether it represents such damage to a reasonable degree of accuracy. Also, to test a large number of specimens under a wide range of variations in fatigue loading was recognized as not being feasible. Therefore, rather than attempting to develop a new cumulative damage theory testing a limited number of specimens under variable fatigue loads and then determining whether the Miner equation could reasonably be used to predict the failure of these specimens were deemed to be more appropriate.

The laboratory study that provided the necessary data was conducted in 3 phases. Numerous static tests were made on beams and cylinders to provide basic strength information on each batch of concrete, 44 beams were subjected to constant cycle repetitive loads to develop the basic S/N relationship for this study, and 28 beams were subjected to a variety of 2-level cyclic loads to evaluate the Miner hypothesis.

LABORATORY TESTING PROGRAM

Test Specimens and Equipment

For the preceding evaluations, it was considered necessary that numerous specimens be tested to provide as much information on the concrete as possible. The batches of concrete were of sufficient size to make the following specimens: two 6- by 6- by 64-in. beams, three 6- by 6- by 21-in. beams, and three 6- by 12-in. cylinders. From each batch, one 21-in. beam and one cylinder were continuously moist-cured until tested at 28 days of age. The remaining specimens were divided into two test groups, including one cylinder, one 6- by 6- by 21-in. beam, and one 6- by 6- by 64-in. beam. Each of these groups is moist-cured for 7 days, and then moved into an air-drying laboratory storage area until time of test. The air-drying period ranged from about 175 to 550 days.

The concrete mix that was used for this study was designed for a 28-day compressive strength of 5,500 psi, a maximum slump of 3 in., and an air content of $5\frac{1}{2}$ percent. The coarse and fine aggregates were high-quality crushed limestone and a natural quartz sand respectively. The cement was a Type I non-air-entraining material. The air content was adjusted by adding Protex, a neutralized vinsol resin. All materials met the requirements of the appropriate ASTM specifications.

For most of the preceding static tests, conventional laboratory testing machines were used. However, special equipment was used for the static and fatigue tests of the

64-in. beams. The loading equipment was an electronically controlled hydraulic system, which was manufactured by the MTS Systems Corporation. A self-contained structural steel frame was fabricated for these third-point flectural tests. The fixtures conformed to the requirements of ASTM Method C78 [Test for Flexural Strength of Concrete (using Simple Beam With Third-Point Loading)].

Phase 1—Static Tests

Initially all of the specimens from 32 batches of concrete were tested statically to develop basic strength information on the concrete and correlations between test methods. Phase 1 tests are shown in Figure 1. It may be noted that the halves of the broken 64-in. beams were tested in flexure and that the resulting pieces from these and the 21-in. beam tests were tested in compression by the modified cube method. Except for the tests of the 64-in. beams, all of these tests were also made on the fatigue test group specimens. Thus, a considerable amount of static test data was accumulated in this laboratory study.

Phase 2—Constant Cycle Fatigue Tests

In the phase 2 series of tests, the 64-in. beams from 44 specimen groups were subjected to constant cycle fatigue tests to provide data for developing the basic S/N

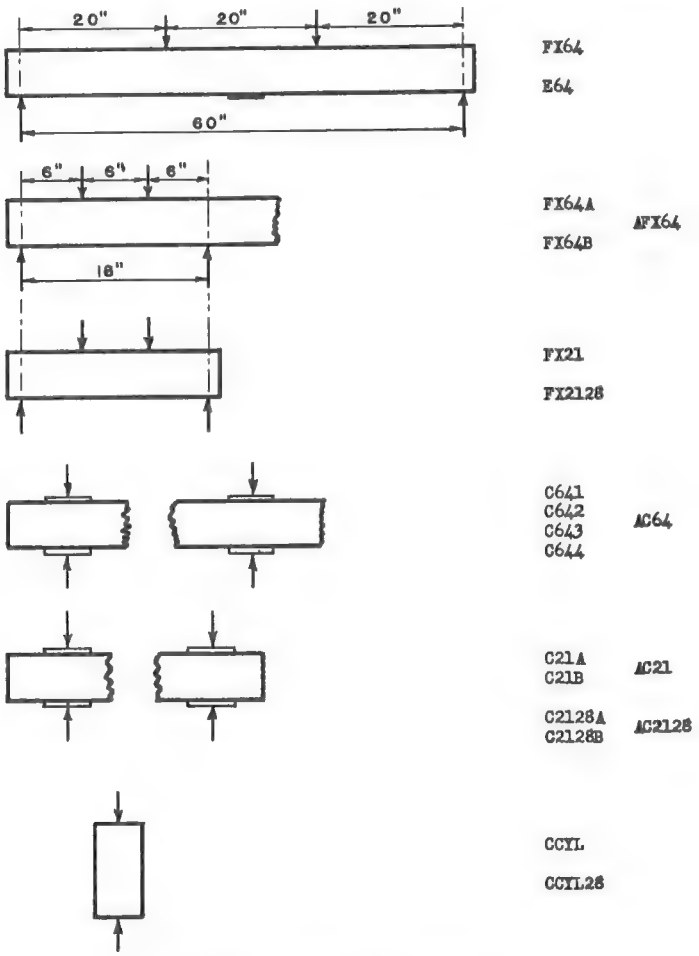

Figure 1. Schematic of static tests.

relationship for this study. The loads were applied in a sinusoidal pattern at a rate of 450 cycles per minute (cpm). Also, the ratio of the minimum to maximum loads was held constant at 0.15.

For these tests the level of the cyclic loads that were applied to each specimen was established arbitrarily. However, it was based somewhat on the age of the specimen and the number of cycles of load the previous specimens had sustained before failing. Because the static strength of these specimens varied, the actual range of applied stress levels (expressed as a percentage of the ultimate) was quite wide.

Phase 3—Variable Load Fatigue Tests

In the phase 3 series of tests, the 64-in. beams from 28 specimen groups were subjected to two levels of repetitive loads. A range of test conditions was provided by varying the magnitude and difference in the loads and the number of cycles at each level. Also, in 8 cases the second load level was lower than the first, whereas in 20 cases it was reversed. The cyclic load pattern, rate, and load ratio were the same as in the constant cycle tests of phase 2.

STATIC TEST DATA AND ANALYSIS

A considerable number of static tests were conducted in this research study to determine the fatigue characteristics of concrete and to provide the data for evaluating the fatigue test results.

As mentioned previously, results of fatigue tests are customarily reported on an S/N diagram. The effects of variables that are not of interest are masked out by normalizing and reporting the actual applied cyclic loads in terms of percentage of the ultimate strength of the specimens. It is therefore necessary to predict the ultimate strength of the specimens that are tested in fatigue, and this is the greatest weakness in the analysis of fatigue test data, especially for concrete. Concrete is not a homogeneous material but is rather a composite of several materials. Many physical and environmental factors cause variations in the strength of test specimens, even within the same batch of concrete. Data from a group of tests may be analyzed statistically to establish empirical relationships or evaluations of their strength. Unfortunately, it is one thing to derive such empirical relationships and yet another to relate that equation to specific test specimens (or to other specimens that were not included in the original set of data). Thus, it is obvious that the accuracy of the S/N relationship is completely dependent on the accuracy of the prediction of the static ultimate strength of the specimens that are tested in fatigue. One further step, as also mentioned, is that the S/N relationship that is developed will then be used to evaluate the results of the variable load fatigue tests.

The static tests that were conducted and the subsequent analysis of those data form a very important part of this study. So that the best possible results would be achieved for the study, several methods of analysis were evaluated and discarded. All were rational and have been used by other researchers. However, the appropriateness of a method had to be evaluated on the basis of the S/N line that it yielded. Certain boundary conditions on the nature of the required line necessitated the selection of the final method of analysis. A few of the methods of analysis that were tried will be briefly commented on before the final approach is discussed.

Single Regression Analysis

When the schedule of tests was set up for this study, the original plan was that tests of the specimens from the 32 static groups would yield an empirical relationship from which the static strength of the 64-in. beams could be predicted with reasonable accuracy. If this could be done, the stresses to be applied in the fatigue tests could be established prior to those tests. This approach proved to be unworkable because there was considerable scatter in the data from the tests of all types of specimens. An examination of the scatter diagrams of comparisons between the various test results revealed that the best one was between flexure tests of the 64-in. beams and the average

for their halves. It was therefore concluded that the prediction of the ultimate strength of the 64-in. beams should be based on tests of the pieces remaining after the fatigue tests. A regression analysis was made on the data from tests of the 32 static specimen groups to develop an equation relating the strength of the 64-in. beams and the average flexural strength of their halves. This was then used with the actual strengths of the halves of a particular beam to predict the flexural strength of that beam after completion of the fatigue test. This value was then used to normalize the applied fatigue stress for developing the desired S/N relationship. When this approach was used, however, it was found that the resulting S/N line was almost flat and completely unreasonable.

Multiple Regression Analyses

The level of scatter within the data from every type of static test precluded the possibility of developing a simple relationship that could be used to predict accurately the static flexural strength of the 64-in. beams. The next approach to the problem was based on the assumption that, because several types of specimens were cast from a single batch of concrete, the data from tests of specimens within a group could be combined to form a better basis for predicting the strength of the 64-in. beams. Accordingly, a multiple linear regression analysis was made on all of the data from tests of specimens from the 32 static groups. The computer program that was used for this analysis computes a sequence of multiple linear regression equations in a stepwise manner. At each step one variable is added to the regression equation (3). Thus, a multiple-term equation was developed that related the data from many strength tests to the flexural strength of the 64-in. beams. This equation was then used to predict the flexural strength of the 64-in. beams tested in fatigue by using the data from many static tests of specimens from their groups. However, when this method was used to normalize the applied fatigue loads, the results indicated that most of the specimens had been subjected to fatigue stresses greater than 100 percent of their ultimate strength. Because this could not be true, it indicated that the relationships between the various types of test data and those of the 64-in. beams might be changing. It was decided to take a closer look at the static data from all phases of the study.

The data from the static tests conducted in all phases of this study are given in Table 1. One section gives the data from the 32 static specimen groups of phase 1, whereas the other section summarizes the data from each type of test from all of the specimen groups. Although it has only limited statistical value, the standard deviation for each test type is also expressed as a percentage of the mean strength value to permit comparison between flexural and compressive strength data.

In some cases there is considerable difference between the values in the 2 sections. One of the major causes for this variation may be attributed to the difference in the

TABLE 1

SUMMARY OF STATISTICAL MEASURES OF STATIC TEST DATA

Type of Test and Specimens Used	32 Static Tests			All Test Groups		
	Mean (psi)	Standard Deviation (psi)	Percentage of Mean	Mean (psi)	Standard Deviation (psi)	Percentage of Mean
Compressive Strength						
Cylinders at 28 days (CCYL28)	5,576	329	5.90	5,767	409	7.09
Halves of 21-in. beams at 28 days (AC2128)	5,927	402	6.78	6,134	352	5.74
Cylinders at test of 64-in. beams (CCYL)	6,235	331	5.31	6,472	464	7.17
Halves of 21-in. beam at test of 64-in. beam (AC21)	7,100	414	5.83	7,283	441	6.06
Quarters of 64-in. beams (AC64)	6,959	483	6.94	7,126	427	5.99
Flexural Strength						
21-in. beams, at 28 days (FX2128)	770	61	7.92	814	63	7.74
21-in. beams, at test of 64-in. beams (FX21)	741	69	9.31	793	70	8.83
Halves of 64-in. beams (AFX64)	694	49	7.06	788	78	9.90
64-in. beams (FX64)	623	65	10.43	—[a]	—[a]	—[a]
Modulus of Elasticity						
64-in. beams (E64)	5.51	0.36	6.53	5.58	0.45	7.65

[a]Not available for beams tested in fatigue.

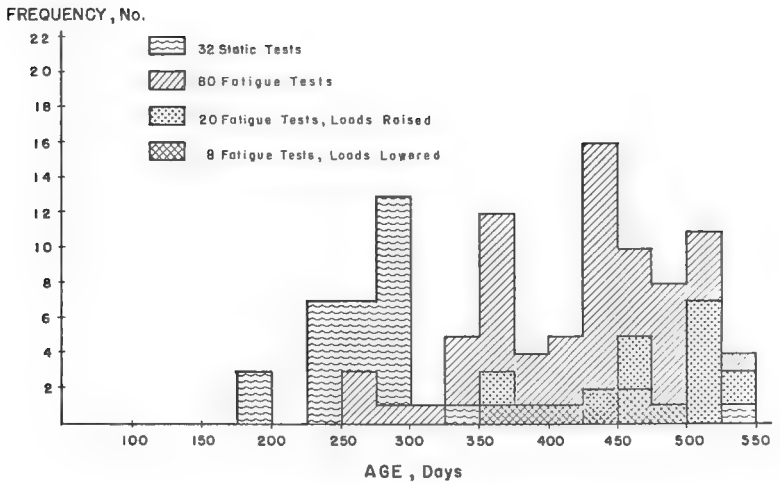

Figure 2. Frequency of tests conducted at various ages.

ages of the specimens. Figure 2 shows the distribution of specimen ages for the various testing plans. The primary cause of the wide variation in age at test was that the specimens were selected at random after all of the specimens were cast.

As a by-product of the computer analysis, the level of correlation among the various types of tests was also determined. The correlation coefficients for the 32 static tests groups are given in matrix form in Table 2. As expected, the degree of correlation among some of the tests is poor. The maximum correlation of any test with the static flexural strength of the 64-in. beams (FX64) is obtained for the average of the flexural strengths of the halves of the broken 64-in. beams (AFX64), which is expected. However, that correlation is only 0.477. This emphasizes the fact that even this correlation cannot be used to accurately predict the static ultimate strength of the 64-in. beams.

A similar correlation matrix relating the static test data for all 112 specimen groups is given in Table 3. A comparison of the 2 matrices shows that the level of correlations is improved considerably when all test values are considered, even though the range of test ages is widened. The strength of the 64-in. beams obviously could not be included in this table because most of these specimens were broken in fatigue. With regard to the average of the strength of the halves of the 64-in. beams, the maximum correlation is obtained for the strength of the companion 21-in. beams (FX21), i.e., 0.584.

Because of this situation, it was concluded that a somewhat indirect method of analysis would be necessary. It was still felt, however, that the multiple regression method

TABLE 2

CORRELATION OF VARIABLES FOR 32 STATIC TEST GROUPS

Specimen	AFX64	FX21	FX2128	AC64	AC21	AC2128	CCYL	CCYL28	E64	LAGE	FX64
AFX64	1.000	0.133	0.126	0.417	0.391	0.336	0.173	0.333	0.065	0.317	0.477
FX21		1.000	0.247	0.035	0.093	0.029	0.017	0.002	0.261	0.027	0.022
FX2128			1.000	0.530	0.248	0.491	0.070	0.374	0.351	0.165	0.165
AC64				1.000	0.742	0.736	0.277	0.680	0.465	0.187	0.394
AC21					1.000	0.732	0.522	0.726	0.431	0.184	0.342
AC2128						1.000	0.437	0.672	0.514	0.204	0.361
CCYL							1.000	0.575	0.430	0.028	0.373
CCYL28								1.000	0.542	0.127	0.240
E64									1.000	0.217	0.312
LAGE										1.000	0.399
FX64											1.000

TABLE 3
CORRELATION OF VARIABLES FOR ALL 112 TEST GROUPS

Specimen	AFX64	FX21	FX2128	AC64	AC21	AC2128	CCYL	CCYL28	E64	LLAGE
AFX64	1.000	0.584	0.480	0.413	0.323	0.435	0.361	0.360	0.094	0.745
FX21		1.000	0.351	0.276	0.276	0.283	0.261	0.214	0.094	0.517
FX2128			1.000	0.505	0.400	0.517	0.310	0.384	0.155	0.473
AC64				1.000	0.638	0.738	0.457	0.623	0.298	0.221
AC21					1.000	0.684	0.521	0.595	0.167	0.150
AC2128						1.000	0.558	0.640	0.248	0.279
CCYL							1.000	0.591	0.287	0.225
CCYL28								1.000	0.161	0.201
E64									1.000	0.073
LLAGE										1.000

of analysis had to be used to obtain the best possible prediction for the static flexural strength of the 64-in. beams. Because much higher correlations among the various types of tests were obtained when the data from all of the test groups were considered (Table 3), it was also concluded that this should form the basis for further analysis.

For this final method of analysis, the computer program was first used to develop a multiple-term regression equation relating the different static tests to the average flexural strength of the halves of the broken 64-in. beams (AFX64) by using the data from all 112 specimen groups. The program was then used to develop a simple linear equation relating the average strength of the beam ends (AFX64) to the strength of the 64-in. beam (FX64) by using the data only from the 32 static test groups. The predicted strength of the 64-in. beams was calculated as follows: The first equation was used to calculate an expected value for AFX64, and then this expected value of AFX64 was used with the second equation to predict the static strength of the 64-in. beam (FX64).

A summary of the first 6 steps of the regression analysis used to develop the first equation is given in Table 4. Table 4 gives the level of correlation (multiple R) that increases as each step is completed and as another variable is added to the equation. The benefit of adding variables drops as each variable is added. This is evident by the reduction in the "increase in R^2" value. To minimize the complexity of the computations and the resulting equations, we decided to terminate the regression equation after the fourth step, where the "increase in R^2" value drops from 0.0451 to 0.0034. The correlation coefficient for the resulting equation is 0.8481, which is a substantial increase over the values shown in the previous correlation matrices. The computer output for the fourth step of the regression analysis provided the coefficients for the desired equation:

$$\underset{}{\text{AFX64}} = \underset{}{-2720} + \underset{(\pm 0.1382)}{0.286\ (\text{FX21})} - \underset{(\pm 0.5592)}{1.36\ (\text{AGE})} + \underset{(\pm 0.0197)}{0.0405\ (\text{C642})} + \underset{(\pm 2658)}{8580\ (\text{LLAGE})}$$

where

TABLE 4
SUMMARY OF REGRESSION ANALYSIS

Step	Variable Entered	Multiple		Increase in R^2
		R	R^2	
1	LLAGE	0.7451	0.5552	0.5552
2	C642	0.7898	0.6237	0.0686
3	AGE	0.8211	0.6743	0.0506
4	FX21	0.8481	0.7194	0.0451
5	C2128B	0.8502	0.7228	0.0034
6	CCYL28	0.8506	0.7236	0.0008

Note: Summary of statistical values for each step of regression analysis relating results of individual tests to the average flexural strength of the halves of the 64-in. beams (AFX64).

AFX64 = average flexural strength of ends of 64-in. beam;
FX21 = flexural strength of companion 21-in. beam;
AGE = test age for 64-in. beam and companion specimens;
C642 = compressive strength, second strongest quarter of 64-in. beam; and
LLAGE = loglog of AGE.

The equation contains two "age" terms; however, one is negative. The combination of the two gives a curved relationship

for the strength of the specimens with age, as drying and other changes occur. The 95 percent confidence limits for each coefficient are given in the equation in parentheses. Thus, each term in the following equation is significant.

The second equation, which relates the flexural strength of the 64-in. beam to the average for the halves, is given as follows:

$$FX64 = 159 + 0.667\ (AFX64)$$

where FX64 is static flexural strength of 64-in beam.

The effectiveness of the first equation to predict the average flexural strength of the halves of the 64-in. beams is shown in Figure 3. It is felt that the quality of this prediction is good, considering the level of scatter associated with the data from each type of test. It may be noted that the values for the 32 static tests fall together along the lower portion of the 45 deg comparison line.

S/N FATIGUE TEST DATA AND ANALYSIS

In the second phase of this study the 64-in. beams from 44 specimen groups were subjected to constant cycle fatigue tests to develop the basic S/N relationship necessary for evaluating the results of the variable load fatigue tests. A summary of the test conditions and the S/N prediction are given for each specimen in Table 5. The actual range in applied stresses was very wide. These data are plotted on the S/N diagram shown in Figure 4.

The S/N line was established by using two boundary conditions from previous concrete fatigue research. First, the main portion of the S/N relationship is represented as a straight, descending line when plotted on a semilog basis. Second, the initial portion of the S/N line is not straight, but rather it curves downward from 100 percent to meet the linear portion of the line. The exact number of cycles at which the two portions of the line should intersect is not well established. This initial portion of the S/N line represents the low cycle fatigue region. That is, specimens that are loaded in this range of their ultimate strength are subject not only to the effects of simple fatigue but also to other fracture phenomena as well. The explanation of the fracture mechanics involved will not be discussed, but the general nature of this situation is recognized to influence the analysis of the data.

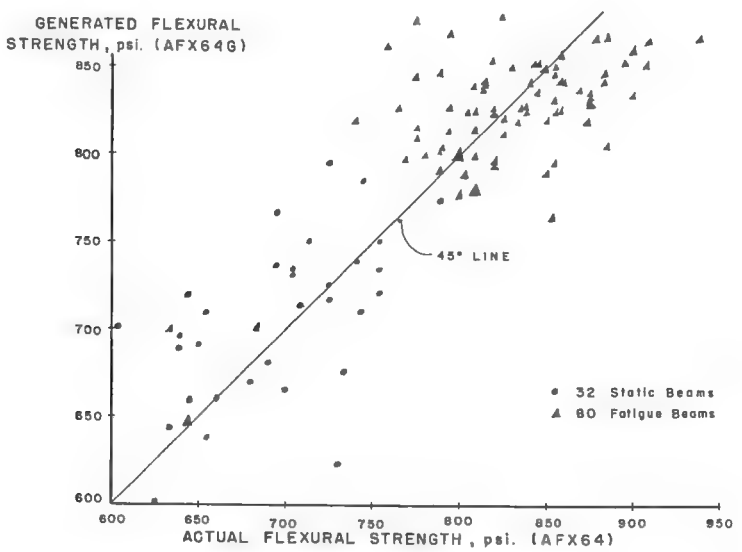

Figure 3. Average flexural strength of halves of 64-in. beam, generated versus actual.

TABLE 5
SUMMARY OF S/N FATIGUE TEST DATA

Beam	Stress Range (psi)	Maximum Stress (psi)	Maximum Stress S (percent)	Actual Cycles n	Predicted Cycles N	Damage d (n/N)
6	350	418	67	5,700	317×10^7	0.00
8	389	458	73	107,695	189×10^5	0.01
9	369	442	75	885	3,437,980	0.00
30	461	544	78	324,000	265,711	1.22
32	339	398	59	3,247,000	29×10^{11}	0.00
35	496	583	80	89,345	48,211	1.85
36	472	555	76	1,965,150	1,464,440	1.34
42	519	611	83	1,729	3,726	0.46
44	519	611	86	1,658	288	5.76
45	496	583	80	3,965	48,211	0.08
47	519	611	86	9,500	288	32.99
48	519	611	85	43,405	676	64.20
51	519	611	83	3,457	3,726	0.93
54	567	666	92	26	6	4.33
55	567	666	93	478	4	109.89
57	519	611	83	3,578	3,726	0.96
64	519	611	84	266	1,587	0.17
71	496	583	81	197,845	20,536	9.63
73	472	555	78	3,904,462	265,711	14.69
74	519	611	86	202	288	0.70
75	496	583	82	53,438	8,747	6.11
76	496	583	81	490	20,536	0.02
79	496	583	80	361,856	48,211	7.51
82	519	611	82	130	8,747	0.01
88	496	583	82	9,010	8,747	1.03
93	496	583	85	3,400	676	5.03
94	567	666	96	24	2	11.65
98	519	611	88	1,621	50	31.02
99	472	555	79	461	113,182	0.00
101	496	583	83	115,440	3,726	30.98
102	567	666	93	79	4	18.16
103	472	555	79	340	113,182	0.00
104	519	611	90	16	14	1.17
105	472	555	79	75,175	113,182	0.66
108	519	611	85	849	676	1.26
109	519	611	85	259,842	676	384.34
110	519	611	84	19,415	1,587	12.23
111	519	611	89	4,011	24	168.53
113	496	583	84	5,041	1,587	3.18
114	567	666	94	140	3	42.42
116	519	611	89	579	23	24.33
118	472	555	80	2,055	48,211	0.04
122	496	583	87	25,902	123	211.14
126	567	666	96	3	2	1.46

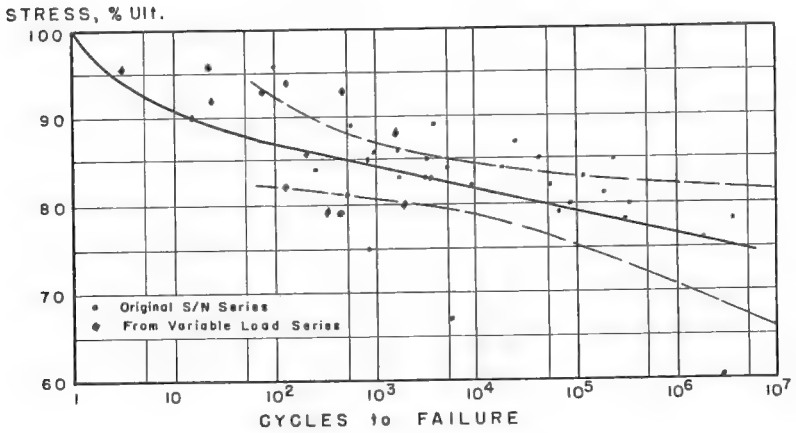

Figure 4. S/N diagram for monotonic fatigue tests.

The S/N line that was developed for this study is shown in Figure 4. It may be noted that 11 points represent specimens from the variable load fatigue series, which failed prior to changing of the cyclic loads. The linear portion of the S/N line was established by neglecting the specimens that failed at less than 70 cycles, and the computer was used to calculate a regression line through the remaining points. The equation for this portion of the line is as follows:

$$\text{Stress, percent ultimate} = 92.6 - 2.70 \text{ (log cycles)}$$
$$(\pm 1.914)$$

The 99 percent confidence limits for the slope of the line is shown in parentheses beneath that term in the equation. The 99 percent confidence band for the linear portion of the S/N line is also shown in Figure 4. It has been stated that the Miner theory postulates that fatigue damage occurs linearly with an increase in cycles of load. The data given in Table 5 and the S/N line were used to calculate the apparent damage, d, for each of the specimens. These values are also given in Table 5. Although it is difficult to evaluate the apparent damage, the very wide range is interesting. It may be noted that the apparent damage at failure ranges from 0.00 to 384.34.

The S/N relationship that has been established is the best result of several methods of analysis. There is obviously considerable scatter of the data points plotted on the diagram. This scatter is due primarily to errors in accurately predicting the strength of the individual test specimens. However, this was caused by the basic variations in strength within and between the specimens cast from each batch of concrete.

VARIABLE LOAD FATIGUE TEST DATA AND ANALYSIS

In the third phase of this study, 28 of the 64-in. beams were subjected to two levels of repetitive loads to develop some information on the cumulative damage characteristics of plain concrete. Although the number of load variations was limited, the following variables were included: the stress and the number of cycles at the first level, the direction of change to the second stress level, and the magnitude of change in stresses.

Because the number of tests that could be run was limited, the testing plan was designed to provide a range of conditions that could be used to evaluate the Miner hypothesis. This theory is based on the assumption that fatigue damage will occur in proportion to the work done on the specimens and that the resulting damage may be expressed by the ratio of the number of cycles of stress at a particular level to the corresponding number of cycles to cause failure at that same level (2). In other words, a specimen subjected to n_1 cycles of load at a constant stress level S_1, which would cause the specimen to fail after N_1 cycles, will use up 100 (n_1/N_1) percent of its fatigue life. Additional repetitions of load at different stress levels will cause damage at the same proportional rate.

If the Miner theory is appropriate, the damage created under the two levels of stress could be accumulated to yield a set of values that could be compared against the S/N diagram. If the resulting points fell within the scatter of the S/N points, it could be said that damage occurred on a linear basis.

Accordingly, the data from this phase of testing were evaluated as follows: The S/N line and the normalized maximum stresses were used to calculate the number of cycles at the second stress level necessary to cause the damage, d, theoretically created at the first level and yielded n_1'. This value was added to the actual number of cycles that were applied at the second stress level, and an equivalent total number of cycles was obtained at the second stress level, n_2^*. These calculations were made with the computer. In equation form the preceding may be expressed as follows:

$$n_1/N_1 = d_1$$
$$d_1 (N_2) = n_1'$$
$$n_1' + n_2 = n_2^*$$

TABLE 6
DATA FROM VARIABLE FATIGUE TESTS WITH LOADS LOWERED

Beam	Maximum Stress S_1 (percent)	First Level Cycles n_1	Damage d_1 (n_1/N_1)	Equivalent First Level Cycles n_1'	Maximum Stress S_2 (percent)	Second Level Cycles n_2	Damage d_2 (n_2/N_2)	Stress Change (percent)	Total Cycles n_2^*	Total Damage d^*
78	85	1,000	1.48	922,677	77	42,954	0.07	7	965,631	1.55
67	86	1,000	3.47	922,677	78	633,634	2.38	8	1,556,311	5.85
66	86	2,000	6.94	1,845,353	78	1,043,742	3.93	8	2,889,095	10.87
72	86	2,000	6.94	1,845,353	78	405,135	1.52	8	2,250,488	8.46
92	92	100	16.67	26,453	84	1,363	0.86	8	27,816	17.53
119	93	50	11.49	3,310	86	1,774	6.16	7	5,084	17.65
91	93	100	22.99	15,542	85	12,786	18.91	8	28,328	41.90
124	97	50	29.94	666	89	41,763	1,754.75	8	42,429	1,784.69

The test data and the results of the preceding calculations are given in Tables 6 and 7 for the tests in which the stress level was lowered and raised respectively. The theoretical damage created at the 2 stress levels has been indicated. The extreme values are due to scatter of the points about the S/N line, which emphasizes the error that could be created by not recognizing the effect of variation in strength of concrete on its fatigue life.

The preceding information for each specimen was used to plot points that are shown in Figure 5 and that represent the equivalent total number of cycles at the second stress level versus that stress level. The equation for the regression line through the data is as follows:

$$\text{Stress, percent ultimate} = 92.7 - 1.88 \text{ (log cycles)}$$
$$(\pm 1.132)$$

The 99 percent confidence limits for the slope of the line are shown beneath that term in the equation. The 99 percent confidence band for the line is also shown in Figure 5. The results of these tests were evaluated by comparing this regression line with the S/N line and its 99 percent confidence band. This comparison is shown in Figure 6. The line representing the variable load fatigue test data falls within the 99 percent band for most of its length.

TABLE 7
DATA FROM VARIABLE FATIGUE TESTS WITH LOADS RAISED

Beam	Maximum Stress S_1 (percent)	First Level Cycles n_1	Damage d_1 (n_1/N_1)	Equivalent First Level Cycles n_1'	Maximum Stress S_2 (percent)	Second Level Cycles n_2	Damage d_2 (n_2/N_2)	Stress Change (percent)	Total Cycles n_2^*	Total Damage d^*
53	69	12,000	0.00	100	84	6,262	3.95	15	6,362	3.95
33	69	24,000	0.00	0	85	4,905	7.26	16	4,905	7.26
50	69	24,000	0.00	0	85	3,460	5.12	16	3,460	5.12
120	69	96,000	0.00	0	85	32,080	47.45	16	32,080	47.45
77	70	48,000	0.00	0	85	172,571	255.26	15	172,571	255.26
41	70	48,000	0.00	0	86	167	0.58	16	167	0.58
34	71	12,000	0.00	0	87	905	7.38	16	905	7.38
123	71	24,000	0.00	0	87	3,735	30.45	16	3,735	30.45
43	76	3,000	0.00	8	83	43,932	11.79	7	43,940	11.79
83	76	6,000	0.00	15	83	571	0.15	7	586	0.15
86	76	6,000	0.00	7	84	2,833	1.78	8	2,840	1.78
68	77	12,000	0.02	13	85	19,625	29.03	8	19,638	29.05
37	78	3,000	0.01	3	86	2,776	9.64	8	2,779	9.65
59	78	12,000	0.04	13	86	34,547	119.96	8	34,560	120.00
80	78	12,000	0.04	13	86	387,995	1,347.30	8	388,008	1,347.34
38	79	3,000	0.03	3	87	521	4.24	8	524	4.27
46	79	3,000	0.03	3	87	18,909	154.15	8	18,912	154.18
69	79	6,000	0.05	7	87	7,015	57.19	8	7,022	57.24
40	80	3,000	0.06	3	88	1,943	37.19	8	1,946	37.25
70	80	6,000	0.12	3	89	1,737	72.98	9	1,740	73.10

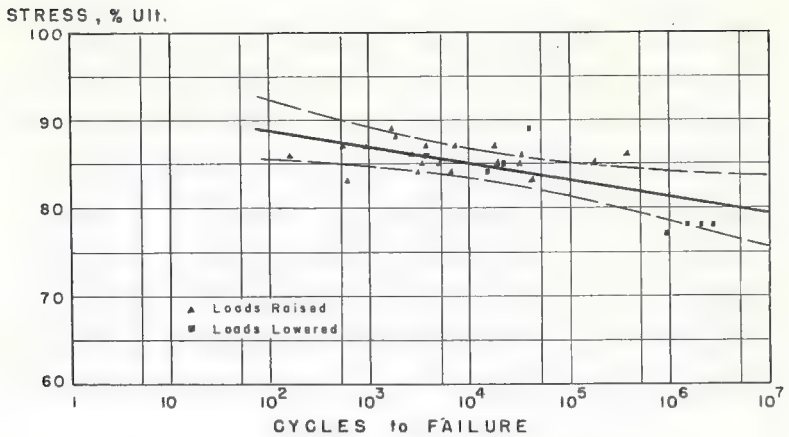

Figure 5. Effect of 2 levels of fatigue loading on fatigue life.

Whether these 2 lines are significantly different was determined by considering 2 statistical factors. The appropriate terms and their confidence limits in the preceding equation show that the slopes of the 2 lines are not statistically different and that their intercepts at the vertical axis are almost identical. Also, the standard error of fit for the variable load data points to the S/N line has been compared against the corresponding value for the S/N points with respect to the S/N line. The F-ratio for this comparison was computed to be 1.63. Therefore, the variable load test data are not significantly different from the S/N test data. Therefore, the conclusion was that there is no evidence of a significant difference in the 2 lines shown in Figure 6.

PREVIOUS PLAIN CONCRETE FATIGUE RESEARCH

As mentioned previously, there has been considerable research on the fatigue characteristics of plain concrete. How do the results of this study relate to earlier studies? Rather than to examine those studies in detail, it is perhaps more appropriate to comment on one of the main findings of this study and to relate this finding to one of the previous studies. That is, it has been found that the accuracy of the S/N relationship is

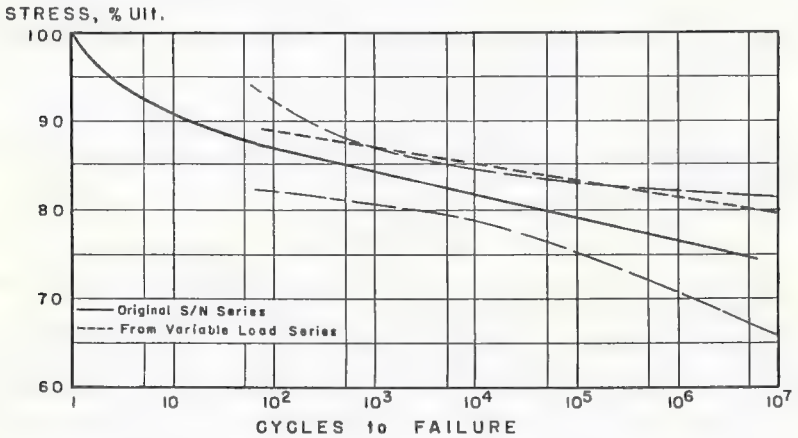

Figure 6. Comparison of cumulative damage line with S/N line.

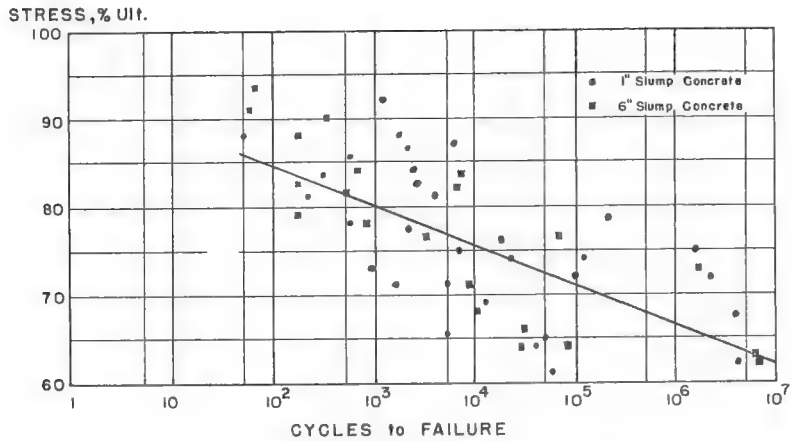

Figure 7. S/N diagram developed by Murdock and Kesler (4).

dependent on the accuracy of the normalizing static strength prediction. As the accuracy diminishes, the level of scatter of the data points increases, and the position and slope of the S/N line are changed.

The S/N diagram reported in a related fatigue study conducted by Murdock and Kesler (4) is shown in Figure 7. For these tests of beams, the normalizing value was the average flexural strength of the halves of the broken beams. The variation in the indicated percentage of ultimate strength for the specimens, which failed at the same number of cycles, is about twice as large as that shown in Figure 4.

Therefore, it is concluded that many of the previously reported S/N relationships for concrete may leave something to be desired but that their use for comparative purposes within a study is probably reasonable. However, the true accuracy of those S/N relationships may be questionable.

CONCLUSIONS

1. The accuracy of the S/N line representing the fatigue strength of concrete is very dependent on the accuracy of the prediction of the static strength that is used to normalize the data.
2. The Miner hypothesis represents the cumulative damage of plain concrete due to variations in fatigue loading in a reasonable manner.
3. Concrete should not be stressed to a level where the effect of fatigue is a real possibility. Because of the local, or gross, variations in the strength of concrete, fatigue effects may become critical at about 70 percent of the static ultimate strength.

ACKNOWLEDGMENTS

The study reported here is a portion of a major investigation that is being conducted by the Office of Research of the Federal Highway Administration (5) on the life expectancy of highway bridges.

REFERENCES

1. Murdock, J. W. A Critical Review of Research on Fatigue of Plain Concrete. Eng. Exp. Station, Univ. of Illinois, Bull. 475, 1965.
2. Miner, M. A. Cumulative Damage in Fatigue. Trans. ASME, Vol. 67, 1945.
3. Dixon, W. J. BMD-Biomedical Computer Programs. Univ. of California, 1968.
4. Murdock, J. W., and Kesler, C. E. Effect of Range of Stress on Fatigue Strength of Plain Concrete Beams. ACI, Jour. Proc. Vol. 30, No. 2, Aug. 1958.
5. Ballinger, C. A. The Effect of Load Variations on the Flexural Fatigue Strength of Plain Concrete. U.S. Dept. of Transportation, Federal Highway Admin., Office of Research, Aug. 1971.

USE OF SILICONE ADMIXTURE IN BRIDGE DECK CONCRETE

H. L. Patterson, Michigan Department of State Highways

This report is the third in a series that resulted from a cooperative study, originally started in 1963 and sponsored jointly by the Dow Corning Corporation of Midland, Michigan, and the Michigan Department of State Highways, to determine the effects of using a silicone admixture in bridge deck construction. The previous reports dealt with the construction and initial inspection of the Scotten Avenue bridge over Michigan Avenue in Detroit and of the Coe Road bridge over US-27 in Isabella County.

•THE EFFECTS OF SILICONES on concrete have been investigated for several years by the Dow Corning Corporation, a major producer of silicones. Their initial efforts were directed toward hardened concrete sealants, but more recently the company has been interested in the use of silicones as an admixture in concrete. This led to the development of DC-777, an admixture that is a water-soluble, straw-colored, liquid-reactive polysiloxane containing 100 percent silicone and weighing approximately 8.45 lb/gal. Dow Corning engineers found that, when it is added to concrete in the amount of 0.3 percent by weight of the cement, it produced the following characteristics: substantially retarded the set of the concrete (Table 1); entrained a significant amount of air; increased the bond, compressive, and flexural strengths; reduced the net water-cement ratio; and increased the resistance to scaling on concrete of low or moderate air content when ice-removal salts were used.

TEST BRIDGES

Scotten Avenue Over US-12 (Michigan Avenue)

Dow Corning personnel presented a summary of laboratory studies to Michigan Department of State Highways (MDSH) representatives in Midland on April 25, 1963, and in Lansing on May 9, 1963. At this time it was decided to select a bridge whose deck would test the effectiveness of the admixture. The Scotten Avenue bridge over Michigan Avenue in Detroit, originally constructed in 1941, was scheduled to receive a deck replacement under a major maintenance contract. It was decided to use the admixture in conjunction with blast-furnace slag coarse aggregate on this deck.

The structure is a 2-span, through plate girder design, 141 ft long with a clear roadway of 42 ft. Curb, sidewalk, and girder encasement pours on both sides of the deck result in an overall width of 62 ft 8 in. The northeast and southwest deck pours were to contain the silicone admixture concrete, whereas the northwest and southeast pours were to be of conventional air-entrained concrete. Construction was completed in October 1963. This bridge receives heavy urban traffic and heavy winter salting for snow removal. Figure 1 shows profile and approach views of this bridge as it appeared in 1969.

Coe Road Over US-27

The second structure selected in the study is a 4-span, prestressed concrete I-beam bridge that carries Coe Road, a rural county road, over US-27, a limited-access,

Sponsored by Committee on Chemical Additions and Admixtures for Concrete.

divided highway, 6 miles north of Alma. The silicone admixture in conjunction with limestone coarse aggregate was used on this bridge. The bridge has a 24-ft roadway and a total length of 208 ft. All but 13 ft of the west half of the bridge deck was constructed with silicone admixture concrete, whereas the remainder was constructed with conventional air-entrained concrete containing a water-reducing and set-retarding admixture. Construction was completed in October 1964. This bridge receives light rural traffic and no salting in the winter. Figure 2 shows the profile and approach views of the bridge as it appeared in 1969.

TABLE 1

COMPARISON OF HOURS OF SETTING TIME

Temperature (F)	Normal Concrete[a]		Concrete With 0.3 Percent DC-777[a]	
	Initial	Final	Initial	Final
40	10¼	15¼	52	63
60	6	8	31¼	37
80	4	5¼	23	29
100	2	3	15	24

[a]Determined by ASTM Method C 403 (Test for Time of Setting of Concrete Mixtures by Penetration Resistance).

Figure 1a

Figure 1b

Figure 1. Scotten Avenue bridge over Michigan Avenue: (a) general view of bridge deck looking northwest and (b) profile view looking west along Michigan Avenue.

Figure 2a

Figure 2b

Figure 2. Coe Road bridge over US-27 south of the village of Shepherd: (a) general view of bridge deck from the west approach and (b) k profile view looking northwest.

Eastbound M-78 Over the Grand Trunk and Western Railroad

The third structure selected in the study is a 3-span steel stringer bridge carrying eastbound M-78, a limited-access, divided highway, over the Grand Trunk and Western Railroad southwest of Flint. The bridge has a deck width of 38 ft 6 in., is 203 ft long, and has end spans that cantilever over their piers to support the suspended center span. The silicone admixture in conjunction with concrete containing gravel coarse aggregate was used on this bridge. The bridge deck and curb pours of the center span are cast with the silicone concrete, whereas the end spans have normal concrete that is air entrained and contains a water-reducing and set-retarding admixture. At the date of the construction of this bridge, Dow Corning engineers had modified their silicone admixture such that it could be used with regular air-entrained cement without entraining an excessive amount of air. The modified material was designated DC-777B. Construction was completed in September 1967, and the bridge currently receives heavy traffic and moderate salting for snow removal. Figure 3 shows profile and approach views of the bridge as it appeared in 1969.

EVALUATION

Slag Coarse Aggregate

The Scotten Avenue bridge deck in urban Detroit was covered with a concrete mix containing blast-furnace slag coarse aggregate and 6 sacks/cu yd of cement. The concrete was mixed in transit by ready-mix trucks, placed by a crane-lifted concrete

Figure 3a

Figure 3b

Figure 3. Eastbound M-78 bridge over the Grand Trunk and Western Railroad, southwest of the city of Flint: (a) general view of bridge deck looking west and (b) profile view looking northeast.

bucket, and hand screeded and finished. The deck concrete was cured with 4-mil white polyethylene and applied as soon as the surface moisture was gone.

Slag coarse aggregate has the advantage in bridge deck construction of reducing the bridge deck dead load by 10 percent, minimizing surface and internal disruptions caused by freeze-thaw vulnerable deleterious materials, and being cheap and readily available in this area. It has the disadvantages of being brittle, containing small amounts of iron, and having a high water-absorption capacity.

Because the original silicone admixture entrained air, Type I cement was used throughout the deck; an air-entraining admixture was added to supply the necessary air for the normal concrete.

Data given in Table 2 show that the water-cement ratio of the normal concrete was higher than that of the silicone concrete. This is because the deck was constructed before the Michigan Department of State Highways adopted water-reducing and set-retarding admixtures for use in bridge deck concrete to accommodate machine finishing. To achieve a 4-in. slump required that the water-cement ratio of the normal concrete be significantly higher than that for the silicone concrete because the silicone admixture acted as an internal lubricant in the mix. Thus, the silicone admixture effectively reduced the amount of water required to obtain a 4-in. slump.

TABLE 2
CHARACTERISTICS OF FRESH CONCRETE

Bridge	Coarse Aggregate	Concrete	Pour Date	Span	Cement		Net Water-Cement Ratio	Fine Aggregate/ Total Aggregate (percent)	Slump (in.)	Air (percent)	Admixture per Sack[a]
					Type	Sacks/ Cu Yd					
Scotten Avenue	Slag	Normal			I	6	0.49	50	4.1	6.6	2.5 oz AE
		Silicone			I	6	0.40	49	4.7	7.3	0.3 lb DC-777
Coe Road	Limestone	Normal			I	6	0.40	42	4.1	6.2	3.0 oz WR and SR, 1.5 oz AE
		Silicone			I	6	0.39	42	4.1	8.1	0.3 lb DC-777
M-78 Deck	Gravel	Normal	8-14-67	1	IA	6	0.43	35	4.0	6.5	4.0 oz WR and SR, 0.5 oz AE
		Silicone	8-11-67	2	IA	6	0.43	35	4.0	7.5	0.25 lb DC-777B, 0.25 oz AE
		Normal	8-16-67	3	IA	6	0.42	35	4.5	7.1	4.0 oz WR and SR, 0.5 oz AE
Curb	Gravel	Normal	8-25-67	1	IA	6	0.44	33	3.0	8.5	3.0 oz WR and SR, 1.38 oz AE
		Silicone	8-30-67	2	IA	6	0.44	33	3.3	7.6	0.25 lb DC-777B, 0.25 oz AE
		Normal	8-29-67	3	IA	6	0.44	33	3.0	7.9	3.0 oz WR and SR, 1.25 oz AE

[a]AE = air-entrained agent; WR = water-reducing agent; and SR = set-retarding agent.

In the laboratory, the performance of the silicone concrete field specimens was superior to that of the normal concrete in both strength and shrinkage measurements (Table 3). This could have been the combined effect of 2 factors: first, the beneficial effect of the silicone admixture; and, second, the lower water-cement ratio of the silicone concrete. The measurements are the average of several specimens that were sampled at various times during the pour. The compressive strength, flexure strength, and shrinkage measurements were measured respectively from the 4- by 8-in. cylinders, 3- by 4- by 16-in. beams, and 3- by 3- by 15-in. prisms cast with stainless steel end studs. The complete test data for the bridge are contained in the original report (1).

A field inspection was conducted 6 years after the deck was poured and showed the entire deck to be functioning well. Figure 4 shows a diagram of all the deterioration features that were visible at the time of inspection. The plastic shrinkage cracks and

TABLE 3
LABORATORY TEST RESULTS OF FIELD SPECIMENS

Bridge	Coarse Aggregate	Concrete	Span	Average Compressive Strength (psi)		Average Flexural Strength (psi)		Shrinkage (percent)		
				7-Day	28-Day	7-Day	28-Day	7-Day	28-Day	3-Month
Scotten Avenue	Slag	Normal			4,610		660		0.017	0.044
		Silicone			6,080		860		0.009	0.036
Coe Road	Limestone	Normal			5,800		—		0.008	0.030
		Silicone			5,420		—		0.010	0.033
M-78 Deck	Gravel	Silicone	2	3,670	4,200	710	880	0.035	0.051	
		Normal	3	3,450	4,200	610	720	0.036	0.049	
Curb	Gravel	Normal	1	3,240	3,350	640	800	0.024	0.050	
		Silicone	2	3,450	3,860	710	830	0.042	0.059	

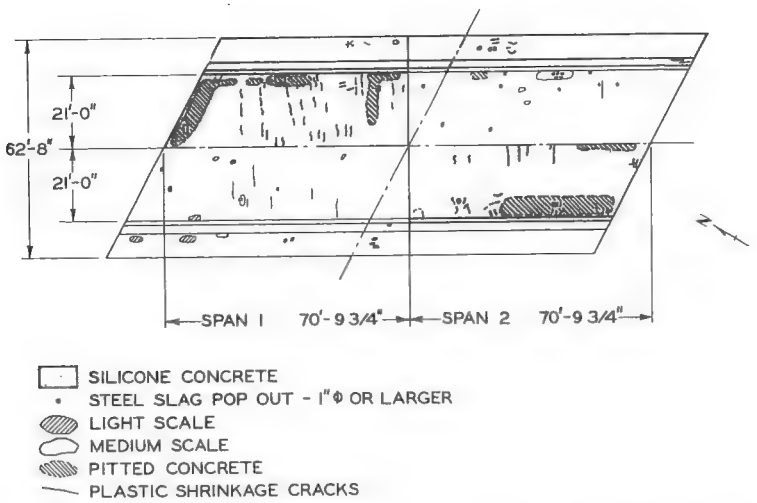

Figure 4. Surface deterioration observed on Scotten Avenue bridge deck containing slag coarse aggregate.

large pitted areas were generally confined to the silicone concrete, whereas the scaled areas and rusted iron pop-outs were generally confined to the normal concrete.

The plastic shrinkage cracks in the silicone developed within 36 hours after finishing and were prominently visible at that time. Three known conditions could have contributed to their formation: (a) the silicone concrete took 36 hours to set; (b) the slag aggregate, with its great absorption potential, had adequate time to absorb a significant amount of mix water; and (c) the polyethylene sheeting, with which the deck was cured, could have allowed air movement underneath if it was not properly sealed around its perimeter. The first 2 factors are considered to be the most critical on this project.

The pitted areas seem to have been produced by traffic abrasion, to which slag aggregate appears to be vulnerable. On successive annual inspections, it was noted that surface features photographed the first year could not be identified the second year. Although this abrasion was by no means confined to the silicone concrete, it was more distinct there because of the unfavorable location it occupied on the bridge deck with respect to traffic. That is, the bridge was on a vertical curve and the nature of the traffic pattern was such that vehicles would be braking as they left either end of the bridge deck where the silicone concrete was located.

The few small scaled areas and scattered iron pop-outs on the bridge appeared to be confined to the normal concrete pours. This would indicate that the silicone was effective in preventing these types of deterioration. Figure 5 shows some of the most prominent deterioration features found on the deck.

Limestone Coarse Aggregate

In the bridge deck of rural county Coe Road, the concrete mix contained limestone coarse aggregate and 6 sacks/cu yd of cement. Limestone coarse aggregate (6AA) has the advantage in bridge deck construction of providing a uniform, dense material that has a high compressive load capacity and low absorption. Because of these properties, it is very resistant to freeze-thaw deterioration.

Limestone coarse aggregate has the disadvantage of producing a harsh mix, being relatively soft, and being relatively expensive. The harshness is caused by the irregular angular shape of the crushed limestone and can only be rectified by increasing the percentage of the aggregate in the mix. This increases the volume of the mortar,

Figure 5a

Figure 5b

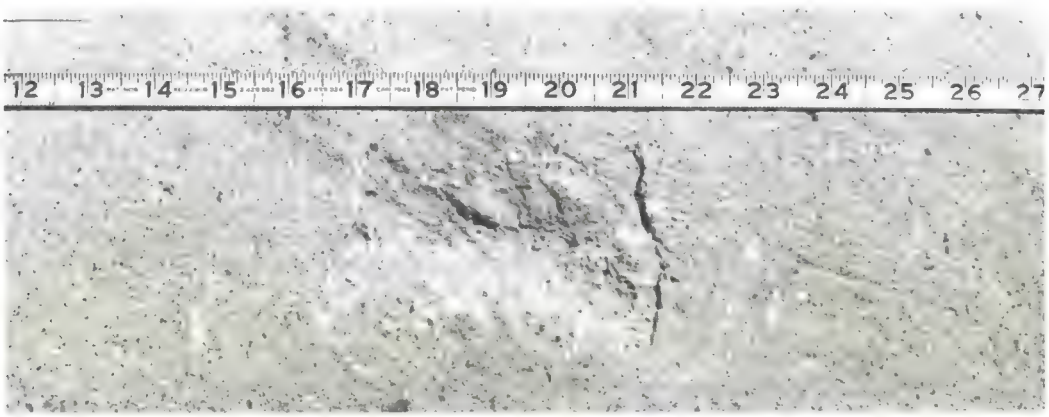

Figure 5c

Figure 5. Deterioration on the Scotten Avenue bridge: (a) typical plastic shrinkage cracks found in silicone concrete, (b) light pitting to which slag aggregate appears vulnerable, and (c) 3- by 5-in. scale spot caused by volume expansion of rusting iron.

dilutes its cement content, and increases the water-cement ratio. The softness of the limestone makes it vulnerable to traffic abrasion.

As with the Detroit bridge, Type I cement was used throughout the deck because the silicone admixture entrained the air. A water-reducing set-retarding admixture and an air-entraining admixture were added to the control or normal concrete. The concrete was mixed in transit by ready-mix trucks, placed by a crane-lifted bucket, and finished by a transverse screeding machine. The concrete was sprayed with a white curing membrane applied at 200 sq ft/gal soon after finishing.

Table 2 gives the water-cement ratio, the rest of the mix proportioning, and the slump; these were nearly the same for both the silicone and normal concretes. They differed only in that the silicone concrete contained about 2 percent more entrained air.

Table 3 gives the results of the tests of the field specimens that were cured and tested in the laboratory. The normal concrete, aided by its water-reducing and

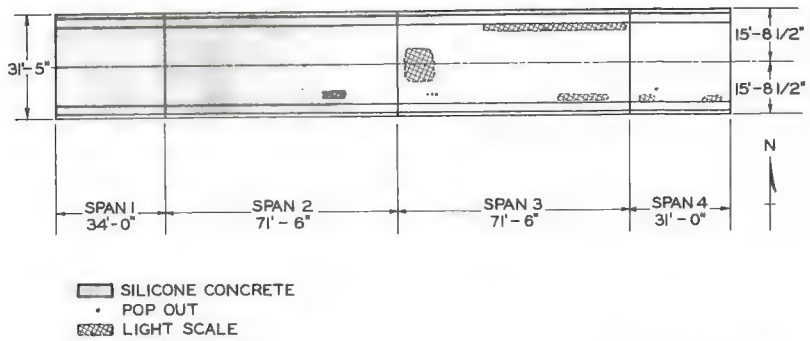

Figure 6. Surface deterioration observed on Coe Road bridge deck containing limestone coarse aggregate.

set-retarding admixture, produced very impressive results, even slightly surpassing the performance of the silicone concrete. The compressive strength and shrinkage measurements were obtained from the 4- by 8-in. cylinders and 3- by 3- by 15-in. prisms cast with stainless steel end studs. No flexure strength beams were cast for this bridge. The complete test data for this bridge are contained in the original MDSH report (2).

A field inspection was conducted 5 years after the bridge was constructed, and showed the concrete to be in excellent condition. Figure 6 shows a diagram of the deterioration features on the deck that were visible at the time of the inspection. The silicone portion of the deck was completely unblemished except for 1 small scale spot. The normal concrete portion of the deck had developed a few areas of light scale and a very few pop-outs. These pop-outs were probably caused by deleterious materials that were introduced at the batching plant of the concrete company.

Gravel Coarse Aggregate

In the limited-access, divided-highway bridge deck on M-78, the concrete mix contained gravel coarse aggregate (6AA) and 6 sacks/cu yd of cement. The concrete was mixed in transit by ready-mix trucks, placed by a crane-lifted concrete bucket, and

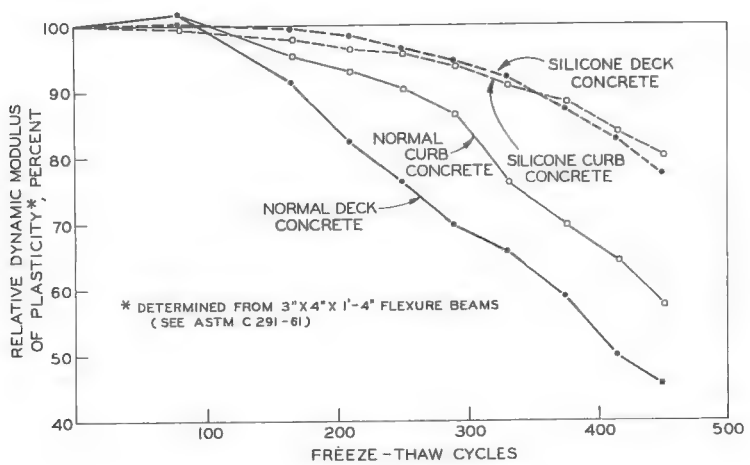

Figure 7. Internal freeze-thaw durability of beams cast from gravel coarse aggregate concrete used in M-78 bridge.

finished by a longitudinal screeding machine. The concrete was cured with a white membrane curing compound applied at 200 sq ft/gal.

Gravel has the advantage of being readily available, relatively cheap, and composed of an assortment of smooth rounded stones that will produce a very workable mix. Because of its workability, the percentage of fine aggregate can be minimized and produce a strong rich mortar. Gravel has the major disadvantage of being composed of a random assortment of rock types, some of which are considered to be deleterious.

Because freeze-thaw susceptible aggregates generally have low specific gravities, the quality of gravel can be improved by the heavy media process that separates the lighter particles from the heavier ones. Although this process improves the aggregate, it by no means makes it ideal because some stones of marginal quality are retained. When freeze-thaw conditions cause these frost-susceptible particles to disintegrate, they disrupt the concrete that surrounds them and make it vulnerable to further damage.

In 1967, when this deck was poured, the Dow Corning Corporation had incorporated a defoaming agent into its silicone admixture that allowed it to be used with conventional air-entrained cement. This modified version of the original admixture was designated DC-777B. Thus, all the cement used in this bridge was Type IA.

Table 2 gives the important properties of the fresh concrete used throughout the deck and curb pours of this bridge. The silicone concrete data are from span 2, and the normal concrete data are from spans 1 and 3. Little difference exists between the properties shown for the 2 types of concrete.

Table 3 gives the results of some of the laboratory tests run on field specimens. The silicone concrete in every case tested higher in both compression and flexure. In shrinkage, however, the normal concrete shrank less than the silicone concrete.

For this bridge, scaling slabs and freeze-thaw beam specimens were cast in addition to the compression (4- by 8-in. cylinders), flexure (4- by 4- by 16-in. beams), and shrinkage (3- by 3- by 15-in. prism) specimens. They were all covered with polyethylene film at the bridge site and allowed to harden before being moved to the moist-curing room in the laboratory.

By means of dynamic testing apparatus, the fundamental transverse vibration frequencies of the 3- by 4- by 16-in. freeze-thaw beams were measured initially and at subsequent regular intervals throughout the rapid freeze-thaw testing. Figure 7 shows the relative dynamic modulus of elasticity plotted against freeze-thaw cycles. The results of this testing indicate the silicone concrete to be superior to normal concrete in resisting internal freeze-thaw damage; this apparently was the result of a resistance to absorption that the silicone furnished to deeply embedded deleterious particles.

The scaling slabs were 9 in. wide, 12 in. long, and $2\frac{1}{2}$ in. thick and had a 1-in. high mortar dike around the perimeter to retain water. During the testing procedure, the slabs were placed on a mobile rack and pushed into the freezer at night. They were withdrawn in the morning, thus giving a freeze-thaw cycle per day (about 0 to 70 F). At the end of each 15 cycles, the slabs were returned to the concrete laboratory, scrubbed under running water, and set up to dry; their surface condition was then studied, evaluated, and photographed. On alternate days during the first 60 cycles, the slabs were placed in ponds of water and a 3 percent salt solution. Figure 8 shows the scaling slabs of silicone deck concrete before and after 45 freeze-thaw cycles. Although the slabs developed several pop-outs, they developed only light scale.

Figure 9 shows scaling slabs cast of normal concrete before and after 45 freeze-thaw cycles. The surface not only developed many pop-outs but also developed extensive medium scale. Figure 10 shows the observed severity of the scale on all of the normal and silicone concrete scaling slabs through 200 freeze-thaw cycles. The evaluating rating system ranges from 1 to 5, where 1 represents no scale and 5 represents heavy scale. The values shown are the average ratings for 3 specimen slabs of each concrete pour. A comparison of Figures 8 and 9 shows that the silicone concrete has much more resistance to frost-inflicted scaling than the normal air-entrained concrete. It would appear from Figure 8 that frost-susceptible particles lying close to the top surface of the concrete receive little protection, but the same type lying slightly deeper appear to be better protected.

The field inspection of this bridge made 2 years after the bridge was completed showed some contrasting features with the other bridges described in this report.

Figure 8a

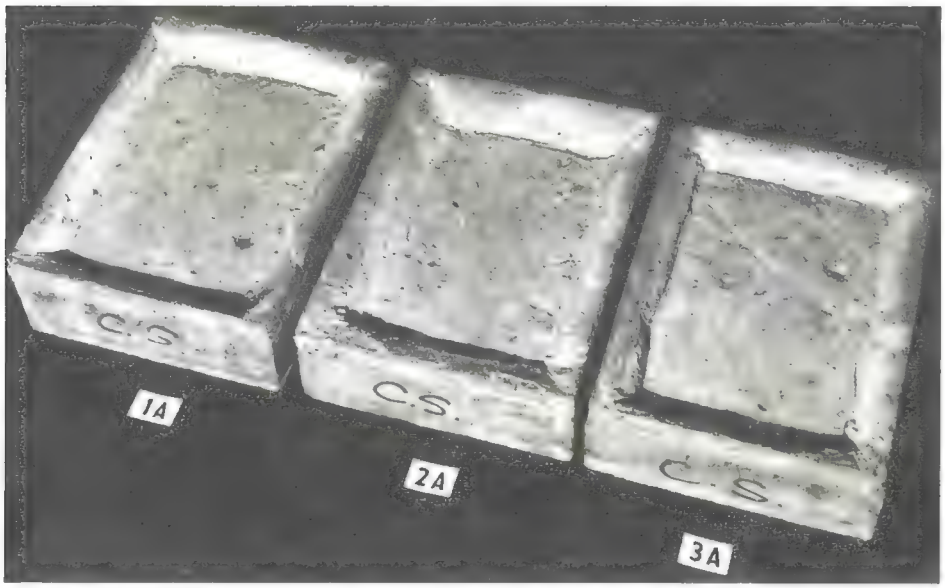

Figure 8b

Figure 8. Laboratory scaling slabs cast from silicone deck concrete used in span 2 of M-78 bridge (a) before testing and (b) after 45 freeze-thaw cycles.

Figure 9a

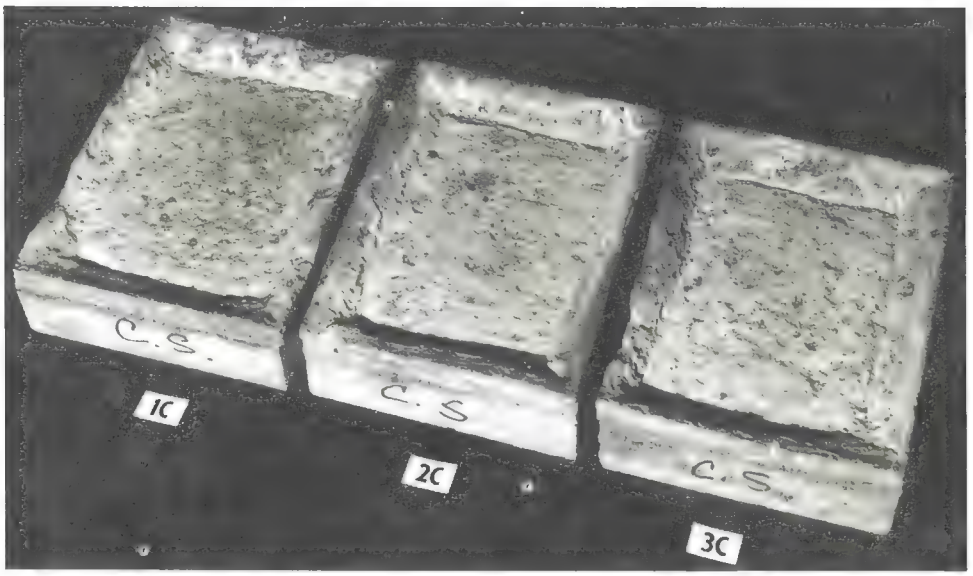

Figure 9b

Figure 9. Laboratory scaling slabs cast from normal deck concrete used in span 3 of M-78 bridge (a) before testing and (b) after 45 freeze-thaw cycles.

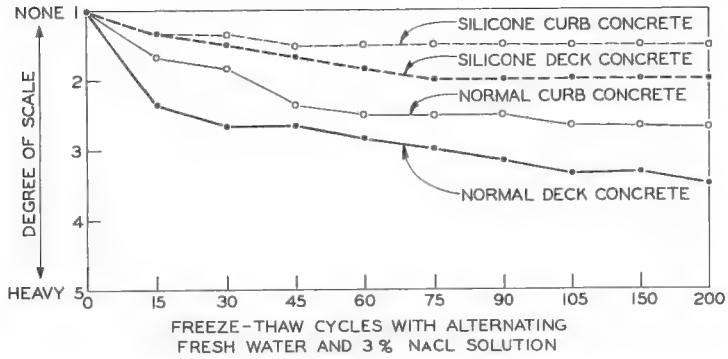

Figure 10. Surface freeze-thaw durability of scaling slabs cast from gravel coarse aggregate concrete used in M-78 bridge.

Figure 11 shows a diagram of the deterioration features that were visible at the time the deck was inspected; included are pop-outs and craze cracking in all 3 spans and light scale in span 3. The most prominent of these were the numerous pop-outs that developed uniformly over the entire deck surface; they developed in a pattern consistent with laboratory observations and suggested that the silicone admixture provided little protection for the frost-susceptible particles in the gravel lying close to the top surface of the concrete. Figure 11 also shows that both types of concrete developed large areas that were craze cracked. This type of cracking is generally the result of early surface shrinkage and could be caused by conditions similar to those that produce plastic shrinkage cracks.

Scaling is minor on this deck, being confined mainly to the south curb line in span 3 where the longitudinal screeding machine left the heaviest concentration of laitance. Because this thin layer of silt and cement was weak and brittle, it was soon removed by weathering and traffic abrasion and now gives the specious impression that the rapid destruction of the concrete is imminent; however, the concrete below laitance generally presents a more formidable surface. Figure 12 shows some of the prominent deterioration features described previously.

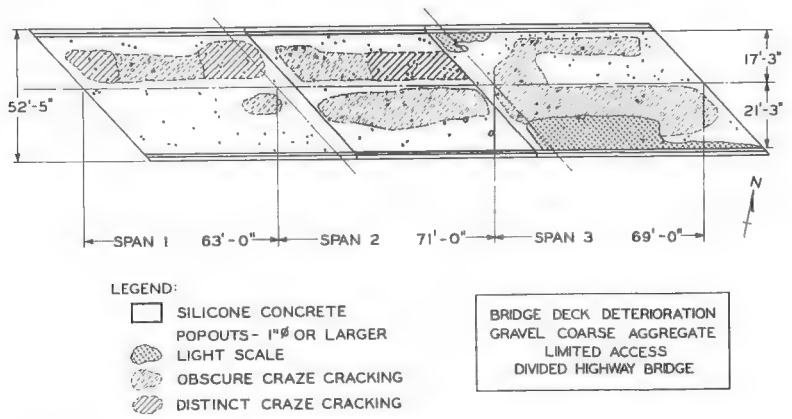

Figure 11. Surface deterioration observed on M-78 bridge containing gravel coarse aggregate.

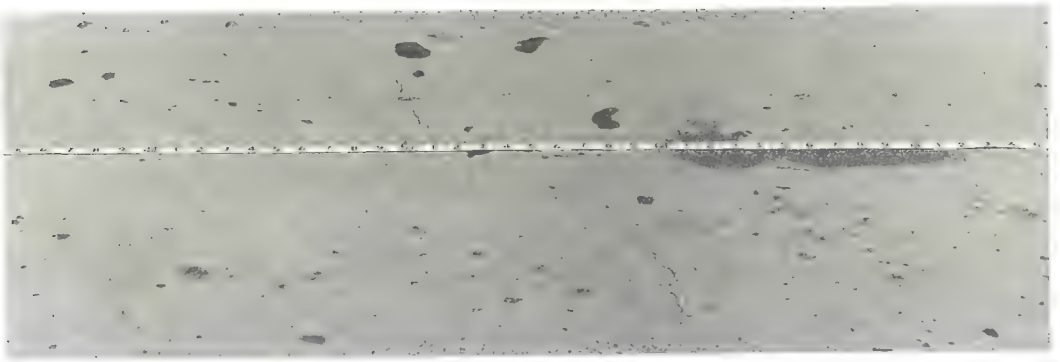

Figure 12a

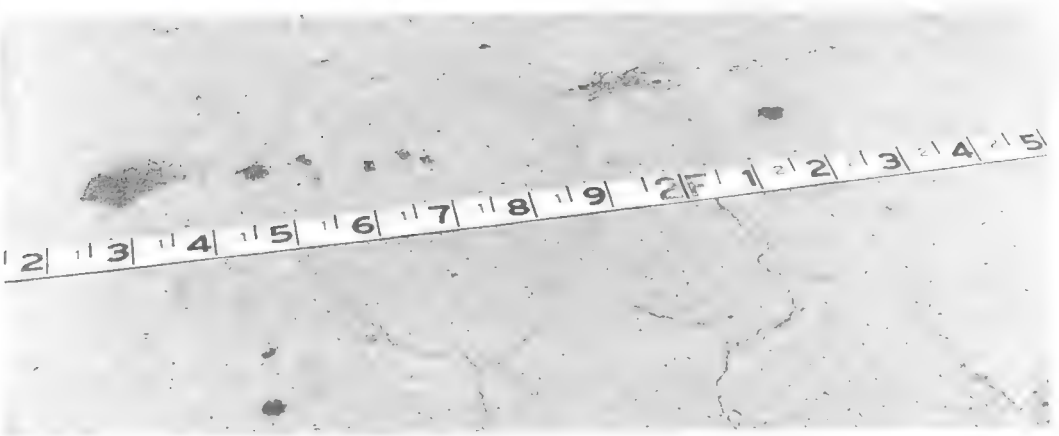

Figure 12b

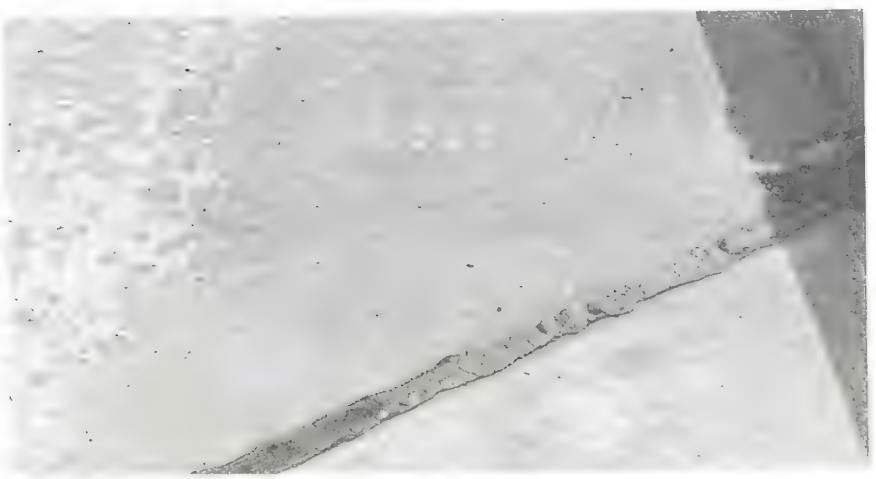

Figure 12c

Figure 12. Deterioration on M-78 bridge included (a) pop-out concentration in traffic lane of span 2 and typical across entire deck, (b) distinct craze cracking area in traffic lane of span 2, and (c) light scaling of thin laitance coat along south curb line in span 3.

CONCLUSIONS

The basic liquid silicone admixture DC-777, which was developed by Dow Corning, altered the properties of plain concrete in the following ways:

1. It entrained air;
2. It excessively retarded the set;
3. It served as an internal lubricant, permitting a reduction in mix water;
4. It raised the unit strength; and
5. It increased the resistance to freeze-thaw deterioration.

The basic admixture was later modified and designated DC-777B for use with regular air-entrained cement.

When compared with normal air-entrained concrete to which water-reducing and set-retarding admixtures have been added, the strength advantages of the silicone admixture concrete are somewhat reduced but still include greater resistance to freeze-thaw deterioration.

The silicone admixture seems to function equally well with any of the 3 coarse aggregates described in this report; blast-furnace slag, limestone, and gravel. Although it offers excellent protection to the concrete against scaling, it affords less protection to frost-susceptible particles found in gravel and the iron particles found in slag. The deleterious particles that appeared to be particularly susceptible were those lying immediately at the surface; those embedded deeper in the concrete appeared to receive some protection. This conclusion is based on the superior performance of the silicone concrete in the dynamic modulus freeze-thaw testing conducted in the laboratory.

Although two of the bridges developed some type of shrinkage cracks in the silicone concrete, it was not conclusive that the admixture's set retardation was the main cause; however, it could have contributed significantly in the high-porosity slag concrete that was cured with polyethylene film. The limestone concrete developed no shrinkage cracks, and the craze cracking in the gravel concrete was common to both the silicone and the normal concrete.

In general, the liquid silicone admixture DC-777B could be described as being beneficial to the concrete, particularly in retarding the formation of scale as observed on all 3 test bridges. Rapid freeze-thaw testing conducted in the laboratory revealed the treated concrete to have a superior resistance to internal freeze-thaw breakdown. Whereas the test bridges have shown the silicone concrete to be somewhat superior to normal concrete, they are not old enough at this time to establish a substantial superiority.

The quantity price of the admixture is about $3.50 per pound and would add $6.00 to the cost of a cubic yard of concrete containing 6 sacks of cement, when used at the recommended rate of 0.3 pound of silicone per sack of cement.

REFERENCES

1. Brown, M. G., and Merrill, R. H. Use of a Silicone Admixture in Bridge Deck Concrete. Michigan Department of State Highways, Res. Rept. R-463, June 1964.
2. Merrill, R. H., and Zapata, C. A. Use of a Silicone Admixture in Bridge Deck Concrete. Michigan Department of State Highways, Res. Rept. R-529, Sept. 1965.

MICROSTRUCTURE AND STRENGTH OF THE BOND BETWEEN CONCRETE AND STYRENE-BUTADIENE LATEX-MODIFIED MORTAR

J. E. Isenburg and D. E. Rapp,
The Dow Chemical Company, Midland, Michigan;
E. J. Sutton,* City of Midland; and
J. W. Vanderhoff,* Lehigh University, Bethlehem, Pennsylvania

Various surface preparations were used in resurfacing concrete with a latex-modified mortar. A 1-in. mortar cap was applied to the circular surface of 14-day old, high early strength concrete cylinders treated in various ways. After aging 14 days, several cylinders of each group were fractured in a shear bond test, and an unfractured cylinder was sawed to provide a ½-in. cube that included the interface between concrete and mortar. These cubes were fractured normal to the interface, producing a surface free of sawing artifacts. After they were examined in the scanning electron microscope, these sections were fractured again to simulate the shear bond test and then reexamined. Several performance variations are explained by the scanning electron photographs.

•CONSIDERABLE RESEARCH EFFORTS for the past 15 years have been devoted to the use of styrene-butadiene and vinylidene chloride copolymer latexes in the modification of portland cement systems. These materials have been used to resurface old concrete floors, roads, and bridges where the bond strength of a thin-mortar overlay is extremely important (1, 2). The purpose of this study is to show the effect of various parameters on the physical properties and morphology of styrene-butadiene latex-modified mortar overlays on aged concrete substrates, i.e., to reproduce in the laboratory the various methods of resurfacing the deteriorated surfaces of concrete highways and bridge decks and to compare these methods according to the shear bond strength and morphology of the composite. The parameters studied were the various techniques for the preparation of the concrete substrate surface and for the application of the latex-modified mortar to this substrate.

SHEAR BOND STRENGTH TESTS

Preparation of Specimens

The mix used for the concrete substrates is given in Table 1. The substrates were prepared in the form of cylinders (3.4 in. diameter, 6.5 in. height) by casting the mix in a cardboard carton. The circular top surface was finished by troweling, and the cylinders were cured under wet towels for 24 hours at room temperature. The cartons were then cut away, and the concrete cylinders were placed upright on the troweled ends and were cured in a fog room for 13 days at 73 F and 100 percent relative humidity (RH). The compressive strengths of these cylinders at 7 and 14 days were about 5,000 and 6,000 psi respectively.

*When this research was performed, Messrs. Sutton and Vanderhoff were with The Dow Chemical Company.

Sponsored by Committee on Basic Research Pertaining to Portland Cement and Concrete.

TABLE 1
CONCRETE SUBSTRATE MIX

Component	Parts by Weight
Crushed dolomitic limestone, 25A[a]	293
Natural sand, 2NS[a]	200
High early strength portland cement	100
Water	61.4
Total	654.4
Compressive strength of 4- by 8-in. cylinders, psi	
14 days	6,070
28 days	6,530

[a]The aggregates meet the designated specifications of the Michigan Department of State Highways.

TABLE 2
MORTAR OVERLAY MIXES

Component	Parts by Weight	
	Overlay Containing Latex	Control Overlay
Natural sand, 2NS	324	324
Styrene-butadiene copolymer latex, 48 percent solids	31	—
High early strength portland cement	100	100
Water	21.4	61.4
Total	476.4	485.4
Air content, percent[a]	8.0	8.8
Compressive strength of 4- by 8-in. cylinders, psi		
14 days	5,150	6,010
28 days	5,350	5,900

[a]ASTM Method C 185-59 (Standard Method of Test for Air Content of Hydraulic Cement Mortar).

The mixes used for the overlays are given in Table 2. The concrete cylinders that had aged for 14 days were removed from the fog room and the troweled ends were sandblasted to prepare the surface for the application of the overlay. Then a section of another carton was taped around the sandblasted end, forming a cylindrical mold with the top 1 in. above the sandblasted surface. The surface was wet, a thin layer of the latex-modified mortar was brushed into it to ensure good contact, and then the rest was added and tamped in. Finally, the top was struck to form a 1-in. thick mortar layer. The composite was damp-cured for 24 hours and was then cured for 14 days at 73 F and 50 percent RH. In addition, 7 variations of this standard sample were prepared: composite was aged 7 instead of 14 days before testing; composite was aged 3 days before testing; overlay was "vibrated on" the substrate instead of being brushed and tamped; substrate was a 2-year-old specimen taken from a road; substrate was sandblasted but not wet; substrate was wet but not sandblasted; and overlay was of control mortar mixture without latex.

The control mortar overlay was damp-cured for 24 hours and then for 14 days at 100 percent RH in a fog room. Five specimens were prepared for each variation. After the appropriate aging time, four of these were fractured in the shear bond strength test, and the fifth specimen was sectioned and examined by scanning electron microscopy.

TABLE 3
SHEAR BOND STRENGTH

Sample	Shear Bond Strength, psi[a]	Probability That Strength of Standard Sample Is Greater
Standard	474	—
Composite		
Aged 7 days	391	97
Aged 3 days	319	99
Overlay vibrated on	418	90
Two-year-old concrete substrate	428	69
Substrate not wet	528	—[b]
Substrate not sandblasted	385	94
Control (without latex)	249	99 —[c]

[a]Average of 3 specimens for 2-year substrate; average of 4 specimens for all others.
[b]Because 528) 474, probability that substrate not wet) standard = 90 percent.
[c]Also probability that 7-day composite) 3-day composite = 94 percent and probability that 2-year substrate) control = 97 percent.

Shear Bond Strength Test Results

After aging, the cylinders were tested in shear bond (1). Observations were made of the mode of fracture, i.e., through the overlay or through the substrate. The average values of the shear bond strengths are given in Table 3. In general, the shear bond strengths of the latex-modified mortar are nearly twice as great as that of the control mortar.

Statistical Analysis of Results

These averages are derived from the results of only 4 tests, which showed some experimental scatter. The usual methods of statistical analysis are not applicable in this case because of the small number of specimens and the expectation that the statistical distribution of test results are not necessarily a normal distribution.

Therefore, these data were analyzed by the Wilcoxon Test (3), which was developed to treat cases of this kind. As an example of the Wilcoxon Test, the following comparison between the standard sample and the 7-day composite sample gives individual values of the shear bond strength of each sample ranked in decreasing order: standard—508, 496, 478, and 413 psi; and 7-day composite—418, 404, 379, and 364 psi. These values are then combined and ranked according to the highest, second-highest, third-highest, and so forth: standard—1st, 2nd, 3rd, 5th, sum 11; and 7-day composite—4th, 6th, 7th, 8th, sum 25.

The disparity between the preceding sums is 25 - 11, or 14. From the tables given in Siegal's Study (3), the probability is only 0.029 that a disparity equal to or greater than this value will occur as a random variation. The results of these comparisons are given in the last column of Table 3. The data given in Table 3 show that the shear bond strength increased progressively with aging times of 3, 7, and 14 days. This was corroborated by the mode of fracture: completely at the interface in the 3-day samples; entirely through the substrate at some distance from the interface in the 14-day samples. Also, the brushing technique in the latex-modified mortar gave higher strengths than the vibrating technique. For the surface preparation, the unwet but sandblasted sample displayed higher strengths than the wet and sandblasted sample, which in turn displayed higher strengths than the wet but not sandblasted sample. In all comparisons, the shear bond strengths of the latex-modified samples were significantly greater than those of the control sample. The only comparison of doubtful significance was that between the standard and the 2-year-old concrete substrate samples; however, the latter sample had only 3 specimens, with considerable experimental scatter.

SCANNING ELECTRON MICROSCOPY

Preparation of the Specimens

For examination in the scanning electron microscope (4), the fifth (untested) cylindrical specimen of each sample was sectioned with a diamond saw to produce a ½-in. cube, which contained almost equal amounts of the overlay and the substrate. This cube was fractured perpendicularly to the interface to produce two ¼-in. slabs, each showing an interior fracture surface spanning the interface between the overlay and the substrate. This ¼-in. slab was positioned on the sample mounting stub, coated under vacuum with evaporated gold, and examined in the Stereoscan Mark IIa scanning electron microscope. (This equipment is manufactured by the Cambridge Instrument Company, England, and is distributed by Kent Cambridge Scientific, Inc., Morton Grove, Illinois.) In some cases, color optical photomicrographs were made before the slabs were metalized, so that, when the sample was examined in the scanning electron microscope, the interface could be located and the various types of particles—limestone and sand grains—could be identified by their color, luster, and texture.

For some microscope specimens, the shear bond strength test was simulated by removing the ¼-in. slab from the mounting stub after examination, clamping the concrete end in a vise with the interface aligned with the lips, and pushing on the protruding end until it fractured. The 2 pieces were then remounted on the stub so that the salient features of the morphology of the interface could be compared. Qualitatively, the results correlated with the shear bond strength tests. Those specimens that fractured through the interface in the shear bond strength test usually gave clean fractures through the interface in the microscope samples. Also, those stronger samples that fractured through the concrete substrate usually did so in both cases.

Results of Scanning Electron Microscopy

Let us first consider the particle size and expected appearance of the ingredients used. The 25A crushed dolomitic limestone contains particles in the size range of 0.09 to 0.5 in. (2.4 to 13 mm). The 2NS natural sand passes a No. 4 sieve and is retained on a No. 100 sieve, which corresponds to the size range of 0.006 to 0.2 in. (0.15 to 4.8 mm). The average particle size of the latex is about 0.2 μm (0.0002 mm), and its particle size distribution is relatively narrow. Because the scanning electron

microscope offers a wide range of magnifications, a relatively large area (about 3 mm square) of each specimen was examined first at low magnification. Under these conditions, the limestone and sand grains could be identified easily by their shape or by reference to the optical color photomicrographs. Moreover, in most cases, the interface between the overlay and the substrate could be located precisely. Then, specific features of the morphology in this region thought to be of interest were examined in greater detail by increasing the magnification in regular steps to a much higher value. The morphology of the cement grains was altered by the hydration reactions, and the various crystalline forms observed are described in the following sections. The very small latex particles are perfect spheres in the mortar mix, but when dry the particles coalesce to form a continuous film in which the individual particles lose their identity. Therefore, the latex polymer would be expected to form an amorphous mass of coalesced particles having no distinguishing morphological characteristics.

The first sample described is the control mortar overlay (without latex) on the concrete substrate. Figures 1, 2, 3, and 4 show several series at increasing magnification; all except Figure 1a are scanning electron micrographs. The first series shows a fracture surface that is perpendicular to the overlay-substrate interface. In each micrograph, the interface is marked with arrows labeled I, and the area to be shown at higher magnification in the next micrograph is outlined by the corners; e.g., the outlined area shown in Figure 1b is the subject of Figure 1c. Figure 1a is a black and white copy of a color optical photomicrograph of the specimen before it was metalized. The interface could be seen clearly in the color photograph and was then marked as I

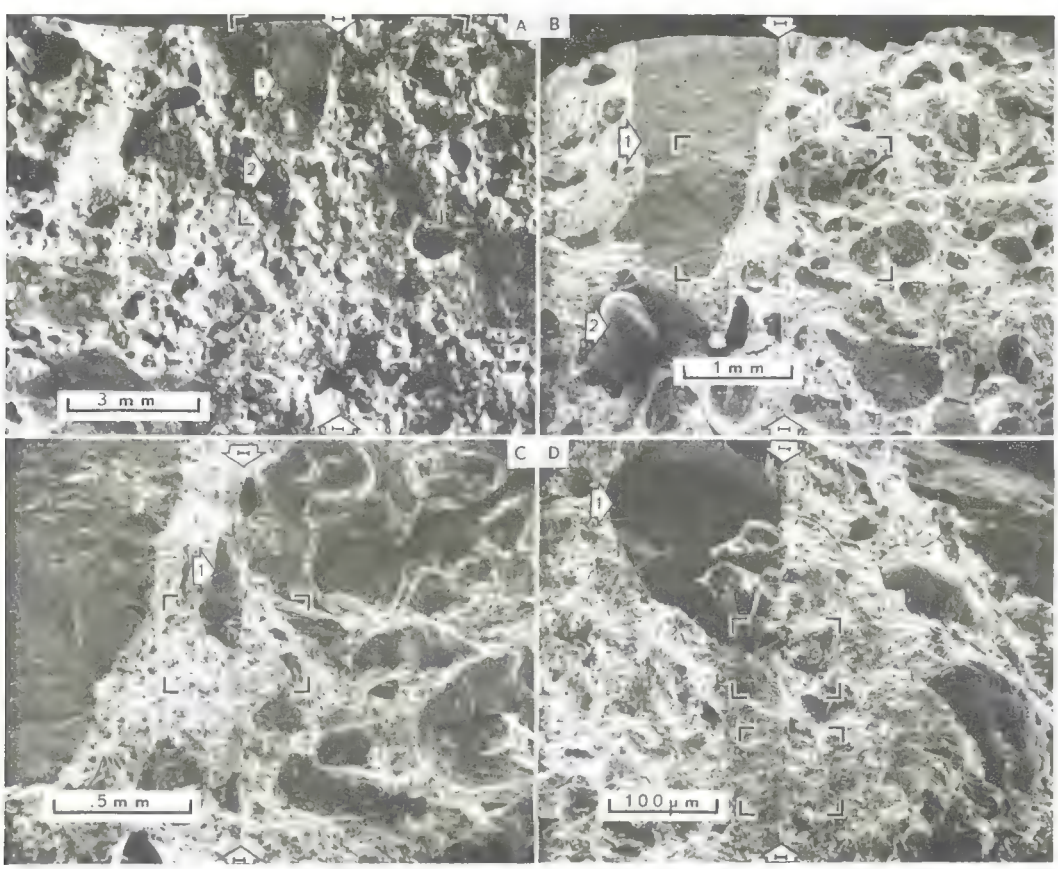

Figure 1. Control sample: overlay substrate interface.

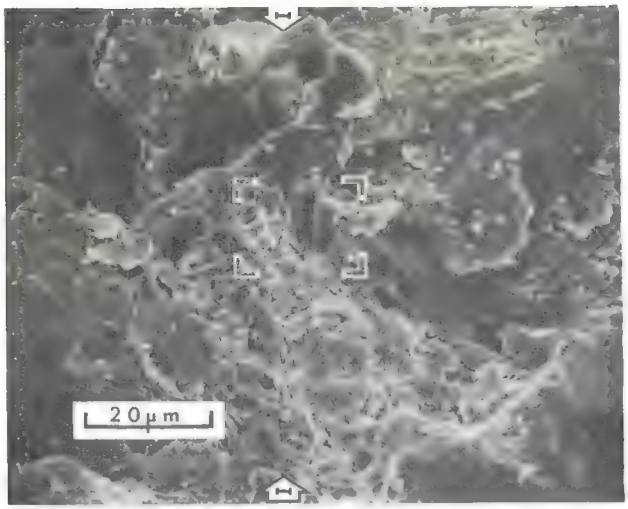

Figure 2a

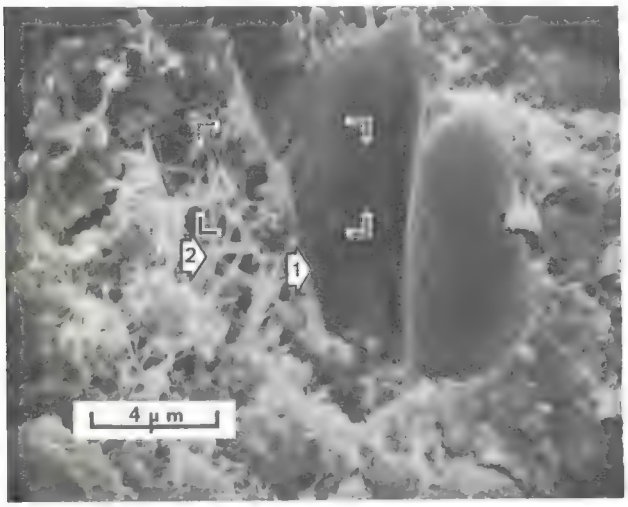

Figure 2b

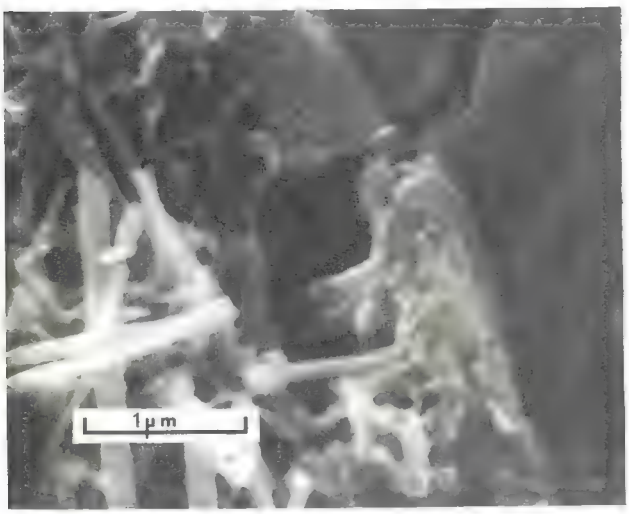

Figure 2c

Figure 2. Control sample: upper outlined area in Figure 1d.

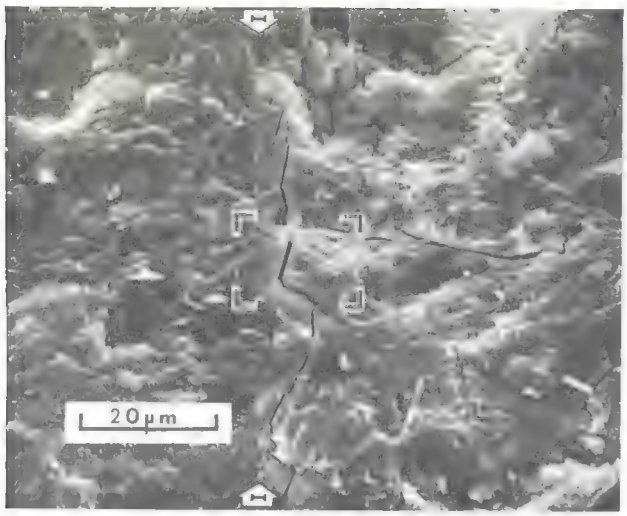

Figure 3a

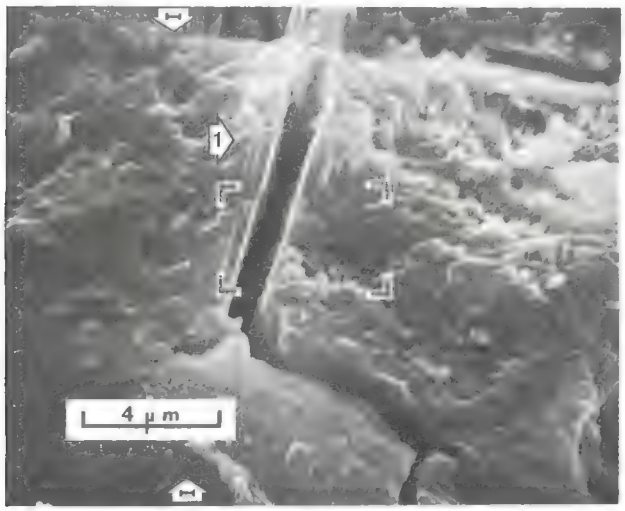

Figure 3b

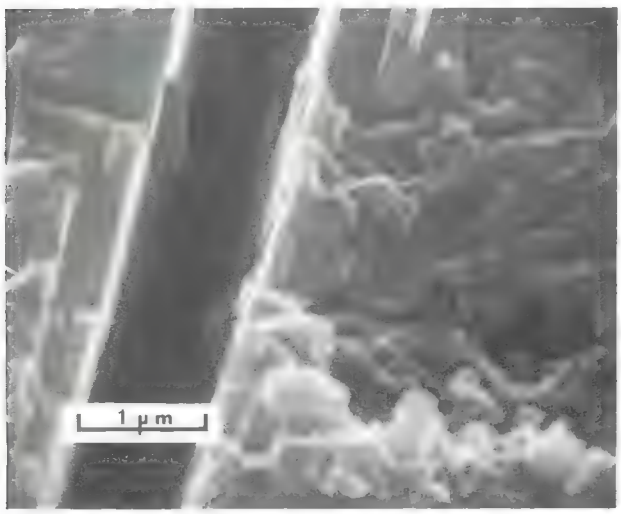

Figure 3c

Figure 3. Control sample: lower outlined area in Figure 1d.

on the black and white copy. The overlay is to the right and the substrate is to the left. A limestone grain (arrow 1) and a silica sand grain (arrow 2) can be identified in the substrate. A comparison of Figures 1a and 1b shows that the outlines of the limestone grain are shown much more clearly by scanning electron microscopy than by optical microscopy. For the silica sand grain, however, the luster and transparency that serve to identify it can be seen only in the optical photomicrograph. The sawed edge of the ½-in. cube can be seen at the top of both figures. The great depth of field of the scanning electron microscope is shown in Figure 1b; the specimen was tilted at an angle of 45 deg to the electron beam, yet almost all of it is in sharp focus.

Figures 1c and 1d show that the overlay-substrate interface is still apparent at higher magnification. Also, a sand grain flush with the surface of the substrate (arrow 1) can be seen in contact with the overlay.

The 2 areas outlined in Figure 1d are shown at higher magnification in Figures 2 and 3; the upper area is shown in Figures 2a, 2b, and 2c and the lower area is shown in Figures 3a, 3b, and 3c. Figures 2a and 3a show that the interface is less distinct at this higher magnification. Both figures show an extensive network of microcracks, which seem characteristic of the control mortar overlay near the interface. Figure 2b shows that the interface can no longer be distinguished and that the microstructure is characteristic of that of portland cement mortar observed at early aging times. One such feature is the layer of hydration products deposited on the surface of the sand grains; e.g., a sand grain was extracted by the fracturing, leaving a smooth imprint (arrow 1). It is also characteristic that the channels between the sand and cement grains are filled with a network of needle-like crystals (arrow 2). The needles and sand grain imprints are shown at higher magnification in Figure 2c. Figures 3a, 3b, and 3c show the microcrack structure of the overlay immediately adjacent to the interface. The fact that the periodic straight cracks are slanted at the same angle suggests that they are the result of cleavage of crystal masses lying along the interface. As shown in Figure 3b, the interface is believed to lie between the I arrows, and arrow 1 shows a structure interpreted as a crystal mass. The width of the microcrack shown in Figure 3c is 0.9 to 1.1 μm. Such microcracks must certainly indicate a point of weakness in the adhesion of the overlay to the substrate.

The 1/2-in. cube specimen was removed from the mounting stub and was fractured again to simulate the shear bond strength test. This new fracture provided a good example of failure at the interface. The specimen was remounted so as to expose the new fracture surface—the interface itself. Thus, Figure 4 shows micrographs of the overlay side of the interface exposed by the shear bond test. In Figure 4a, the edge of the specimen on the left side is part of the fracture surface shown in Figures 1, 2, and 3. The smooth area in the center is where the mortar was in contact with a limestone grain that was removed by the fracture, taking fragments of mortar with it and leaving the fragments of limestone. This was confirmed by examination of the limestone grain itself in the "mate" of the specimen. Figure 4b shows a hole left by the removal of a mortar fragment (arrow 1) and a fragment of limestone still adhering to the mortar (arrow 2). Figure 4c shows, however, that this fracture is not an ideal example of interfacial failure; actually, the failure occurred irregularly on both sides of the interface between the overlay and the substrate. Figure 4d shows irregular fractures through the mortar side of the interface. These fractures exposed channels between sand and cement grains similar to those shown in Figure 2b. These channels were also filled with networks of needle-like crystals (arrow 1). The needles are shown in greater detail in Figures 4e and 4f. In Figure 4f, the parallel striations along the axis of the needles are less than 0.05 μm (500 Å) apart, exemplifying the best resolution obtained to date with our scanning electron microscope.

Thus, Figures 1, 2, 3, and 4 show the following characteristics of the microstructure of the control mortar overlay on a concrete substrate after aging 28 days:

1. The open channels between the sand and cement grains are filled with networks of needle-like crystals;
2. The surfaces of the sand grains are covered with a layered deposit;
3. The overlay is veined with microcracks, some of which follow the overlay-substrate interface for a distance; and

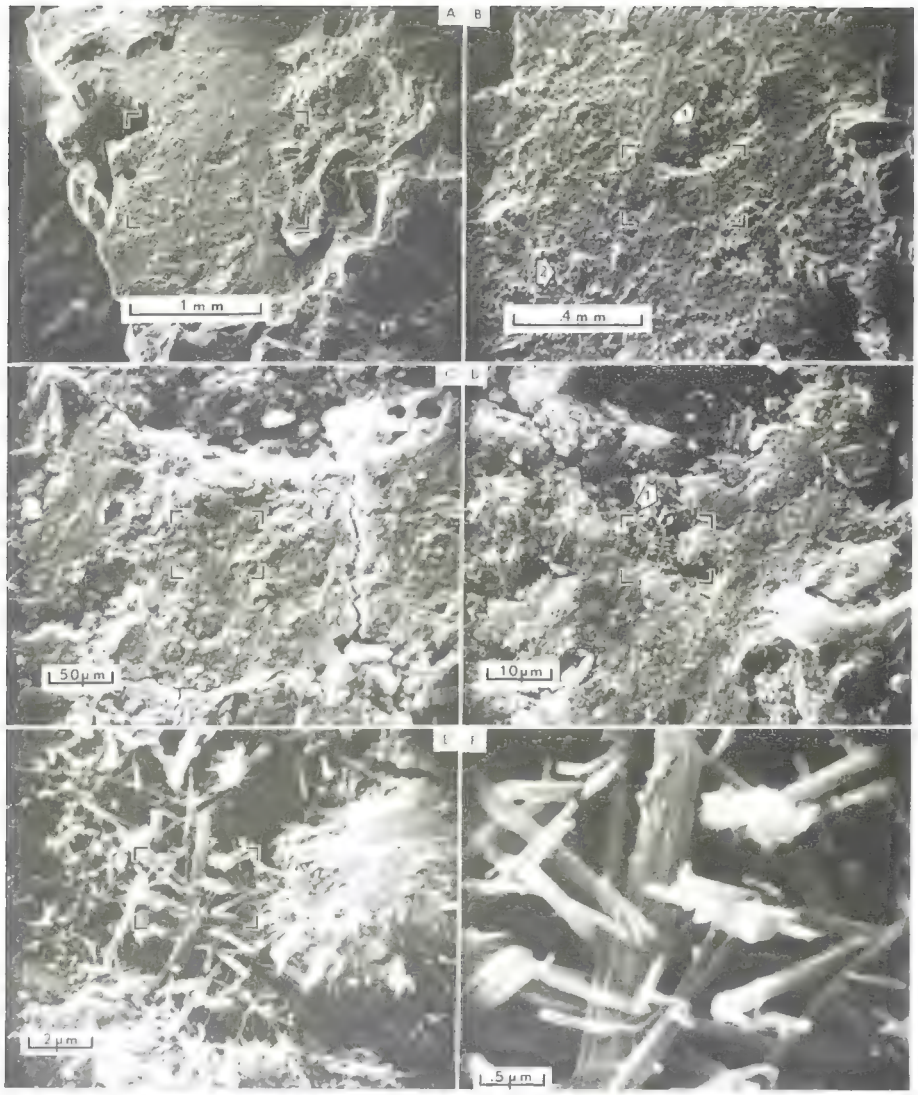

Figure 4. Control sample: overlay side of shear bond fracture.

4. The shear bond test fracture generally follows the interface, but sometimes it passes through weak areas on either side of it.

The technique of examining the samples fractured perpendicularly to the interface, fracturing them again to simulate the shear bond strength test, and then examining the mated interfaces generated by this new fracture has been applied to the other samples of this study. To date, more than 250 electron micrographs of these specimens have been examined. Space permits us to show only a few of the micrographs that demonstrate the usefulness of this technique in explaining the results of the shear bond strength tests.

It was shown previously that the shear bond strength of the latex-containing overlay was lower when the concrete substrate was not sandblasted. Figures 5, 6, and 7 show an explanation for this result. Figure 5 shows the overlay-substrate interface for the standard latex-containing mortar and the unsandblasted concrete substrate. In Figure 5a, the interface marked with the arrows I runs from the lower left to the upper

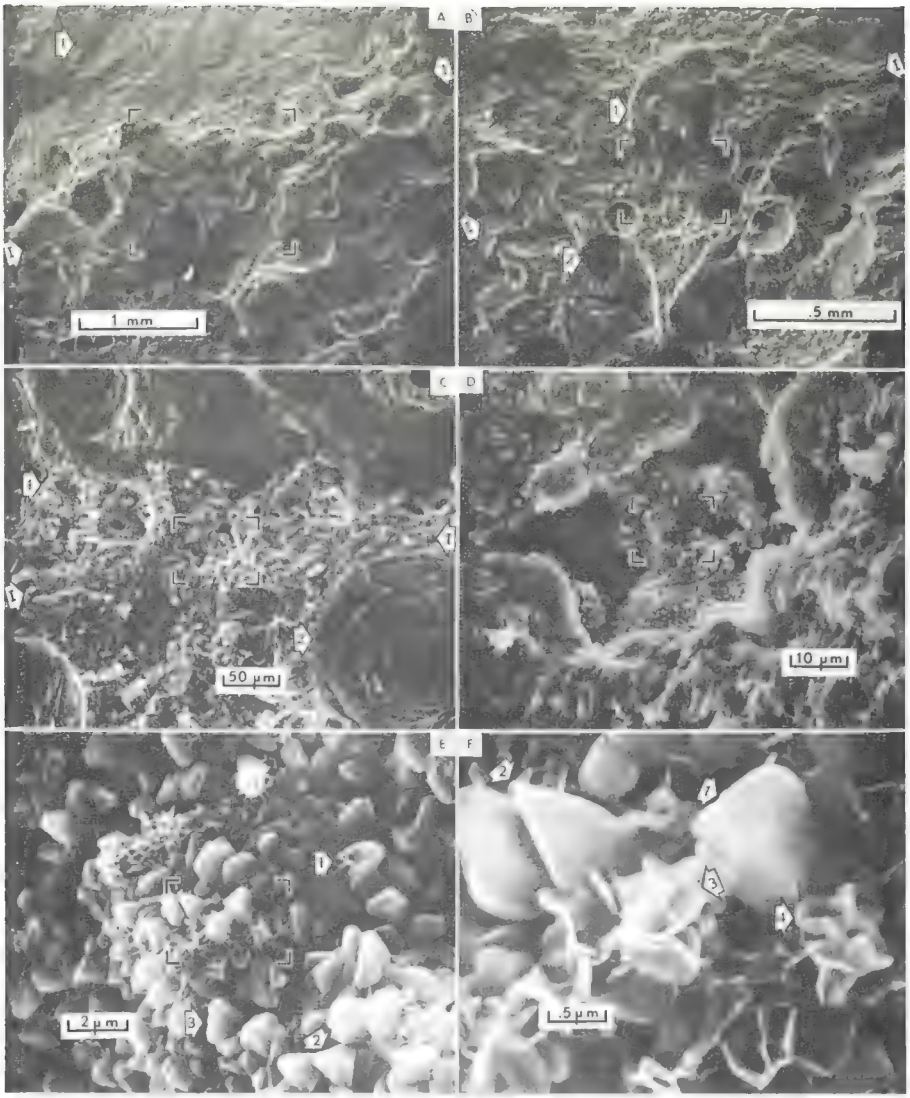

Figure 5. Standard unsandblasted sample: overlay-substrate interface.

right, with the substrate to the left and the overlay to the right. Note the limestone grain (arrow 1) in the substrate less than 1 mm from the interface. Figure 5b shows a sand grain (arrow 1) in the substrate near the interface and several bubble holes in the overlay (arrow 2). These holes are attributed to entrained air bubbles; evidently the fracture plane intersected the bubble hole, revealing it to be a hollow sphere. This interpretation is supported by the presence inside the hole of crystal growths, which are apparently hydration products. Figure 5c shows a string of tiny open pockets along the interface. Inside these is a 10-μm to 100-μm thick layer of material, extending from the interface to arrow 1. Figure 5c also shows the crystals that have grown in the bubble holes (arrow 2). Figure 5d shows that the crystals lining one of the larger pockets are of 2 types; leaf-shaped and granular. Details of the crystal habit of these 2 forms are pointed out in Figures 5e and 5f. These open pockets lined with crystals follow the interface just below the surface of the concrete substrate.

The question as to the prevalence of these pockets is answered by examination of the surface after shear bond fracture. In this case, the failure was judged visually to be present entirely throughout the interface. Figure 6 shows the concrete substrate side of the shear bond fracture specimen. Even at the lowest magnification (Fig. 6a), the failure does not appear to be entirely at the interface. There are plateaus of the original interface interspersed with fuzzy areas and exposed sand grain surfaces, which must have been below the original interface. Figure 6b shows a plateau of the original interface (arrow 1) at higher magnification as well as the perimeter of a fuzzy area (arrow 2) and a deep fracture exposing a sand grain (arrow 3). Figure 6c shows that the fuzzy area is actually a myriad of crystals extending through veins and fissures across the fracture surface. The vein of needle-like crystals (lower framed area) is shown at higher magnification in Figure 6d. Stereoscopic observation of this field confirmed that the needles spanned the vein, because their ends (arrow 1) had been broken off and the mass (arrow 2) is much lower than the surface in the lower right corner to

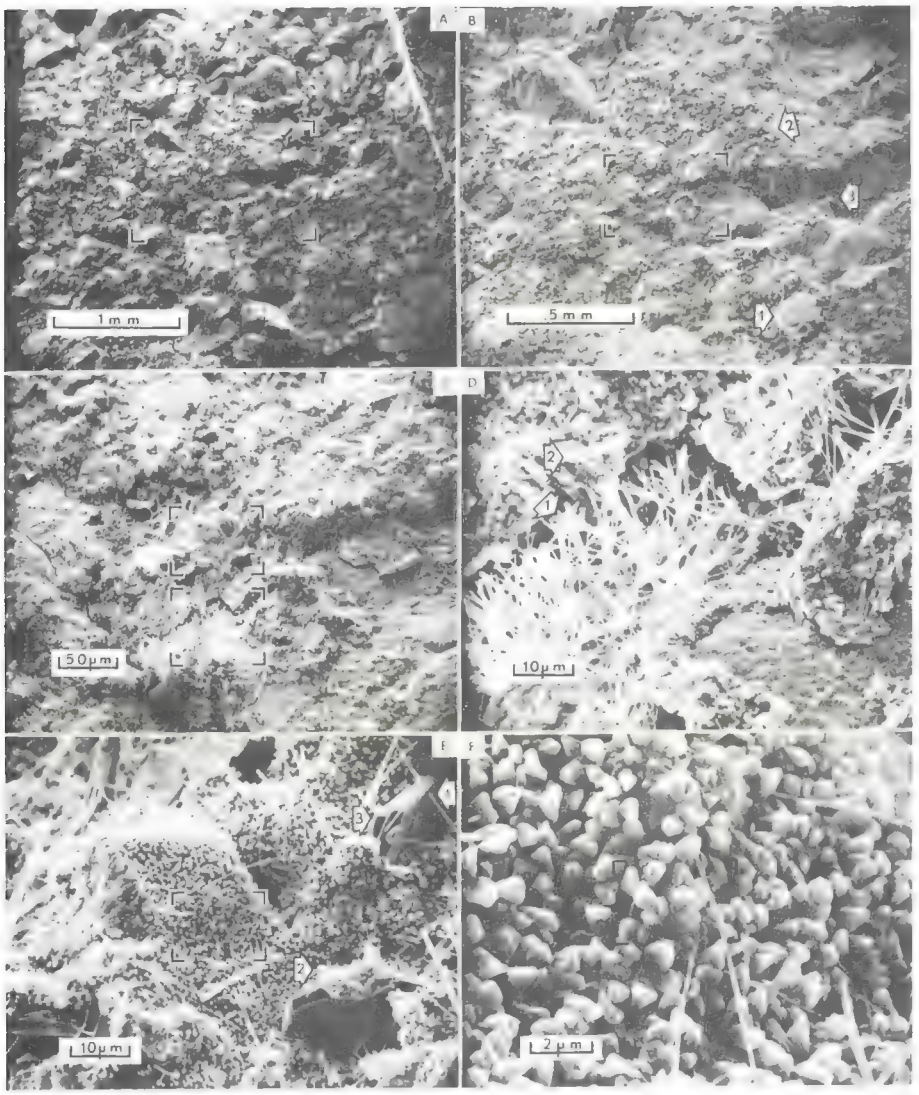

Figure 6. Standard unsandblasted sample: substrate side of shear bond fracture.

which the needles are attached. Figures 6e and 6f show the intercrystallization of several crystal forms; e.g., in one case (Fig. 6e), a needle penetrated a plate (arrow 1). In the lower right corner (Fig. 6e), a piece of amorphous material, probably the original roof of the pocket, is still adhering to a plate (arrow 2). Note the slanted edges of the large plates (arrow 3). Stereoscopic observation suggests that the orientation of these edges is rhombohedral; the crystal form of the tabular plates would then be rhombohedral pinacoids. The granular crystals shown in the background of Figure 6e are of the same size and crystal habit as those shown in Figure 5f; however, in the present case, there are no masses of tiny leaf-shaped crystals. Such observations on crystal morphology will eventually lead us to the identification of these crystals.

Thus, it appears that the pockets lined with crystals are actually "caverns" that extend parallel to the interface for relatively great distances and that constitute a significant proportion of the interfacial area. This is verified by Figures 7a and 7b,

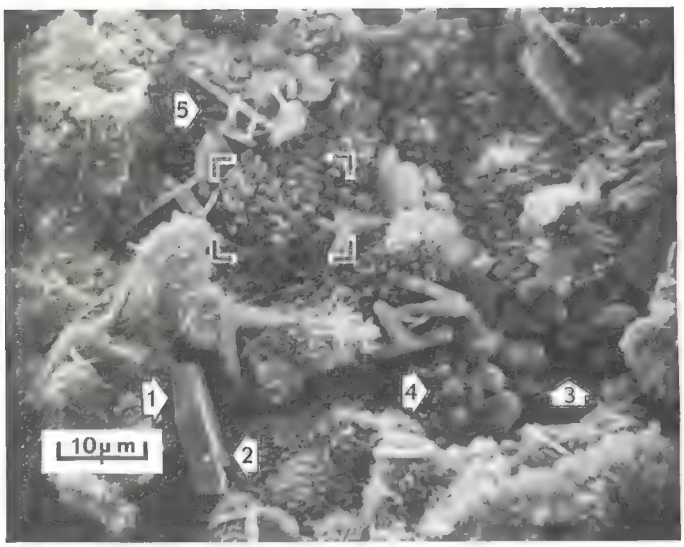

Figure 7a

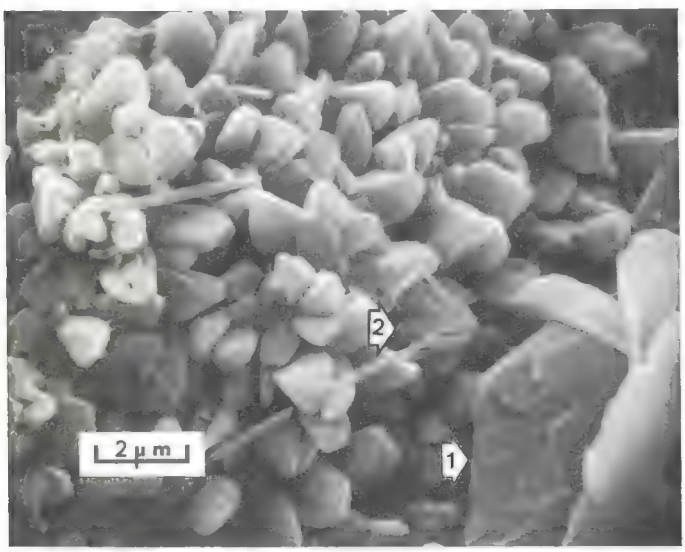

Figure 7b

Figure 7. Standard unsandblasted sample: overlay side of shear bond fracture.

which show the mortar side of the fracture surface corresponding to the substrate shown in Figure 6 (i.e., the roof of the cavern that was split apart by the shear bond fracture). Figure 7a is remarkable in that it shows 5 different crystal shapes, all growing together and lining the roof of the cavern. One large plate (arrow 1) in the form of a rhombohedral pinacoid has a needle (arrow 2) growing out of it. Also seen are the granular ground mass (arrow 3) with its pyramidal shape and the accompanying tiny, twinned, leaf-shaped crystals (arrow 4). Finally, there is a new type of plate crystal (arrow 5), as shown in Figure 7b that is terminated by a series of hexagonal steps (arrow 1). Figure 7b also shows the succession of mineral growth, e.g., the granular crystal (arrow 2) in which a needle has been included, with a subsequent disruption of the growth habit of the grain.

Regardless of the beauty of these crystalline forms, their presence is indicative of a weak bond between the mortar overlay and the concrete substrate. Such crystals can

Figure 8a

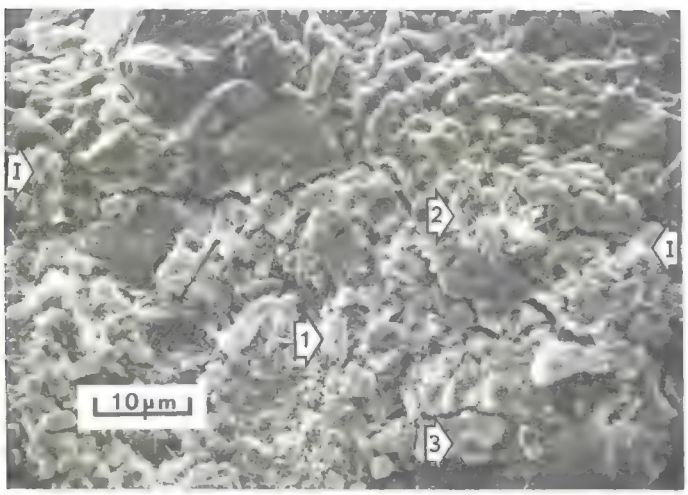

Figure 8b

Figure 8. Standard 3-day composite sample: overlay-substrate interface.

form only in cavities or voids that are filled with liquid or gas. The presence of such cavities or voids decreases the area of contact between the overlay and the substrate. They may be formed either before or after the overlay is applied to the substrate; however, their formation involves materials already present on the surface of the substrate. The absence of both the cavities and the crystals in the sandblasted samples indicates that this or another scarification treatment is necessary to remove these materials.

The next series shows the differences in morphology observed with the standard samples were aged 3, 7, and 14 days. The morphology correlates with an increasing degree of fracture through the concrete substrate, rather than through the mortar overlay or interface. Figures 8 and 9 show the fracture surfaces perpendicular to the overlay-substrate interface, analogous to those shown in Figures 1, 2, and 5. Figure 8 shows the standard sample aged 3 days. Again the interface is marked by arrows, with the substrate above and the overlay below. Figure 8a shows the perimeters of a

Figure 9a

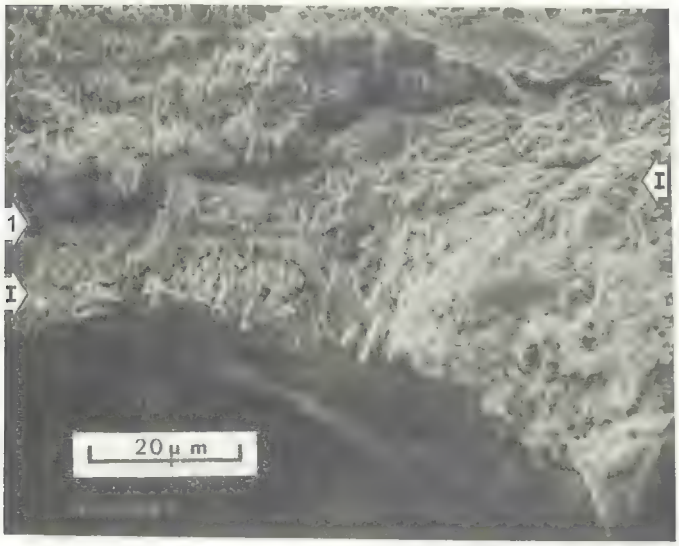

Figure 9b

Figure 9. Standard 7-day composite sample: overlay-substrate interface.

limestone grain (arrow 1) that is flush with the interface. The fractured mass in the limestone grain (arrow 2) is probably calcite because of its rhombohedral form. The large mass (arrow 3) is a sand grain in the overlay mortar. Microcracks can be seen around the peripheries of the sand and limestone grains. Figure 8b clearly shows the microcrack along the mortar side of the limestone-mortar interface. The needle-like crystals lining the channels and fissures (arrow 1) are characteristic of early aging times. The interface can be located only approximately on this scale. A pocket of needles seems to have penetrated the limestone grain (arrow 2), whereas the particle characteristics of the limestone are present in the mortar (arrow 2). Thus, the latex-containing overlay dry-cured for 3 days resembles the control overlay wet-cured for 28 days in that it exhibits needle-filled channels and microcracks on the mortar side of the interface.

Figure 9 shows the standard sample aged 7 days. Again, the interface is marked with arrows and the latex-containing mortar is shown in contact with a limestone grain. These figures show that there are 2 significant differences between 3-day and 7-day aging:

1. The needle-like structures are absent at 7 days (either they have not formed, or they have been covered by the hydration products that formed later); and
2. The microcracks generally follow the overlay-substrate interface but through the substrate adjacent to it, e.g., about 10 μm inside the limestone grain (arrow 1) and the interface is more difficult to locate than in the sample aged 3 days.

The analogous micrographs for the standard sample aged 14 days are not shown because the interface could not be discerned at all at these magnifications. The sample that fractured perpendicularly to the interface showed no microcracks or significant differences in morphology nor any other discontinuities. When this specimen was fractured to simulate the shear bond strength test, the fracture occurred almost entirely throughout the concrete substrate as it did in the actual shear bond test. Thus, the latex-modified overlay became completely integrated with the concrete substrate between 7 and 14 days, under conditions (50 percent RH) that would have severely weakened the ordinary mortar overlay.

Because it is difficult to imagine that a crack present at 3 or 7 days could heal and absent in 14 days, these cracks are assumed to form when the specimen is dried for microscopy under vacuum. The cracks then indicate excessive shrinkage on drying, and they pass through the weakest structures present.

CONCLUSION

The shear bond strength of latex-modified mortar overlays on concrete substrates correlates well with the morphology of the specimens as observed in the scanning electron microscope. The lower bond strength of the control mortar overlay (without latex) correlates with the many microcracks observed throughout the interface between the overlay and the substrate and around the periphery of the sand and limestone grains. The increase in internal and adhesive strength of the latex-modified overlays observed with aging times up to 14 days correlates with the complete integration of the overlay with the substrate, so that the interface can no longer be discerned (it was clearly visible at earlier aging times). The lower bond strengths of the overlay observed when the substrate was not sandblasted before application, correlates with the presence of crystals of various shapes formed in cavities or voids in the interface (neither the crystals nor the voids were observed in the sandblasted sample). These results demonstrate the remarkable utility of the scanning electron microscope for investigating the morphology of portland cement compositions.

REFERENCES

1. Cardone, S. M., Brown, M. G., and Hill, A. A. Latex-Modified Mortar in the Restoration of Bridge Structures. HRB Bull. 260, 1960, pp. 1-13.
2. Shafer, H. H. A Structural Restoration System for Concrete Surfaces. HRB Spec. Rept. 116, abridgment, 1971, pp. 48-50.

3. Siegal, S. Nonparametric Statistics for the Behavioral Sciences. McGraw-Hill, New York, 1956, pp. 75-83.
4. Kimoto, S., and Russ, J. C. The Characteristics and Applications of the Scanning Electron Microscope. American Scientist, Vol. 57, No. 1, 1969, pp. 112-133.

EFFECTS OF COMBINING TWO OR MORE ADMIXTURES IN CONCRETE

C. E. Lovewell and Edward J. Hyland,
Chicago Fly Ash Company

Two laboratory investigations were conducted to determine predictability of performance of concrete mixes with respect to compressive strength and other quality parameters in which mixes were made without admixture and with one or more admixtures. Two programs that were conducted 5 years apart used different sources of materials—air-entrained concrete and non-air-entrained concrete respectively—and two basic concepts or approaches to ascertain equivalency of performance levels. In the first program, the admixture or admixtures were added to the cement. In the second program, cement contents were reduced as made possible for equivalency of performance by use of one or more admixtures. Library research was relied on to give additional background information. Data show that existing concrete technology can serve as a guide in proportioning concrete mixtures containing one or more admixtures and that results can be predicted with reasonable accuracy.

EARLY in 1971, a report (1) was published dealing with admixtures in concrete (accelerators, air-entrainers, water reducers, retarders, and pozzolans). The report contains the latest and most complete information compiled to date on the subject of these classes of concrete admixtures. The objective of this paper is to supplement the information in the report (1) by giving documentary information on some results achieved by use of various combinations of concrete admixtures as differentiated from the use of only 1 type of admixture in a given cubic yard of concrete.

Background information from previously published papers (1, 2, 3) was used in carrying out 2 research programs. The first program dealt with air-entrained concrete and 4 basic mixes involving the use of the following:

Content	Mix
Cement only	A
Cement + fly ash	B
Cement + water reducer	C
Cement + fly ash + water reducer	D

Concrete as made by using these 3 basic mixes: lean, medium, and rich. The admixtures for mixes B, C, and D were in addition to the amount of cement in mix A for each type plus equal (5.0 ± 0.5 percent) air entrainment in all mixes and with appropriate adjustments in aggregates to give equal yield. The principles of mix proportioning developed earlier were used (2), and slump of 4.5 ± 0.5 in. was required throughout. Compressive strength tests were made at 1, 7, and 28 days. The details of the mixes and strength tests are given in Table 1.

Five years later, the second program used fine and coarse aggregates, water reducer, cement, and fly ash from different sources. In this case, actually, 2 different brands of water reducers were used. Another variation was that non-air-entrained

Sponsored by Committee on Chemical Additions and Admixtures for Concrete.

TABLE 1

MIXES USED IN FIRST PROGRAM

Item	Lean, 3.5 Sacks, by Mix				Medium, 4.5 Sacks, by Mix				Rich, 5.5 Sacks, by Mix				FHA Series, by Mix				
	A	B	C	D	A	B	C	D	A	B	C	D	A (5 sacks)	B (4.5 sacks)	B (4.4 sacks)	C (4.25 sacks)	D (3.75 sacks)
								Quantity									
Cement, lb	329	329	329	329	423	423	423	423	517	517	517	517	470	423	414	400	353
Sand, lb	1,635	1,640	1,425	1,510	1,515	1,535	1,325	1,395	1,415	1,435	1,280	1,300	1,485	1,390	1,375	1,575	1,495
1-in. stone, lb	1,635	1,640	1,670	1,705	1,645	1,665	1,690	1,705	1,660	1,685	1,695	1,725	1,675	1,700	1,685	1,670	1,685
Water reducer, fl oz	—	26.3	—	26.3	—	33.8	—	33.8	—	41.4	—	41.4	—	—	—	32.0	28.2
Fly ash, lb	—	—	150	100	—	—	125	100	—	—	100	100	—	75	125	—	100
Air-entraining agent, fl oz	4.5	1.5	9.0	4.0	6.0	1.5	8.0	3.5	6.0	1.5	8.5	4.0	7.0	7.5	7.5	2.0	2.5
Water, lb	280	265	288	265	285	270	290	272	286	272	295	275	282	285	285	265	270
Air, net percent	5.0	5.6	4.9	4.8	5.5	5.4	5.4	5.1	5.4	5.2	4.8	4.8	4.7	5.0	4.8	5.1	4.8
Slump, in.	4.0	4.5	4.5	4.5	4.75	4.75	4.50	4.75	4.50	4.50	4.50	4.50	4.75	5.0	4.25	4.75	5.0
								Average Compressive Strength (psi)									
Age, day																	
1	462	660	790	1,090	813	1,125	1,149	1,533	1,167	1,586	1,462	1,876	1,067	1,120	1,150	1,012	1,185
7	1,574	1,852	1,940	2,234	2,382	2,818	2,712	3,154	3,118	3,466	3,307	3,878	2,707	2,653	2,691	2,600	2,518
28	2,364	2,518	3,100	3,619	3,372	3,837	3,897	4,403	4,285	4,904	4,651	5,405	3,847	3,707	3,925	3,776	3,805

concrete only was made with the 5-, 6-, and 7-sack nominal mixes (2, 3). The mixes contained the following:

Content	Mix
Cement only	A
Cement + water reducer 1	B
Cement + water reducer 2	C
Cement + water reducer 1 + fly ash	D

In this program, tests for compressive strength, modulus of elasticity, and drying shrinkage were made at 3, 7, and 28 days, whereas additional shrinkage measurements only were made at 5, 14, 56, and 90 days. The percentage of water reduction from the control mix A for each of the other mixes was recorded. Each of the concretes containing admixtures contained less cement than the control mix to give approximate equivalency in properties tested. The details of these mixes and their results are given in Table 2.

MATERIALS, MIXTURES, AND SPECIMENS

All of the ingredients for both programs were obtained from commercial sources by testing laboratory personnel. Both cements were Type I and both fly ashes met ASTM Specification C 618, Class F (Tentative Specifications for Fly Ash and Raw or Calcined Natural Pozzolans for Use in Portland Cement Concrete). The sand had a fineness modulus of 2.75, and the 1 in. crushed stone fineness modulus was 7.20 in the first program. These fineness modulus figures were 2.63 and 6.97 in the second program.

There were 153 compressive strength cylinders made and tested, 3 for each of the 3 test ages, for the 17 mixes made in the first program, and 108 cylinders, 3 for each of the 3 test ages, for each of the 12 mixes, plus twelve 3- by 3- by 10-in. prisms for drying shrinkage measurements, in the second program.

In the first program, the fly ash or water reducer or both were in addition to the amount of cement used in the control mix A, and adjustments were made in aggregates, water, and air-entraining agent to maintain yield, slump, and air content constant within reasonable limits throughout. Some of the information from the study by Lovewell and Washa (3) was used.

Consistency was maintained in the second program by holding the coarse aggregate weight constant for all mixes and adjusting the fine aggregate weight and water as needed to maintain yield and slump. The reduction in cement content and amounts of fly ash or water reducer or both to compensate for equivalency in properties to the control mix A were estimated from background information from the first program and elsewhere (3, 4) and proportioning techniques given in ACI Standard 211.1-70 (Recommended Practice for Selecting Proportions for Normal Weight Concrete).

TEST RESULTS

In the first program in which air-entrained concrete only was used, one or more admixtures was added to the same amount of portland cement at 3 levels (lean, medium, and rich). The purpose was to learn whether all tested admixture combinations would yield concrete that was of satisfactory quality, with expected increased strength, and free from detectable abnormalities. The Federal Housing Administration (FHA) series differed in that the 5-sack FHA mix A was used as a control mix with which four other mixes, which were redesigned to include one or more admixtures (in addition to air), were compared. The intention here was to determine whether all 5 mixes would pass physical tests required by FHA minimum property standards for concrete used for housing.

Strength curves shown in Figure 1 yielded 4 distinct curves for compressive strengths at ages of 1, 7, and 28 days respectively. These may be used by an engineer to select any 1 of 4 mixes that will serve as a trial mix for satisfying a specific need.

TABLE 2

MIXES USED IN SECOND PROGRAM

Item	Lean				Medium				Rich			
	Mix A (5 sacks)	Mix B (4.4 sacks)	Mix C (4.4 sacks)	Mix D (3.85 sacks)	Mix A (6 sacks)	Mix B (5.25 sacks)	Mix C (5.25 sacks)	Mix D (4.85 sacks)	Mix A (7 sacks)	Mix B (6.25 sacks)	Mix C (6.25 sacks)	Mix D (5.95 sacks)
Quantity												
Cement, lb	470	414	414	362	564	494	494	456	658	588	588	550
Sand, lb	1,550	1,525	1,600	1,535	1,465	1,480	1,540	1,465	1,360	1,395	1,430	1,350
Stone, lb	1,750	1,750	1,750	1,750	1,750	1,750	1,750	1,750	1,750	1,750	1,750	1,750
Fly ash, lb	—	—	—	100	—	—	—	100	—	—	—	100
Water reducer 1, fl oz	—	16.6	—	14.5	—	19.8	—	18.3	—	23.5	—	22.0
Water reducer 2, fl oz	—	—	12.4	—	—	—	14.8	—	—	—	17.6	—
Water, lb	290	260	275	255	290	265	275	260	300	275	285	270
Water reduction, percent		10.3	5.2	12.1		8.6	5.2	10.3		8.3	5.0	10.0
Slump, in.	4.0	4.25	4.0	4.25	3.75	4.0	4.25	4.25	4.0	3.75	4.0	4.25
Average Compressive Strength (psi)												
Age, day												
3	1,825	1,527	1,503	1,444	3,071	3,059	3,124	2,706	3,891	4,285	4,592	3,655
7	3,018	2,818	2,777	2,871	3,920	4,055	4,256	4,056	4,645	5,294	5,400	4,846
28	4,327	4,327	3,985	4,433	5,512	5,600	5,394	5,812	6,272	6,850	6,438	6,921
Drying Shrinkage (percent)												
Age, 28 days[a]					0.025	0.016	0.025	0.013				
Modulus of Elasticity (10^6 psi)												
Age, day												
3	3.63	3.57	3.60	3.61	3.92	4.08	4.16	4.00	4.20	4.41	4.49	4.30
7	4.23	4.19	4.02	4.23	4.51	4.61	4.51	4.31	4.72	4.91	4.92	4.70
28	4.57	4.52	4.26	4.46	4.91	5.04	4.83	5.09	5.09	5.49	5.40	5.52

[a]Drying shrinkage tests made only at the 6-sack level, because of lack of equipment and personnel to carry on simultaneous tests at all 3 levels.

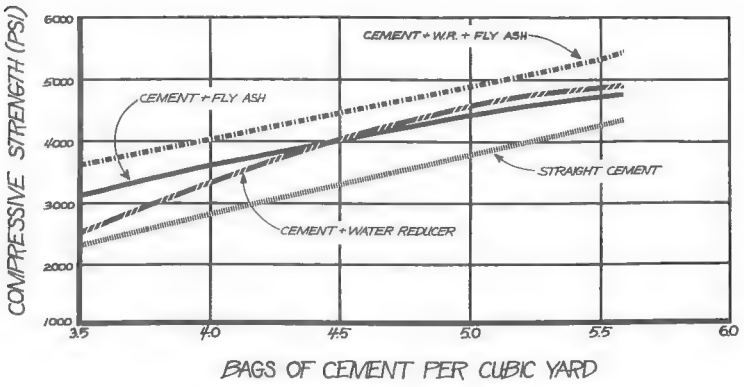

Figure 1. Compressive strength of first program air-entrained concrete tested after 28 days.

For example, the engineer may want 3,000 psi at 28 days along with finishing and placing properties equivalent to those associated with 5 sacks of cementing material with this particular set of aggregates. Reading upward in Figure 1 from 5.0 sacks of cement, we intersect the straight cement curve at 3,850 psi. Then reading across to the left we see that the same strength should be achieved by using 4.4 sacks of cement plus water reducer, 4.4 sacks of cement plus fly ash, or 3.75 sacks of cement plus water reducer plus fly ash. The engineer's strength requirement is satisfied (and there is a suitable factor of safety). Previous experience with such mixes or test slabs, as provided for in ACI Standard 302-69 (Recommended Practice for Concrete Floor and Slab Construction), would reveal adequacy of placing and finishing characteristics of each.

Five years later in the second program, non-air-entrained concrete was made at the nominal levels of 5, 6, and 7 sacks/cu yd by using materials from sources other than those in the first program and by using proportioning techniques recommended in ACI Standard 211.1-70.

Although the non-air-entrained mixes in the second program ranged from 5 to 7 sacks of cement and the air-entrained mixes in the first program ranged from 3.5 to 5.5 sacks of cement, the similarity in trends of the 2 mixes is remarkable. Figure 2 shows that

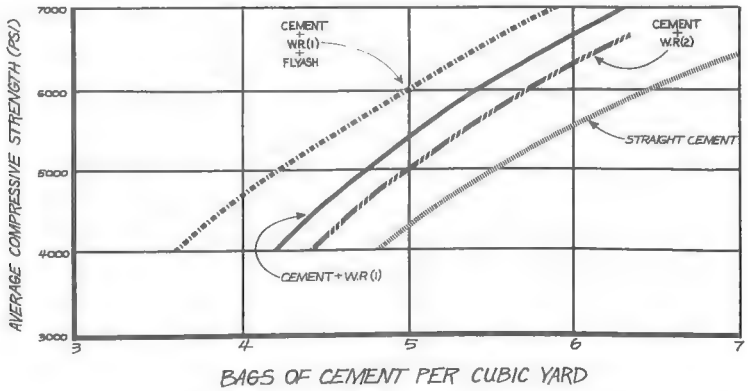

Figure 2. Compressive strength of second program non-air-entrained concrete tested after 28 days.

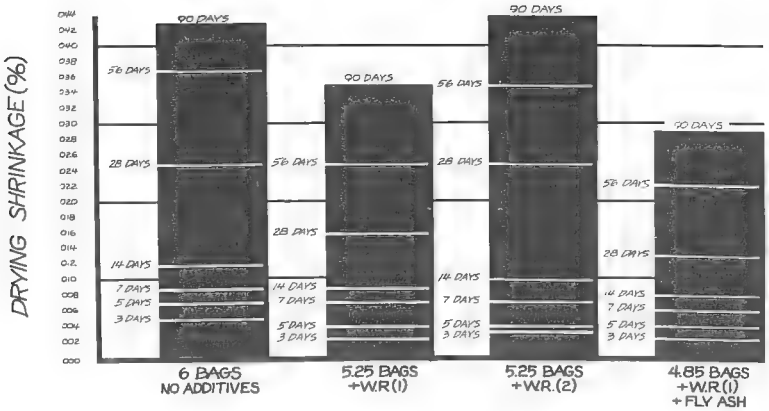

Figure 3. Drying shrinkage of medium mixes of non-air-entrained concrete.

5,000-psi (laboratory strength) concrete was made with 5.5 sacks of cement or with 5.0 sacks plus water reducer 2 or with 4.8 sacks plus water reducer 1 or with 4.3 sacks plus water reducer 1 plus fly ash.

Figure 3 shows drying shrinkage measurements at various ages for the second program medium mixes. The lowest shrinkage values consistently are shown for mix D. Figure 4 shows modulus of elasticity measurements for these same mixes. Because all mixes were intended by design to have roughly equivalent strengths, it is not surprising that the moduli of elasticity likewise are roughly equivalent.

Library research has revealed that, as early as 1951, Davis combined fly ash with a water-reducing agent and an air-entraining agent in concrete and found higher strengths at all ages as compared to the control mix (5). No adverse effects were noted. In another instance, Lovewell in a panel discussion quoted ready-mix production of 7,500-psi non-air-entrained concrete with $8\frac{3}{4}$ sacks of portland cement plus 100 lb of fly ash plus a water-reducing admixture with a 28-day deviation of only 8 percent (6). In still another instance, the Kentucky Department of Highways (7) compared air-entrained concrete as follows: 6 sacks of portland cement/cu yd (control); 5 sacks of cement plus 94 lb of fly ash (experiment A); and 5 sacks of cement plus 140 lb of fly ash (experiment B). Field tests made in accord with ASTM Method C 31 (Standard Method for Making and Curing Concrete Compression and Flexure Test Specimens in

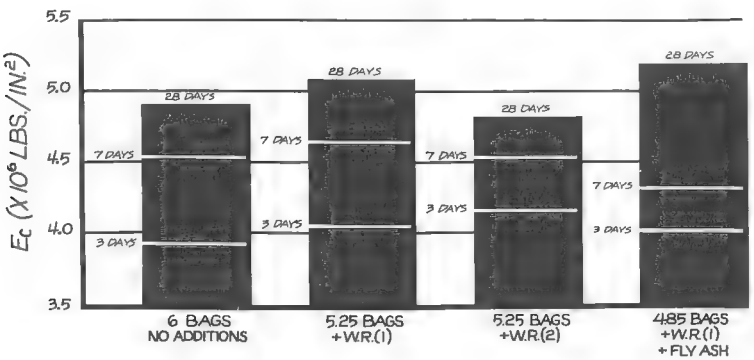

Figure 4. Modulus of elasticity measurements of medium mixes of non-air-entrained concrete.

the Field) revealed an average 28-day compressive strength of 4,970 psi (control), 4,903 psi (experiment A), and 4,779 psi (experiment B). Flexural strengths at 28 days were 1,129 psi (control), 1,080 psi (experiment A), and 1,175 psi (experiment B). Again, no adverse effects were noted.

Another interesting combination of admixtures was used on the Smith Mountain Dam on the Roanoke River in Virginia. Three basic mixes were used: a 4-in. aggregate mix for the concrete arch dam, a 2-in. aggregate mix for the power house, and a $^3/_4$-in. aggregate mix to finish off certain sections of the power house. Retarder, fly ash, and air entrainment were used in all 3 mixes. The 4-in. mix contained 235 lb. Type II cement and 101 lb fly ash for an average 28-day compressive strength of 3,512 psi for 254 cylinders tested. The 2-in. mix contained 329 lb. Type II cement and 82 lb fly ash for an average 28-day strength of 3,778 psi for 178 cylinders tested. The $^3/_4$-in. mix contained 423 lb. Type II cement and 94 lb fly ash retarder, for an average 28-day strength of 4,245 psi for 64 cylinders tested. Although mass concrete is of special interest to only a few engineers, highway engineers would find the 2-in. mix comparable to paving mixes and the $^3/_4$-in. mix similar to concrete in highway structures. No adverse effects of this combination of fly ash, retarder, and air was reported.

Wallace and Ore (8) in 1959 reported on heavily populated test data, both laboratory and field, on the effect of water-reducing, set-retarding admixtures in structural as well as in lean mass concrete. Nine pozzolans (4 fly ash and 5 natural pozzolans), 3 Type I and 9 Type II cements, and 12 admixture agents were used. The agents by classification were ammonium lignin sulfonate (two in solution, two in powder form), hydroxylated carboxylic acid (one in solution), and calcium lignin sulfonate (three in solution, three in powder, and one in powder form with accelerator). Series I "was designed to determine the effects of seven commercial water-reducing agents on retardation of set, water reduction, strength development, and durability of concrete containing $1^1/_2$-in. maximum-size aggregates when added in various dosages with a variety of cements at a constant cement factor." In Series II, "4 lignin-type and 1 hydroxylated carboxylic acid WR agents were used in concrete containing $^3/_4$-, $1^1/_2$-, and 6-in. maximum-size aggregates of relatively good quality. A single Type II cement was used, with and without pozzolan replacement. Effects of the agents on compressive, tensile, and shearing strengths were determined from concrete containing various size aggregates and having various water to cement-plus-pozzolan (w/c + p) ratios. Also, the use of a lignin-type agent with aggregates of marginal or poor quality was studied." In Series III, "one hydroxylated carboxylic acid WR agent and several lignin-type WR agents with good water-reducing effects were selected for use in the mass concretes." Volume change, temperature rise, permeability, workability, strength, and durability were determined. Compressive strength data included test results of 1,820 cylinders 6- by 12-in. and 111 cylinders 18- by 36-in. made in the laboratory and 591 cylinders

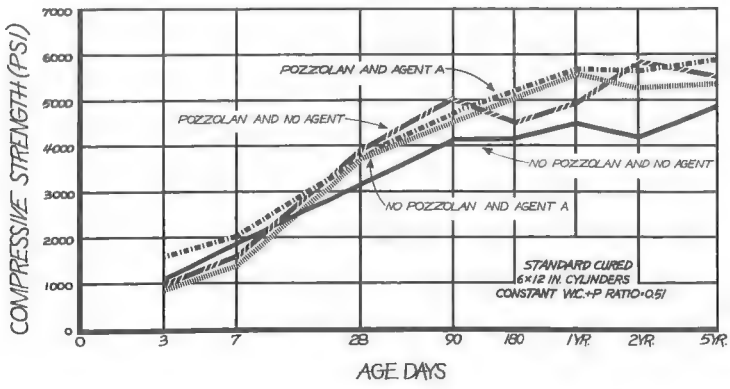

Figure 5. Typical compressive strengths of Wallace and Ore cylinders corresponding to first program mixes.

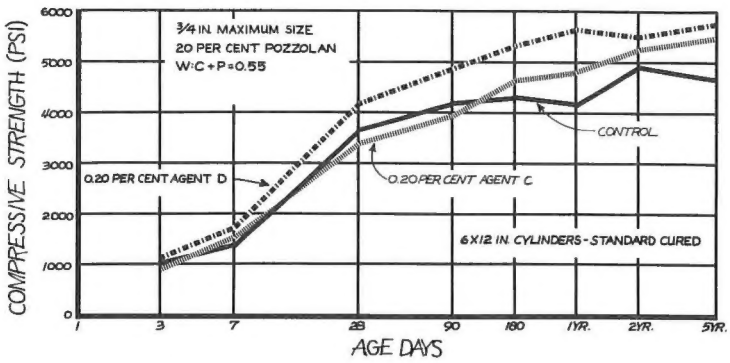

Figure 6. Typical compressive strengths of Wallace and Ore cylinders corresponding to second program mixes.

6- by 12-in. made for field control tests. The report stated, "The test for compressive strength was emphasized because experience has shown that this test provides a good over-all index of the quality of air-entrained concrete."

Tests at 5 years revealed no abnormalities with any of the combinations of admixtures. A typical chart of strengths to 5 years is shown in Figure 5 in which the pozzolan or water-reducing agent or both are added to maintain a constant water-cement plus pozzolan ratio and yield 4 curves very similar to those in the first program.

Figure 6 shows the comparison of mixes with 20 percent cement replaced by pozzolan plus water-reducing agent C (lignin sulfonate) and water-reducing agent D (hydroxylated carboxylic acid) respectively and the control mix with no pozzolan and no agent, all with w/c + p ratio of 0.55. This roughly corresponds to the second program except that there is no mix with pozzolan replacement and with no water-reducing agent included. Here, again, no deleterious effects are noted to 5 years of age.

TABLE 3

EQUIVALENT MINIMUM CEMENTING MATERIAL CONTENTS PER CU YD FOR 4-IN. SLUMP

28-Day Compressive Strength (psi)	Maximum Size of Aggregate (in.)	Total Water per Cu Yd of Concrete (gal)	Mix A[a] (sacks)	Mix B[b] (sacks)	Mix C[c] (sacks)	Mix D[d] (sacks)
		Non-Air-Entrained Concrete				
2,500	1	36	4½	4	3¾[e]	3¼[f]
3,000	1	36	5	4¼	4¼[e]	3¾[f]
3,500	1	36	5½	4¾	4¾[e]	4¼[f]
3,750	1	36	5¾	5	5¼[g]	4½[f]
4,000	1	36	6	5¼	5½[g]	4¾[c]
5,000	1	36	7	6¼	6½[g]	5¾[f]
		Air-Entrained Concrete				
2,500	1	34	4½	4	3¾[e]	3¼[f]
3,000	1	34	5	4¼	4¼[e]	3¾[f]
3,500	1	34	5¾	5	5¼[g]	4½[f]
3,750	1	34	6¼	5½	5¾[g]	5[f]

[a]Portland cement only.
[b]Portland cement plus water reducer as defined in ASTM C-494, Type A. Amounts should be used according to manufacturers' directions (usually a specified amount per sack of portland cement).
[c]Portland cement plus fly ash as set forth in ASTM C-618, Class F. Amounts should be used as indicated.
[d]Portland cement plus water reducer plus fly ash.
[e]125 lb fly ash.
[f]100 lb fly ash.
[g]75 lb fly ash.

With the wealth of information on the subject, it was inevitable that tables of trial concrete mixes, giving estimated equivalent concrete mixes to achieve specified results, would materialize. Table 3 gives data for such trial concrete mixes as specified in the Concrete Industries Yearbook for 1970 (9).

CONCLUSIONS

1. The first and second research programs and considerable library research reveal that pozzolans with water-reducing agents or with water-reducing and retarding agents and with and without air entrainment can be used in concrete without creating abnormalities. All pozzolan ingredients should be checked for compliance with respective applicable ASTM standards, and trial mixes should be made to check compliance of such mixes with specified quality parameters.
2. Although the authors are aware of the successful addition of calcium chloride to mixes containing combinations of admixtures described here, no published information of this type was revealed in the authors' library research.
3. It is concluded that predictable results may be secured by using combinations of admixtures of suitable quality and by using proper mix proportions established by trial batches.

REFERENCES

1. Admixtures in Concrete: Accelerators, Air Entrainers, Water Reducers, Retarders, and Pozzolans. HRB Spec. Rept. 119, 1971, 32 pp.
2. Timms, A. G., and Grieb, W. E. Use of Fly Ash in Concrete. ASTM, Proc. Vol. 56, 1956, pp. 1139-1160.
3. Lovewell, C. E., and Washa, G. W. Proportioning Concrete Mixtures using Fly Ash. ACI Jour., Proc. Vol. 54, June 1958, pp. 1,093-1,102.
4. Cannon, R. W. Proportioning Fly Ash Concrete Mixes for Strength and Economy. ACI Jour., Nov. 1968, pp. 969-979.
5. Davis, R. E. What You Should Know About Pozzolans. Engineering-News Record, April 5, 1951.
6. Control of Cementing Medium in Concrete. National Ready Mixed Concrete Assn., Silver Springs, Md., NRMCA Publ. 132, April 1970.
7. Hughes, R. D. Experimental Concrete Pavement Containing Fly Ash Admixtures. Kentucky Department of Highways, July 1966; NTIS, PB 173-733, Springfield, Va.
8. Wallace, G. B., and Ore, E. L. Structural and Lean Mass Concrete as Affected by Water-Reducing, Set-Retarding Agents. ASTM, STP 266, 1959, pp. 38-96.
9. Concrete Industries Yearbook, 1970. Pit and Quarry Publ., Chicago, Ill.

THE NATIONAL ACADEMY OF SCIENCES is a private, honorary organization of more than 700 scientists and engineers elected on the basis of outstanding contributions to knowledge. Established by a Congressional Act of Incorporation signed by Abraham Lincoln on March 3, 1863, and supported by private and public funds, the Academy works to further science and its use for the general welfare by bringing together the most qualified individuals to deal with scientific and technological problems of broad significance.

Under the terms of its Congressional charter, the Academy is also called upon to act as an official—yet independent—adviser to the Federal Government in any matter of science and technology. This provision accounts for the close ties that have always existed between the Academy and the Government, although the Academy is not a governmental agency and its activities are not limited to those on behalf of the Government.

The NATIONAL ACADEMY OF ENGINEERING was established on December 5, 1964. On that date the Council of the National Academy of Sciences, under the authority of its Act of Incorporation, adopted Articles of Organization bringing the National Academy of Engineering into being, independent and autonomous in its organization and the election of its members, and closely coordinated with the National Academy of Sciences in its advisory activities. The two Academies join in the furtherance of science and engineering and share the responsibility of advising the Federal Government, upon request, on any subject of science or technology.

The NATIONAL RESEARCH COUNCIL was organized as an agency of the National Academy of Sciences in 1916, at the request of President Wilson, to enable the broad community of U.S. scientists and engineers to associate their efforts with the limited membership of the Academy in service to science and the nation. Its members, who receive their appointments from the President of the National Academy of Sciences, are drawn from academic, industrial, and government organizations throughout the country. The National Research Council serves both Academies in the discharge of their responsibilities.

Supported by private and public contributions, grants, and contracts, and voluntary contributions of time and effort by several thousand of the nation's leading scientists and engineers, the Academies and their Research Council thus work to serve the national interest, to foster the sound development of science and engineering, and to promote their effective application for the benefit of society.

The DIVISION OF ENGINEERING is one of the eight major Divisions into which the National Research Council is organized for the conduct of its work. Its membership includes representatives of the nation's leading technical societies as well as a number of members-at-large. Its Chairman is appointed by the Council of the Academy of Sciences upon nomination by the Council of the Academy of Engineering.

The HIGHWAY RESEARCH BOARD, an agency of the Division of Engineering, was established November 11, 1920, as a cooperative organization of the highway technologists of America operating under the auspices of the National Research Council and with the support of the several highway departments, the Bureau of Public Roads, and many other organizations interested in the development of transportation. The purpose of the Board is to advance knowledge concerning the nature and performance of transportation systems, through the stimulation of research and dissemination of information derived therefrom.

HIGHWAY RESEARCH BOARD
NATIONAL ACADEMY OF SCIENCES—NATIONAL RESEARCH COUNCIL
2101 Constitution Avenue Washington, D. C. 20418

ADDRESS CORRECTION REQUESTED